



6-1960

Interface Phenomena During Gas-Liquid Mass Transfer Operations

John Wallace Mottern

University of Tennessee - Knoxville

Recommended Citation

Mottern, John Wallace, "Interface Phenomena During Gas-Liquid Mass Transfer Operations." PhD diss., University of Tennessee, 1960.

https://trace.tennessee.edu/utk_graddiss/2945

This Dissertation is brought to you for free and open access by the Graduate School at Trace: Tennessee Research and Creative Exchange. It has been accepted for inclusion in Doctoral Dissertations by an authorized administrator of Trace: Tennessee Research and Creative Exchange. For more information, please contact trace@utk.edu.

To the Graduate Council:

I am submitting herewith a dissertation written by John Wallace Mottern entitled "Interface Phenomena During Gas-Liquid Mass Transfer Operations." I have examined the final electronic copy of this dissertation for form and content and recommend that it be accepted in partial fulfillment of the requirements for the degree of Doctor of Philosophy, with a major in Chemical Engineering.

H. F. Johnson, Major Professor

We have read this dissertation and recommend its acceptance:

R. M. Boarts, Hilton A. Smith, J. A. Cooley, P. F. Pasqua

Accepted for the Council:

Dixie L. Thompson

Vice Provost and Dean of the Graduate School

(Original signatures are on file with official student records.)

May 24, 1960

To the Graduate Council:

I am submitting herewith a thesis written by John Wallace Mottern entitled "Interface Phenomena During Gas-Liquid Mass Transfer Operations." I recommend that it be accepted in partial fulfillment of the requirements for the degree of Doctor of Philosophy, with a major in Chemical Engineering.

H. Johnson
Major Professor

We have read this thesis and recommend its acceptance:

Alton A. Smith

Ren Boats

J. A. Cooley

[Signature]

J. Cooley

Accepted for the Council:

Adm. Mantling
Dean of the Graduate School

INTERFACE PHENOMENA DURING GAS-LIQUID
MASS TRANSFER OPERATIONS

A Dissertation
Presented to
the Faculty of the Graduate School
University of Tennessee

In Partial Fulfillment
of the Requirements for the Degree
Doctor of Philosophy

by
John Wallace Mottern
June 1960

ACKNOWLEDGEMENT

The author wishes to acknowledge indebtedness to the following persons and organizations for help and guidance during his graduate studies: Dr. H. F. Johnson who supervised this experimental investigation; Dr. R. M. Boarts for his advice and for financial assistance in the form of assistantships and instructorships; Dr. P. F. Pasqua, of the Nuclear Engineering Department, who allowed the author to use the department's Donner Analogue Computer; Dr. M. E. Whately, of the Oak Ridge National Laboratory, who programmed the digital computer solution of some partial differential equations; and the Oak Ridge National Laboratory for the use of the Oracle Digital Computer. Later in this investigation a Pace Analogue Computer in the Chemical Engineering Department was used, and this proved to be very useful.

During his graduate studies, the author received additional financial assistance in the form of fellowships from the following companies: Monsanto Chemical Company, Phillips Petroleum Company, Tennessee Eastman Corporation, and The Texaco Company. The author expresses his gratitude to these companies for the much needed financial help, and to Dr. Boarts for arranging this assistance.

Appreciation is extended to Mr. E. H. Honeycutt and Mr. Bobby L. McGill of the Shop, who constructed the absorption cell.

SUMMARY

By the use of photographic techniques, the absorption rates of single CO_2 bubbles suspended in downward flowing aqueous monoethanolamine (MEA) solutions were determined for various MEA and CO_2 liquid concentrations. It was found that a linear correlation of the experimental data could be obtained by plotting the mass of the bubble to the one-third power versus absorption time. Such a correlation indicates that the absorption rate per unit area is constant. The absorption rates were found to increase with MEA concentration and to decrease with total absorbed CO_2 concentration (that physically absorbed and chemically combined). However, because of excessive scatter in the experimental data, no satisfactory correlation of the absorption rates with liquid concentrations could be found.

Theoretical analyses of various absorption models were made. Analogue and digital computers were used when the differential equations could not be solved analytically. For two normal MEA it was found that the best explanation of the experimental rate, 4×10^{-6} gm-mole/cm²-sec, was given by the model of steady-state diffusion with simultaneous irreversible second order chemical reaction in a stagnant film of thickness 5×10^{-3} cm. The differential equations involved with this proposed model can best be solved by analogue computer.

In the course of the investigation several absorption models were solved analytically. Although the results indicate that the models did not apply, details of the analyses are given in Appendix A for academic interest. Appendices B and C contain the details of the theoretical analyses by digital and analogue computers.

TABLE OF CONTENTS

CHAPTER	PAGE
I. INTRODUCTION	1
II. LITERATURE SURVEY	8
III. THEORY	11
Penetration Theory	14
Film Theory	17
Digital Solutions of the Diffusion Equations . .	23
Correlation of Experimental Data	38
Addendum	40
IV. EXPERIMENTAL APPARATUS AND PROCEDURE	45
Experimental Apparatus	45
Experimental Procedure	50
Analysis of Experimental Data	53
V. EXPERIMENTAL RESULTS	56
VI. CONCLUSIONS AND RECOMMENDATIONS	80
Recommendations	82
NOMENCLATURE	84
LIST OF REFERENCES	87
APPENDIX	
A. SOLUTIONS OF EQUATIONS 3.2 AND 3.3	93
B. DETAILS OF DIGITAL MACHINE SOLUTION OF EQUATIONS 3.2 AND 3.3	111
C. ANALOGUE SOLUTION OF EQUATIONS 3.2 AND 3.3	119

APPENDIX	PAGE
D. ANALYSIS OF ERRORS IN DETERMINING BUBBLE SIZE . .	137
E. SAMPLE CALCULATIONS AND EXPERIMENTAL DATA	150
VITA	173

LIST OF TABLES

TABLE	PAGE
I. Conditions Run on the Digital Computer	26
II. Concentration Gradients from the Digital Computer, Case 1	117
III. Apparent Horizontal and Vertical Diameters and Their Ratio, Reel 6, Take 4	147
IV. F' Values for Reel 6, Take 4	148
V. Experimental Data, Reel 3, $B_0=1.49$	154
VI. Experimental Data, Reel 4, $B_0=1.95$	156
VII. Experimental Data, Reel 6, $B_0=2.97$	159
VIII. Experimental Data, Reel 7, $B_0=1.06$	163
IX. Experimental Data, Reel 8, $B_0=6.06$	165
X. Least Squares Parameters a and b and the Percentage Variance in b	170

LIST OF FIGURES

FIGURE	PAGE
1. Cross Section of Flow Channel Showing Theoretical Velocity Profile	6
2. Concentration Gradients, Penetration Theory	15
3. Concentration Gradients, Film Theory	18
4. Computer Results, Case 2	28
5. Computer Results, Cases 1 and 3	29
6. Computer Results, Case 4	31
7. Absorption Results Calculated from Digital Computer Results	33
8. Schematic Diagram of Experimental Apparatus	46
9. Diagram of Absorption Cell	48
10. Typical Frames from a Single Take	54
11. Typical Mass-Time Plot, Reel 3	57
12. Typical Correlations of Experimental Data	59
13. Typical Correlations of Experimental Data	61
14. Rate versus CO ₂ Concentration, Reel 3	66
15. Rate versus CO ₂ Concentration, Reel 4	67
16. Rate versus CO ₂ Concentration, Reel 6	68
17. Rate versus CO ₂ Concentration, Reel 7	69
18. Rate versus CO ₂ Concentration, Reel 8	70
19. Rate versus Free MEA Concentration, Reel 4	73
20. Rate versus Free MEA Concentration, Reel 6	74

FIGURE	PAGE
21. Rate versus Free MEA Concentration, Reel 8	75
22. Rate versus Temperature, Reel 8	76
23. Correlation of Rate as Suggested by Equation 5.10, Reel 8	79
24. Schematic Diagram, First Order Case	123
25. Concentration-Time Curves from Analogue Computer .	124
26. Analogue Results	126
27. Analogue Results	127
28. Schematic Diagram for Analogue Solution, Second Order Case	130
29. Analogue Solution, Second Order Case	131
30. Computer Diagram for Steady-State Solution	134
31. Steady-State Concentration Profiles, $x_F=3.16 \times 10^{-4}$ cm	135
32. Optical View of Bubble	138

CHAPTER I

INTRODUCTION

During the past two decades mass transfer research has taken place at such a pace that the state of the art is now on a par with that of heat transfer. Indeed, some of the theoretical results obtained in heat transfer are directly applicable to mass transfer. Quite often important developments in mass transfer are not basically new but rather applications of already developed heat transfer principles. In spite of this now rather high degree of sophistication in mass transfer knowledge there are as yet some unanswered questions. The present dissertation describes and reports on the results of an experimental investigation designed to look into and answer some of these questions.

One of the often studied types of mass transfer is the absorption of a gas by a liquid. This is no accident since such a system lends itself well to experimentation, and further, there are many well known industrial applications of gas absorption. Some examples are distillation, gas scrubbing, and humidification. Industry is interested in the economical design of equipment and this requires a knowledge of the process. It is the quest for this knowledge that has spurred on research in the gas absorption field for the last

decade or so. Even if there were no pressure from industry there would still be incentive to carry on research in this field, that incentive being simply trying to find out what is going on when a gas is absorbed by a liquid. This is the viewpoint taken by the so-called pure scientist and is actually the one adopted by the author in this investigation, although the author does not claim to be a scientist or even a reasonable facsimile.

Two possibilities exist initially for a gas once it is absorbed by a liquid. One is that nothing happens and the other is that the gas may react chemically with some component in the liquid phase. The first case is known as physical absorption, an example of which would be the dissolution of oxygen in water. The second case is denoted sometimes as gas absorption accompanied by chemical reaction or more briefly as chemisorption.

In application, equipment utilizing chemisorption is one of two basic types, packed towers where the liquid flows downward over some type of dispersing medium such as Beryl Saddles or rashig rings, and bubble plate towers where the gas passes up through cups on the plates over which liquid is flowing. In both cases the usual procedure is to have the liquid enter the top of the tower and flow counter-currently to the gas entering at the bottom. In the laboratory, prototypes of these towers are built for experimentation, but

little fundamental information is obtained from such investigations. Results are usually presented in the form of correlation of dimensionless groups of the system parameters. Measurements are made only of the end conditions of the tower, that is, of the entrance and exit streams, and thus the effects observed are really gross effects with no insight as to what is actually happening inside the tower. Consequently, in order to gain a more fundamental knowledge of how the molecules move from the gas phase across the gas-liquid boundary and into the liquid phase, the experimenter must resort to other types of absorption apparatus. They may in fact become quite exotic in appearance and would have little industrial application.

One of the most common of these laboratory gas absorbers is the falling film column. The liquid enters the top of a vertical hollow cylinder not unlike a weir and flows down along the inside surface in a thin film. The gas may pass in either direction through the center of the cylinder. Because of the known geometry, the area of the liquid exposed to the gas is known, an obvious advantage over packed or bubble plate contactors. Another apparatus that has come into vogue of late is the laminar jet. Here a cylindrical stream of liquid passes vertically down through an atmosphere of gas from a nozzle into a receiver. Again the geometry is known so that the area of the gas-liquid interface may be

determined. Such apparatus have one limitation however; because of their rather idealized conditions, results obtained from them cannot be applied directly to industrial equipment.

With this in mind the author decided to construct an apparatus with which fundamental knowledge could be obtained and yet results of which could be applied to industrial equipment. One possibility is an apparatus containing a submerged orifice such as a capillary tube whereby the gas is emitted from the tube and rises upward through the liquid. Some investigators have used this type of equipment. Usually the scheme has been to take liquid samples at various times while the gas is bubbling at a constant frequency through the uncirculating liquid. The liquid samples were analyzed for gas concentration. It was then easy to calculate the average absorption rate for the bubbles generated during the time interval between samples. It was decided that the method could be improved by measuring the absorption rate of a single bubble.

The scheme was simply to generate a single bubble in a down-flowing stream of liquid such that the bubble would remain essentially stationary in elevation. Moving pictures were taken of the bubble and the film was analyzed to determine the absorption rate. In order to make the conditions analogous to a bubble rising in a still body of liquid the

flow channel was constructed in a special manner. Figure 1 shows a schematic diagram of the flow channel. The channel has a rectangular cross section. According to hydrodynamic theory (33) the velocity profile for laminar flow of a Newtonian fluid between two very wide parallel plates will be a parabola. But as the fluid passes into a sharply converging section, as shown in the figure, the profile becomes relatively flat over most of the channel. Thus for a bubble trapped in the converging section the fluid velocity will be essentially the same about the bubble. Therefore as far as the bubble is concerned the fluid seems to be infinite in extent and approaching the bubble from infinity. Or looking at it another way, the situation is the same as if the bubble were rising in a still body of liquid, neglecting the effects of the container walls.

It is impossible to trap a bubble in the converging section for if the liquid velocity is just a little too low the bubble will tend to rise, and in so doing it will come into a region of even less velocity and will rise even more rapidly until it escapes on up the column. Exactly the opposite effect will occur if the liquid velocity is too high. The converging section is thus seen to be an instable zone; in contrast, the diverging section below the throat is a stable zone. Here, if the bubble is trapped and the velocity is too low, the bubble will tend to rise into a region of higher

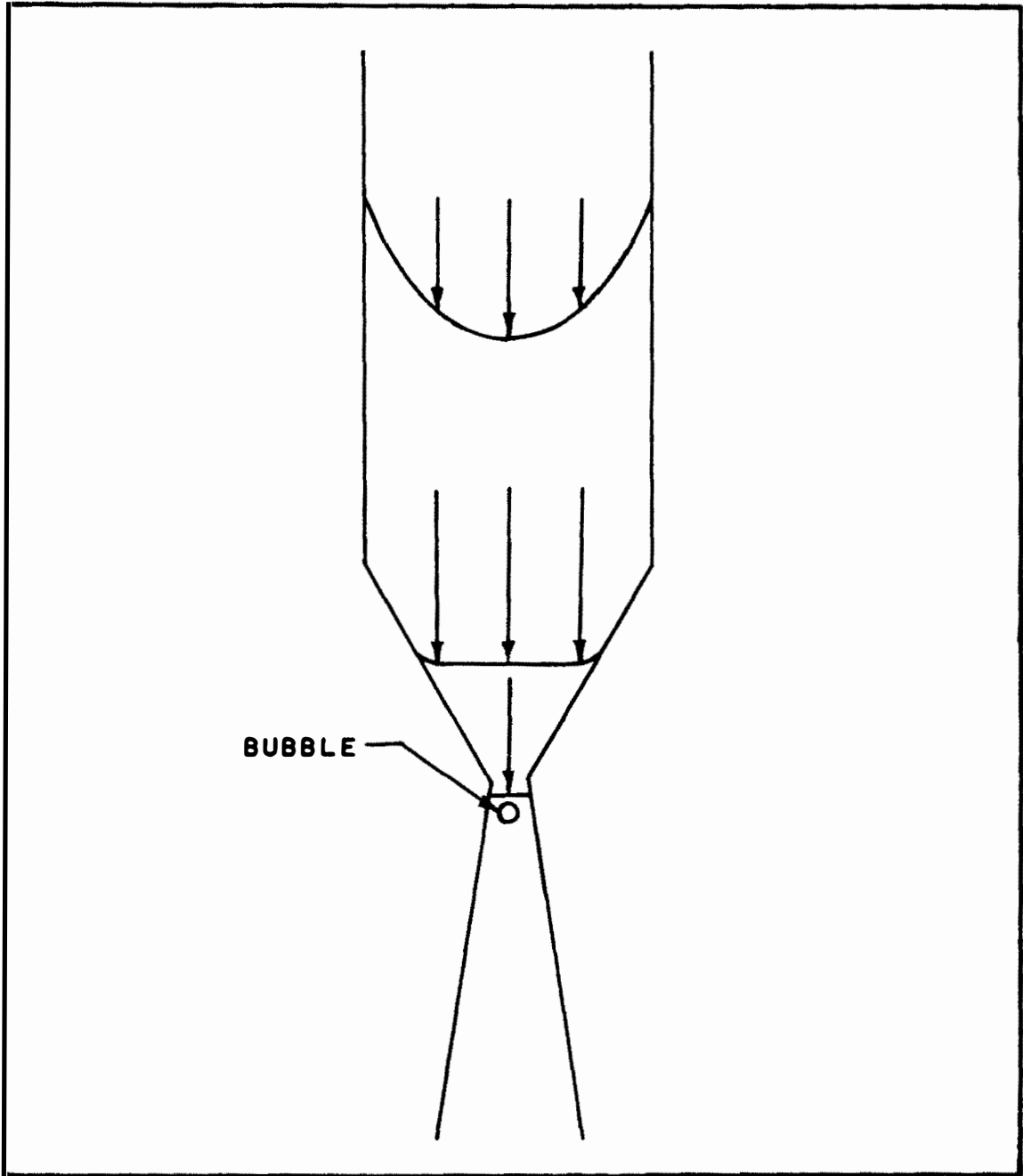


FIGURE 1 CROSS SECTION OF FLOW CHANNEL SHOWING THEORETICAL VELOCITY PROFILE

velocity which in turn will force the bubble back down and vice versa. It is in the diverging section that the bubble is trapped. The purpose of the converging section is to provide the desired velocity profile and in the region just below the throat this profile should persist. The bubble should be trapped just below the throat.

The above experimental procedure was carried out in the present investigation and this thesis is a report on the results. Chapter II contains a short review of the pertinent literature. In Chapter III on theory the author discusses some of the pertinent unanswered questions on gas absorption referred to at the beginning of the present chapter.

Chapters IV and V contain respectively a discussion of the experimental apparatus and procedure and the results of the investigation. Chapter VI summarizes the conclusions and recommendations.

The original data, mathematical developments, and details of theoretical investigations using digital and analogue computers are included in the appendices.

CHAPTER II

LITERATURE SURVEY

It is not intended here to give a complete review of all literature on mass transfer. Nor is it even intended to give a discussion on all literature germane to the present investigation in this chapter. Comments on the work of other investigators will be given later in the text at places where they are pertinent to the discussion. For a general review of mass transfer the reader is referred to the text, "Absorption and Extraction," by T. K. Sherwood and R. L. Pigford (New York: McGraw-Hill Inc., 1952). This is a very excellent book as evidenced by the fact that in recent literature it is one of the most quoted references. For a catalogue of mathematical developments in gas absorption see the doctoral dissertation by Peaceman (34).

As far as could be ascertained little work has been done on the study of stationary drops or bubbles in a moving fluid. Ledig and Weaver (24) in 1924 studied the absorption of a stationary gas bubble by a liquid. Their system was closed except for a capillary tube open to the atmosphere. When a bubble was introduced into the system the liquid in the capillary would rise. Thus they could determine the volume of the bubble as a function of time by recording the liquid level in the tube. Their bubble was held stationary

in an inverted funnel device by the downward flow of liquid. High speed photography was used to record the liquid level but no measurements were made on the bubble itself. A three-stage absorption cycle was detected during the life of a bubble. An initial high rate was the result of the creation of new surface. The next part of the cycle was a steady rate, probably due to "equilibrium conditions." Finally there was a slow rate because of the presence of inert gas and because of decreasing bubble size.

Later Harmerton and Garner (18) studied the absorption of a gas bubble rising in a liquid in a system open to the atmosphere only by a capillary tube. They determined the bubble size by recording the liquid level in the capillary. Motion pictures were made of the bubble in order to determine its rate of ascent. The change in hydrostatic head was taken into account. Their results indicate that there is no difference in the mechanism of absorption and desorption. Garner has been concerned in much of his investigative work with measuring and interpreting the effect of circulation in gas bubbles on absorption rate. In the above article it was deduced that circulation exists in the bubble although it was not detected experimentally. However, the authors noted that circulation should not influence the absorption rate since most of the resistance lies in the liquid film.

Garner and Lane (15) have recently conducted an

investigation on liquid drops suspended in a gas stream. A specially designed wind tunnel, which gave a uniform velocity distribution, was used. Motion pictures were used to determine the bubble size and also to detect internal circulation in the bubble. Here it was found that, indeed, internal circulation does increase the absorption rate above that due to molecular diffusion.

It has been learned by private communication that an investigation similar to the present one is now being conducted at the Carnegie Institute of Technology. No details have been learned, however.

CHAPTER III

THEORY

The theoretical problems involved in mass transfer in bubble systems may be divided into two classes. One is the diffusional mechanism involved when a molecule moves from the interior of a gas bubble across a gas-liquid interface and then into the continuous liquid phase where it may or may not react with some component in the liquid phase. Actually the theory is fairly well understood. Differential equations can be written which are thought to describe the process accurately; but for only the very simple cases can the equations be solved in closed form.

The second class of theoretical problems is related to the hydrodynamics of the absorption process. First of all is the question of the bubble's shape which determines the area available for mass transfer. As mass transfer takes place the bubble will of course decrease in size so that its shape may change from a mushroom configuration to an oblate spheroid and even to a sphere if the gas bubble becomes quite small. Actually the problem is not too difficult. It can be shown that except for large bubbles little error is introduced by assuming that the bubble is spherical even though it may be an oblate or a prolate spheroid. (See Appendix D, Section 3.) Thus it will be assumed from here on that the

geometry is spherical.

The hydrodynamic features of the liquid immediately next to the interface are rather difficult to describe. Indeed, here lies, in the author's opinion, the crux of the problem for mass transfer in bubble systems. Classically, one of two assumptions is made. The first is that a thin film of liquid surrounds the bubble such that transport of matter through the film is by diffusion only. Further it is assumed that the resistance to diffusion lies wholly within the film. The alternate assumption that is often made is that, on the contrary, no laminar film exists about the bubble at the interface. In fact the liquid velocity is assumed to vary continuously away from the interface into the liquid. For a bubble rising in a quiescent liquid the liquid velocity is everywhere zero and the gas in effect penetrates into an essentially infinite body of liquid and the concentration of the gas varies continuously away from the interface. In contrast, if a film exists about the bubble the gas concentration will vary continuously through the film until the film thickness is reached where there is a discontinuity as the concentration assumes the bulk concentration.

Whether a film exists or not is an important but difficult question to answer. Experimentally it may never be proved that a film exists. It would be very thin and hard to see even if its appearance should happen to be different from

the bulk of the liquid. It is not difficult to visualize the existence of a film when a liquid flows past a solid surface. It is thought that the liquid velocity at the surface is zero so that there must be a smooth transition from zero to bulk stream velocity. Thus there should be a region of fluid in which the flow is laminar no matter whether the bulk of the liquid is turbulent or not. At a gas-liquid interface it is not clear whether the velocity is zero. Indeed the assumption is probably invalid since gas is far from being a rigid surface. It is then likely that there is no layer of liquid which is distinctly different from the bulk of the liquid. Pursuing the matter further there are two cases to consider. One is the case of a bubble rising through a quiescent liquid. Now if a film exists it really means that the bubble is dragging some liquid along with it. On the other hand, the liquid may flow down past the bubble in such a fashion that the bubble remains essentially stationary. Under this circumstance the liquid velocity may or may not remain uniform up to the interface. If the fluid were in laminar flow then no laminar film would exist as such, and if there is no flow perpendicular to the interface, then the situation would be the same as for the bubble rising in quiescent liquid with no surrounding film. Actually the case of a stationary bubble is only of academic interest since in practical applications the bubble rises through the liquid. But it will be

shown later that for certain flow conditions the rising bubble and the stationary bubble are really one and the same. In the following discussion it will be assumed that the bubble is rising in a stationary liquid. A further simplification will be made by considering slab geometry, that is, unidirectional mass transfer. The results so obtained can be applied, however, to spherical geometry.

Consider a gas containing some component which is absorbed by the liquid and then undergoes a reaction with some component in the liquid phase. Thus in the liquid



where A will denote both the absorbed gas component and its concentration in the liquid and B denotes the absorbent component, as well as its concentration, in the liquid. The case of irreversible reaction will be of primary interest here and attention will be given to zero, first, and second order reactions.

Penetration Theory. The term "Penetration Theory" has been generally applied to the unsteady-state absorption of a gas by an infinite body of quiescent liquid. The situation is shown in Figure 2, where the concentration gradients of A, B, and the reaction products are plotted as a function of the distance from the interface into the liquid.

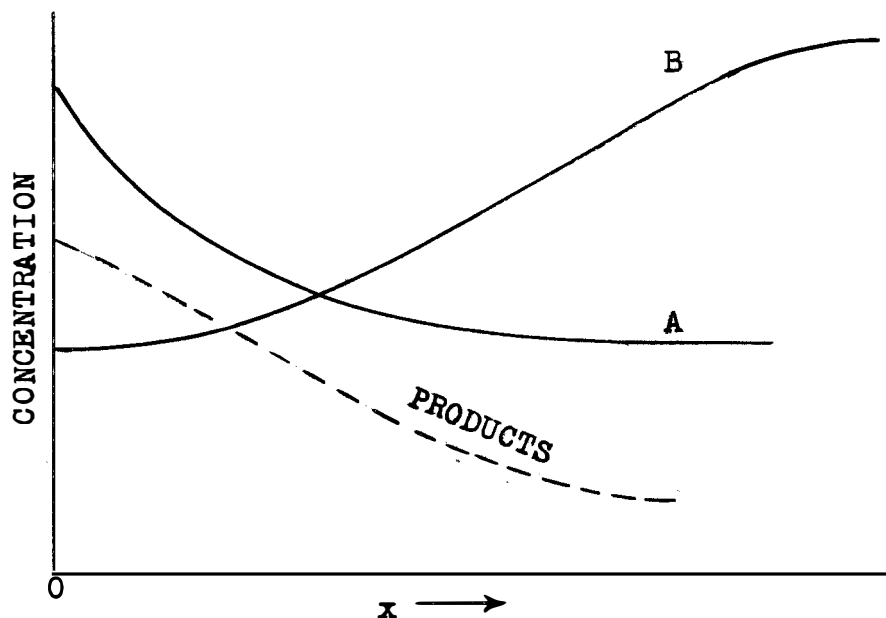


Figure 2. Concentration gradients, penetration theory.

The point $x = 0$ represents the gas-liquid interface. The product curve is dotted since it is not clear at this point how it appears. A material balance about a small element of liquid, dx units thick and with unit area parallel to the interface gives

$$\frac{\partial A}{\partial t} = D_A \frac{\partial^2 A}{\partial x^2} - k'_{AB} \quad (3.2)$$

$$\frac{\partial B}{\partial t} = D_B \frac{\partial^2 B}{\partial x^2} - k'_{AB} \quad (3.3)$$

where

t = time

x = distance

D_1 = diffusivity of component 1

k' = reaction rate constant for the reaction
 $A + B \longrightarrow \text{Products}$

The boundary and initial conditions are

$$A(0, t) = A_1, \quad \left. \frac{\partial B}{\partial x} \right]_{x=0} = 0 \quad (3.4)$$

and

$$A(x, 0) = A_0, \quad B(x, 0) = B_0 \quad (3.5)$$

As $x \longrightarrow \infty$ and for $t=0$, A and B will be the solutions of the differential equations

$$\frac{dA}{dt} = \frac{dB}{dt} = -k'AB \quad (3.6)$$

where, for $t = 0$

$$A = A_0, \quad B = B_0 \quad (3.7)$$

In equation 3.4 the A_1 is assumed to be a constant equilibrium value while $dB/dx = 0$ implies that the liquid B is non-volatile. The initial conditions in equation 3.5 state that at the start of the absorption process the liquid is homogeneous although the concentrations are not necessarily those of chemical equilibrium. Equations 3.2 and 3.3 were derived with the tacit assumption that Fick's First Law holds, namely, that the diffusion rate is proportional to a

concentration gradient; symbolically,

$$N_A \propto - \frac{\partial A}{\partial x} \quad (3.8)$$

where

N_A = rate of diffusion of A, mass/time-area

Solutions of equations 3.2 and 3.3 are known for only very special cases: pure physical absorption, i.e., $k^i = 0$ and equation 3.3 drops out; first order chemical reaction, again equation 3.3 does not appear and $k^i B = \text{new constant} = k$. A rather complete discussion of equations 3.2 and 3.3 may be found in Peaceman's Ph. D. dissertation (34).

It is felt by the author for reasons to be discussed later that the penetration theory as outlined above does not apply to the present investigation. Later it will be shown that a modified penetration theory might better describe the process of gas absorption.

Film theory. It was deduced at the beginning of this chapter that if the penetration theory is not applicable, then some type of laminar film exists near the interface. This particular problem has been investigated for some time. In 1924 Lewis and Whitman (25) proposed such a model for absorption processes and, in fact, the theory has come to be known as the Lewis-Whitman film theory. Figure 3 gives a

sketch of how the concentration gradients might look in a film thickness x_f . Note that a discontinuity occurs at x_f where the concentrations assume the bulk stream values A_0 and

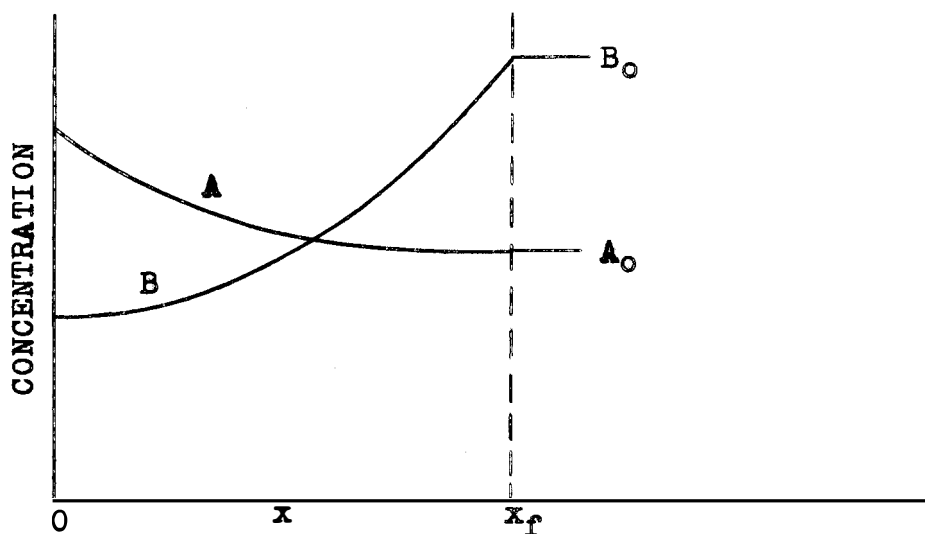


Figure 3. Concentration gradients, film theory.

B_0 . The usual assumptions applied to the film are:

1. The fluid within the film is in laminar flow parallel to the interface. Thus transport of matter through the film is by molecular diffusion only.
2. Steady-state conditions exist in the film.

A material balance about a slice dx gives

$$D_A \frac{d^2 A}{dx^2} - k'_{AB} = 0 \quad (3.9)$$

$$D_B \frac{d^2 B}{dx^2} - k'_{AB} = 0 \quad (3.10)$$

The boundary conditions are:

$$A(0) = A_1, \quad \left. \frac{dB}{dx} \right]_{x=0} = 0 \quad (3.11)$$

and

$$A(x_f) = A_0, \quad B(x_f) = B_0 \quad (3.12)$$

Actually, A_0 and B_0 may not remain constant since they should react according to equations 3.6 and 3.7, but the time for the absorption process is so short that little error is introduced by equation 3.12. Further justification of this point will be given later when the results are applied to the CO_2 -MEA system.

Only for the cases of zero, and first order chemical reaction and for no chemical reaction can solutions be obtained for equations 3.9 and 3.10. Peaceman (34) has discussed these solutions in detail.

Just as the penetration theory might be an idealized situation, so might the film theory. That a film exists is one thing, but whether steady-state exists in the film is quite another. Such a condition would depend first of all on how fast steady-state is obtained, and then on the life of the laminar film. The film will exist of course no longer than the bubble exists. As the film is first formed equations 3.2 and 3.3, with equations 3.4, 3.5, and 3.12 as the boundary conditions, would apply. Such a model could be called a

film-penetration model after Toor and Marchello (43) who used this concept in treating the case of pure physical absorption.

The life of the film may not be anywhere near the life of the bubble. It has been proposed by Higbie (19) and Danckwerts (6)(7)(8) that the film may be periodically replenished in whole or in part. Such an idea has been termed surface renewal model. In essence it is thought that the following happens: A small element of fluid comes to the gas liquid interface where it resides for some period of time during which it absorbs gas. It is then replaced by another element of fluid from the bulk of the liquid. The process is occurring simultaneously all over the interface and the residence times of all of the elements may be the same (Higbie distribution), or they may vary in some statistical or random fashion (Danckwerts distribution). The surface renewal model has particular application to packed towers where the liquid flows down from one piece of packing to the next. During the period when the fluid is between pieces the surface is replenished.

Extension of the idea to bubble geometry is not too far-fetched. As the bubble rises it is continually coming into contact with fresh liquid if no stable film exists. In fact, several investigators (22)(26)(30) have proposed that the residence time is of the order of the time that it takes the bubble to rise a height equal to its diameter. The

notion here is that the liquid element will start at the top of the bubble and travel around the circumference to the bottom where it leaves the bubble. The important point is that except for the case of a stationary laminar film in which steady-state exists, equations 3.2, 3.3, 3.4, 3.5, and 3.12 apply, no matter what the hydrodynamic conditions are at the interface. For example, in the surface renewal models one still has to talk about a small element of fluid of finite area parallel to the interface and of finite depth into the liquid. And while the element is at the surface it will absorb gas according to the above mentioned equations. All that is needed to be done is to solve the equations, which is a problem in diffusion and kinetics, and then determine the size and the residual time of each fluid element, which is largely a hydrodynamic problem. The reader will realize that the last sentence is a slight understatement. The problem is rather complex even if it is properly stated. (It will be pointed out later that there are other complications to consider.) However, in the following pages some solutions to the diffusional phases of the problem will be presented.

As was mentioned previously, Peaceman (34) as well as others (41)(38)(37) have presented solutions for the penetration theory in a semi-infinite liquid and for the steady-state absorption in a laminar film. Equations 3.2 and 3.3 as they

stand have not been solved analytically. Their non-linearity makes the solution somewhat intractable. Perry and Pigford (36) have obtained numerical solutions using a digital computer. Actually they started with a more complicated system of equations in that they took into account the reversibility of the reactions which introduced a third simultaneous partial differential equation. But they did consider the special case of non-reversible reaction as well as other special cases such as infinitely fast reactions. Their solutions were for a semi-infinite liquid. The author has found little work in the literature for the penetration model for a finite liquid depth. As a consequence, equations 3.2, 3.4, 3.5, and 3.7 for $x = x_f$ were solved for a finite liquid depth on the Oracle digital computer located at the Oak Ridge National Laboratories, Oak Ridge, Tennessee, and on a Donner 3100 Analogue Computer at the University of Tennessee Nuclear Engineering Department. Although few details were given in their article, Perry and Pigford's (36) solutions were probably very accurate. They probably used either some type of relaxation method or solved matrix equations. It was mentioned that the machine computing time was about 150 hours. The computer was the Ordrac at the Aberdeen Proving Grounds, Maryland, and this is a relatively slow machine.

Digital solutions of the diffusion equations. It was desired to obtain solutions of equations 3.2 and 3.3 in the form of concentration gradients at various times. The slopes of the A versus x curves at x=0 would give the absorption rate by Fick's First Law. Unfortunately, the last step was not programmed into the computer, and the slopes had to be determined by hand calculations. The overall objective was to determine what set of parameters such as D_A , D_B , x_f , etc., for a given MEA concentration would give an absorption rate comparable to that observed in the laboratory. Since in general the rate varies with time, it is necessary to talk about an average rate which means that the contact time must be known. The contact time can be determined for stagnant film models but not for surface renewal models.

In order to solve the equations the region of interest, namely, $x=0$ to $x=x_f$, must be divided into equal increments, say N in number. Thus the width of each increment will be x_f/N . Then equations 3.2 and 3.3 must be written in finite difference form. Before performing the operation it is convenient to make a substitution of variables. Thus let

$$\alpha = \frac{A}{A_1} \quad \beta = \frac{B}{B_0} \quad x = \frac{x}{x_f} \quad \gamma = \frac{D_A}{x_f^2} t \quad (3.13)$$

Then equations 3.2 and 3.3 become

$$\frac{\partial \alpha}{\partial \gamma} = \frac{\partial^2 \alpha}{\partial x^2} - K_1 \alpha \beta \quad (3.14)$$

$$\frac{\partial \beta}{\partial \tau} = K_2 \frac{\partial^2 \beta}{\partial X^2} - K_3 \alpha \beta \quad (3.15)$$

where

$$K_1 = \frac{k' B_0 x_f^2}{D_A}$$

$$K_2 = \frac{D_B}{D_A}$$

$$K_3 = \frac{k' A_1 x_f^2}{D_A} \quad (3.16)$$

The boundary conditions now are

$$\alpha(x, 0) = \frac{A_0}{A_1} \quad \beta(x, 0) = 1 \quad (3.17)$$

$$\alpha(0, \tau) = 1 \quad \beta(1, \tau) = 1 \quad (3.18)$$

$$\alpha(1, \tau) = \frac{A_0}{A_1} \quad \left(\frac{\partial \beta}{\partial X}\right)_{X=0} = 0 \quad (3.19)$$

In difference form equations 3.14 and 3.15 can be written as

$$\frac{\alpha_{m,n+1} - \alpha_{m,n}}{\Delta \tau} = \frac{\alpha_{m+1,n} - 2\alpha_{m,n} + \alpha_{m-1,n}}{(\Delta X)^2} - K_1 \alpha_{m,n} \beta_{m,n} \quad (3.20)$$

$$\frac{\beta_{m,n+1} - \beta_{m,n}}{\Delta \tau} = K_2 \frac{\beta_{m+1,n} - 2\beta_{m,n} + \beta_{m-1,n}}{(\Delta X)^2} - K_3 \alpha_{m,n} \beta_{m,n} \quad (3.21)$$

where the subscripts m and n refer to the lattice point along the X and γ axes respectively. Two such equations will be written for each lattice point in the $\gamma - X$ network. The procedure is simply to start with the values of α and β at $\gamma = 0$ and calculate new α 's and β 's for a new time at each X value by equations 3.20 and 3.21. Then the procedure is repeated over and over until it is decided to stop. The decision to stop is arbitrary, but the criterion that was used here is when the α and β values did not change significantly from one time to the next. Of course the error involved in the solution depends on the sizes of $\Delta \gamma$ and ΔX . The smaller $\Delta \gamma$ and ΔX are, the more accurate is the solution, but at the same time more computing time is required.

Equations 3.14 and 3.15 were solved for the particular case of absorption of carbon dioxide by aqueous monoethanolamine solutions, **MEA**. At low degrees of carbonation the reaction between CO_2 and **MEA** can be considered irreversible. Further, since the reaction rate is rather fast and since the reaction is irreversible at low degrees of carbonation, the initial CO_2 concentration may be assumed zero as well as the CO_2 concentration in the bulk of the liquid ($x > x_f$). In equations 3.2 and 3.3 A denotes CO_2 and its concentration; B denotes **MEA** and its concentration.

A total of eight cases was run on the computer. Table

I summarizes the various conditions used. Further details concerning the mechanics of the numerical integration are given in Appendix B.

TABLE I
CONDITIONS RUN ON THE DIGITAL COMPUTER

Case	$D_A \times 10^5$ (cm^2/sec)	$D_B \times 10^5$ (cm^2/sec)	X_f (cm)
I	2	0.586	3.16×10^{-4}
IV	2	.586	10^{-2}
V	1	.586	10^{-3}
VI	2	.25	10^{-3}
VII	1	.25	10^{-3}
VIII	5 outputs	1	10^{-3}
	9 outputs	1	10^{-3}

The reaction rate constant, k' , is $3.3 \times 10^6 \text{ cm}^3/\text{gm-mole-sec}$. The interfacial concentration of CO_2 , A_1 , was taken to be the solubility in pure water at 25°C and one atmosphere and is equal to $3.7 \times 10^{-5} \text{ gm-mole/cm}^3$ (9). All the cases are for $B_0 = 2 \times 10^{-3} \text{ gm-mole/cm}^3$. The mesh size was $\Delta X = 2^{-7}$ and $\Delta \tau = 2^{-16}$.

To check on the machine's accuracy the problem was solved for $k'=0$ for which case, pure diffusion, an analytical

solution can be obtained. The result of this computation, denoted as Case II, is given in Figure 4. Another accuracy check was made by running Case I again but with ΔT one-half the original value. This run was labeled Case III and the result is shown in Figure 5 along with the Case I results. Figures 4 and 5 indicate that the machine's results are accurate.

The diffusivities are for the respective components in water. The MEA diffusivity was found by the correlation proposed by Wilke (45). The CO₂ diffusivity was given by Emmert (9). It is not clear what is meant by the diffusivity in the present problem, especially so for MEA which ionizes. A more realistic viewpoint might be to consider CO₂ diffusing through a solution of MEA and water. Thus for 2 N MEA whose viscosity is 2 cp., D_A should be about 1×10^{-5} cm²/sec. Similarly, MEA can be thought of as diffusing through a MEA-water solution and thus $D_B = 0.25 \times 10^{-5}$ cm²/sec. Cases V, VI, VII, and VIII were run in an attempt to take the viscosity effect into account. Case VIII is different from the other three in that two values for D_B were employed. Here it is postulated that the products of the chemical reaction increase the viscosity, producing in turn a proportional decrease in MEA diffusivity. Thus D_B is decreased by approximately one-half after five outputs. By output is meant the readout from the machine after each 256 iterations. At each

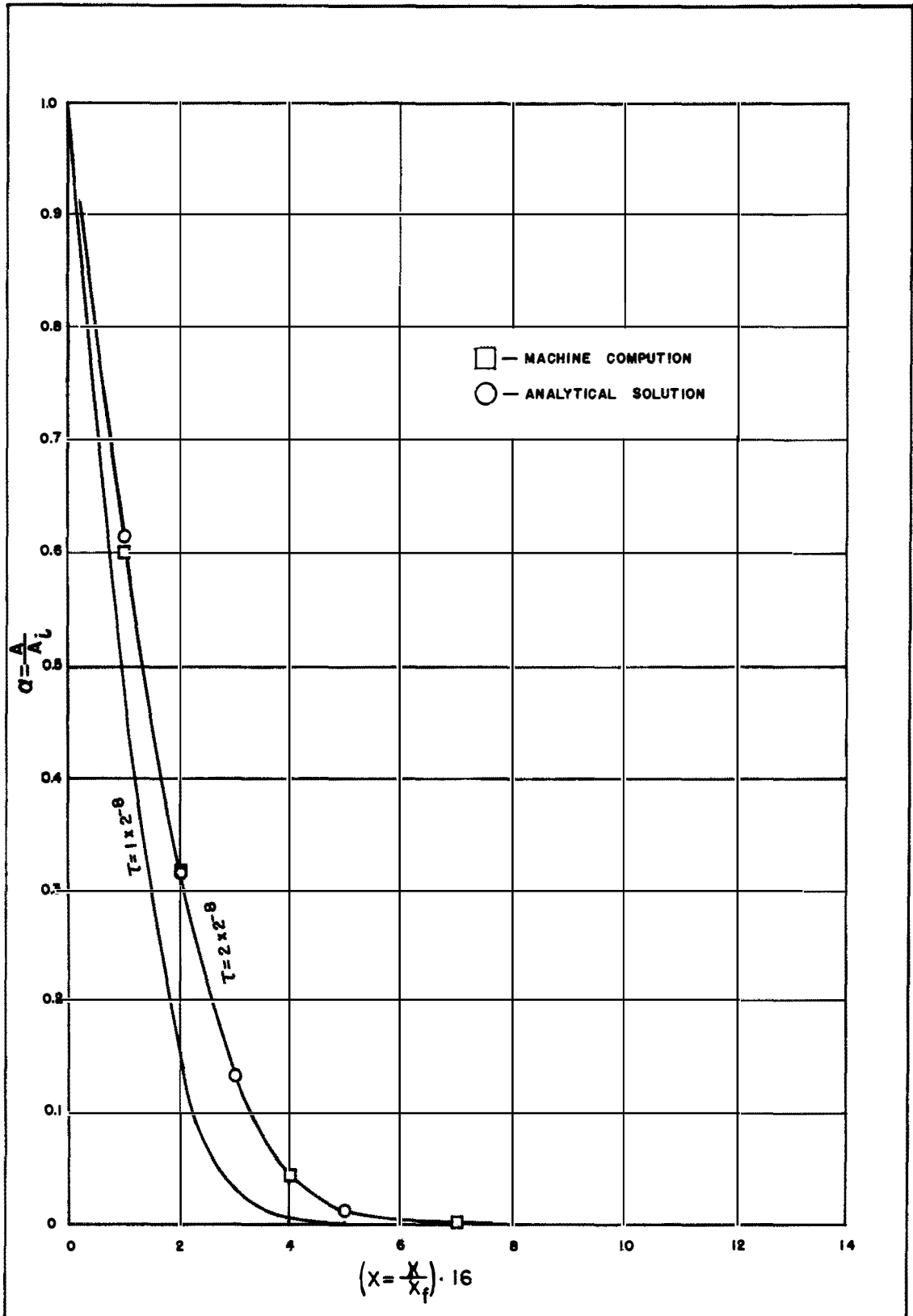


FIGURE 4 COMPUTER RESULTS, CASE II

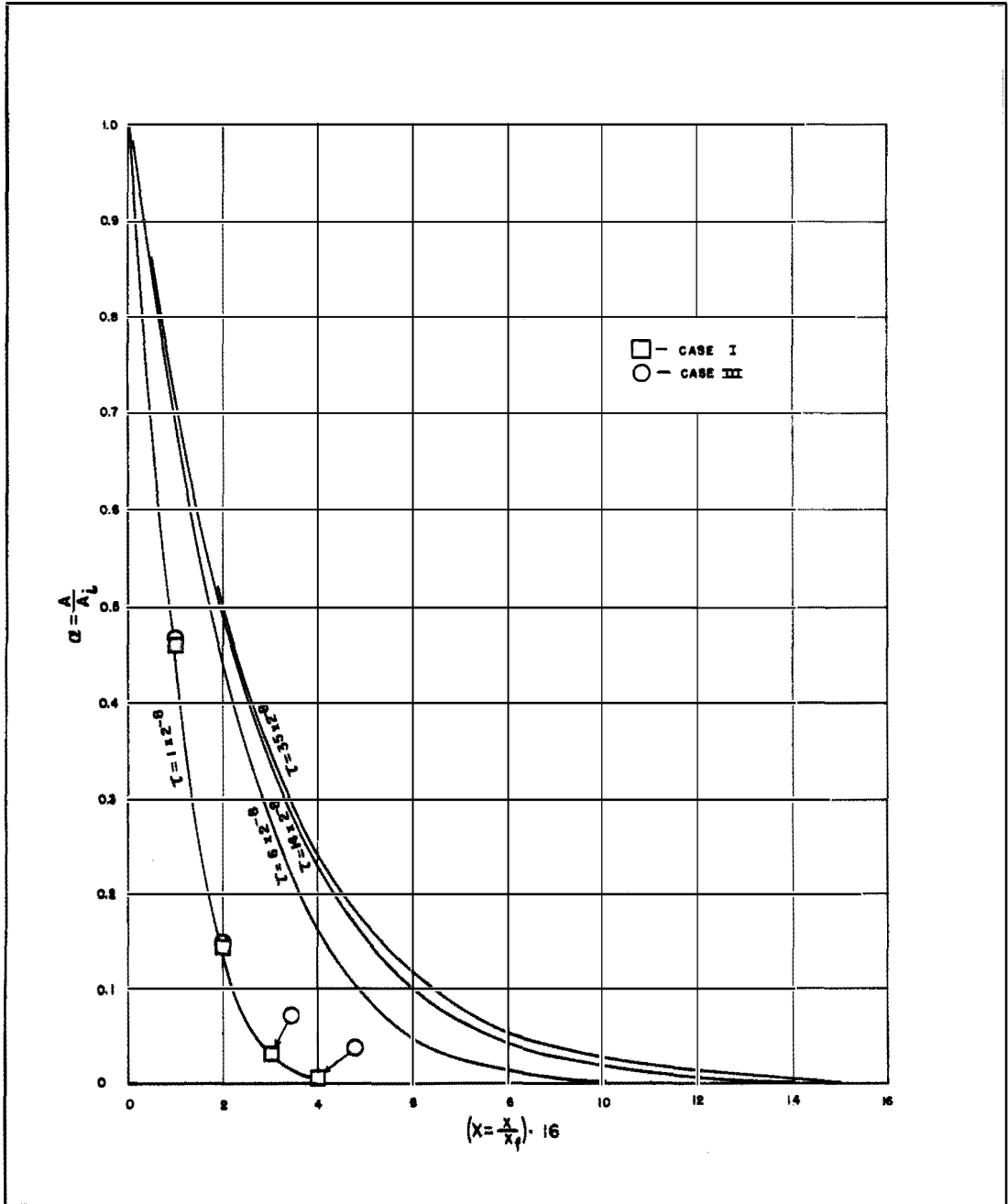


FIGURE 3 COMPUTER RESULTS, CASES I AND III

output the machine printed out results for α and β for $X=n/16$, $n=0,1,2,3,\dots,15$. Also for each output the results were plotted on an oscilloscope, known as a "curve plotter," for every X increment used in the computation. The plotted points were photographed. Appendix B gives details on the computation for γ at each output.

In no case was steady-state, as defined previously, ever reached, although it appears that for Case I (Figure 5) the α curves seem to be near a steady state value for low values of X . Some 2-1/2 hours of machine time were required to produce 35 outputs in Case I. Frequently, however, where the α values at some X appear to approach a constant value, the β values do not. In Case I which is for a rather thin film β decreases only slightly in each output, but the rate of decrease is not very different from 1 to the 35th output. On the other hand, in Case IV which is for a thick film, β decreases rapidly while α does not change fast. Figure 6 shows some of the β curves for Case IV. There is not enough α present to show on a plot of this scale in X . All of the above curves were plotted from the printed results.

As was mentioned previously, provision was not made in the computing program for the calculation of the absorption rates. It would have been easy to do, since

$$N_A = -D_A \left. \frac{\partial A}{\partial x} \right]_{x=0} \quad (3.22)$$

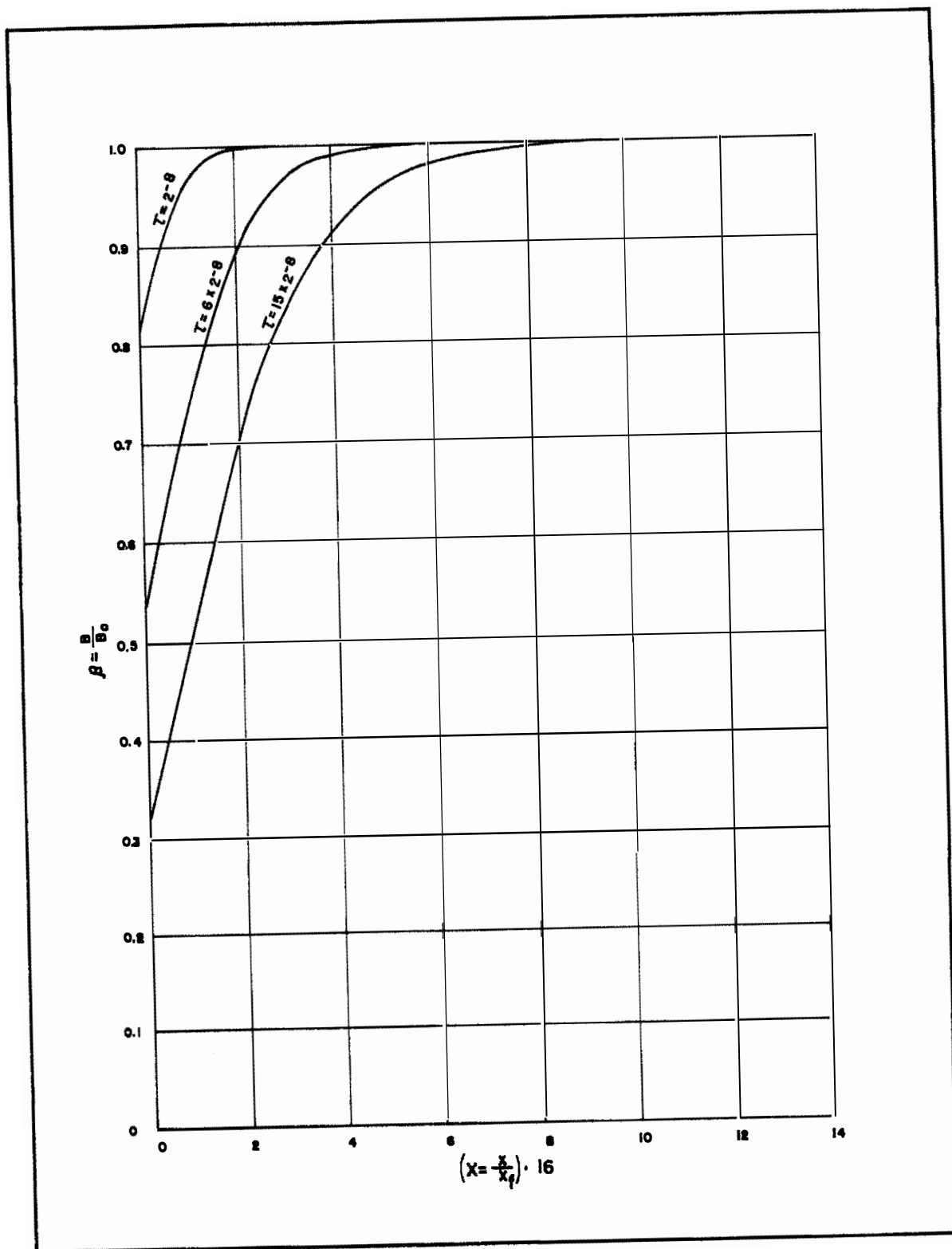


FIGURE 6 COMPUTER RESULTS, CASE IV

or in terms of α and X

$$N_A = \frac{-D_A A_1}{x_f} \left. \frac{d\alpha}{dX} \right|_{X=0} \quad (3.23)$$

The gradients were determined by measurements on the photographs of the curve plotter results. Values of α were determined with a scale and the slopes were determined by Newton's formula:

$$\left. \frac{d\alpha}{dX} \right|_{X=0} = \frac{1}{\Delta X} \left[\Delta\alpha_0 - \frac{1}{2} \Delta^2\alpha_0 + \frac{1}{3} \Delta^3\alpha_0 - \dots \right] \quad (3.24)$$

where $\Delta X = 2^{-7}$ and $\Delta\alpha_0 = \alpha_1 - \alpha_0$. The results are summarized in Figure 7 where a semi-log plot of absorption rate versus actual or real time is given. The log scale is based on two rather than the customary ten. Cases VII and VIII give rates closest to the experimental value.

The results given in Figure 7 indicate that a new definition of steady-state might be needed. Heretofore steady-state implied that the concentration gradients do not change with time. Such a condition was never met in the computer work discussed here. Nevertheless, in Cases V, VI, VII, and VIII, the absorption rates are essentially constant. It appears, then, that the concentration of A at the gas-liquid interface rapidly assumes a steady-state value. This leads immediately to the conclusion that the absorption process is characterized by a surface phenomenon and thus

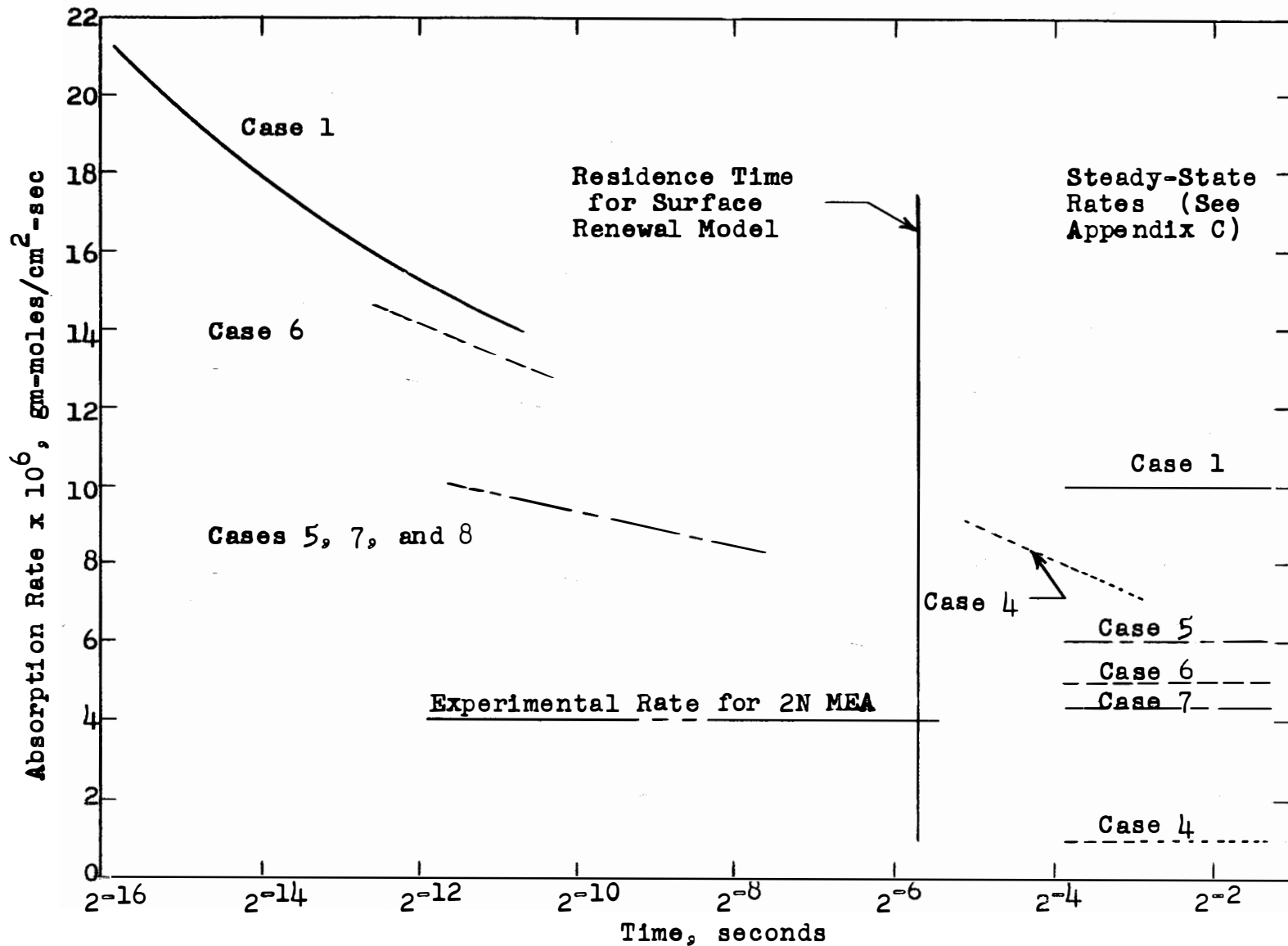


Figure 7. Absorption rates calculated from digital computer results.

the absorption rate should be independent of film thickness. Further, since the time to reach steady-state is much less than the renewal time, the question of which renewal theory is applicable becomes a moot point.

These computer results do point out some interesting facts with regard to existing theories on absorption accompanied by chemical reaction. As has been noted many times previously in the text, the solution to equations 3.2 and 3.3 are at the present intractable. Recourse must then be made to approximate solutions. One of the oldest such solutions is that developed by Hatta (see reference (41), page 321). Hatta assumes the existence of a laminar film in which a gas is absorbed at steady-state conditions. Within the film some component reacts with the gas irreversibly and instantaneously. In other words the gas and the liquid reactant cannot coexist so that there must be a region within the film in which only the gas reactant exists and another region in which the liquid reactant alone exists. The dividing line between the two regions is the reaction zone, or more properly a surface. Its position will be determined by the diffusivities of the gas and the liquid reactant. Using simple algebra one can show for the above model that

$$N_A = \frac{A_1 + (D_B/D_A)B_0}{x_f/D_A} \quad (3.25)$$

where B_0 is the concentration of the liquid reactant in the bulk liquid. Equation 3.25 holds only if the gas is pure in A. The concentration of the gas at the gas-liquid interface (A_1) is an equilibrium concentration corresponding to the gas pressure and is assumed to be given by Henry's law

$$A_1 = \frac{p}{H} \quad (3.26)$$

where p is the gas pressure and H is Henry's Law Constant. The distance of the reaction zone from the gas interface will be less than the laminar film thickness but it may change as the laminar film thickness changes. Thus it can be concluded that the absorption rate will be influenced in part by the hydrodynamic features of the system which is certainly obvious by the appearance of x_f in equation 3.25. The digital computer results indicate that, first of all, some time is required to reach steady-state in the film; secondly, that no reaction zone exists as such since α never goes to zero; and, thirdly, the conclusion as to whether the reaction between CO_2 and MEA can be considered instantaneous depends on the film thickness. For Case I (thin film) β decreases slowly and α increases rather fast at any X , while in Case IV (thick film) β decreases much faster and α increases slowly.

Another semi-theoretical treatment of equations 3.2

and 3.3 was given by Atadan (1) who, in his investigation of the solubility of carbon dioxide in monoethanolamine solutions, made some absorption rate measurements. He concluded that there existed a reaction zone similar to that in Hatta's theory, and he denoted its thickness by $Erzt$. He concluded that $Erzt$ may be something less than x_f but that it was not a function of the hydrodynamics of the liquid. As a consequence the absorption rate is not a function of the hydrodynamics, that is, the degree of agitation in the liquid, as long as the surface area remains the same. A subsequent investigation (31) has verified these conclusions. Atadan did not assume that the CO_2 -MEA reaction was instantaneous but only that it was irreversible.

Sherwood and Pigford (41, page 337) give a solution for unsteady-state absorption of a gas accompanied by a second order instantaneous, irreversible reaction in a stagnant liquid. The reaction zone starts at the interface and moves into the liquid. They found that

$$N_A = \frac{A_1}{\operatorname{erf}(\alpha/D_A)^{\frac{1}{2}}} \left(\frac{D_A}{\pi t}\right)^{\frac{1}{2}} \quad (3.27)$$

where α is the solution of the equation

$$\frac{B}{A_1 r} \exp\left[\left(\frac{\alpha}{D_A}\right)(1-r)\right] \operatorname{erf}\left(\frac{\alpha}{D_A}\right)^{\frac{1}{2}} + \operatorname{erf}\left(\frac{r\alpha}{D_A}\right)^{\frac{1}{2}} = 1 \quad (3.28)$$

and

$$\gamma = \frac{D_A}{D_B} \quad (3.29)$$

A significant point concerning equation 3.27 is that at zero time the rate is infinite, a result which comes up frequently in the treatment of the penetration theory.

Further investigation of equations 3.14 and 3.15 was made with the aid of an analogue computer. Three cases were considered: unsteady-state absorption with first and second order chemical reactions and steady-state absorption with second order reaction. The investigation was moderately successful. Details of the analogue and digital computer work are given in Appendices B and C.

Equations 3.2 and 3.3 for a finite film can be solved for zero and first order chemical reaction. For the first order case one has

$$D_A \frac{\partial^2 A}{\partial x^2} = \frac{\partial A}{\partial t} + kA \quad (3.30)$$

with the boundary conditions

$$A(0, t) = A_1 \quad (3.31)$$

$$A(x, 0) = A_0 \quad (3.32)$$

$$A(x_f, t) = A_0 \quad (3.33)$$

Solutions to equation 3.30 are given in Appendix A. One can

find a solution to 3.30 from Carslaw and Jaeger (3). But it appears that the solution given there does not fit the boundary or the initial conditions. For that reason the details of the solution are given in the Appendix. For zero order reaction the k_A term in equation 3.30 becomes a constant, k'' for example.

Correlation of experimental data. All of the theoretical developments presented in this chapter and in the appendix use a point absorption rate in units of mass per time per area. In some cases rates will be a function of a time. For bubble geometry then the rate is integrated over the surface of the bubble and with respect to time in order to obtain an equation with which to correlate experimental data.

Define the gross rate as

$$Q = N_A \cdot 4 \pi r^2 \quad (3.34)$$

where

N_A = specific absorption rate, moles/time-area

r = radius of the bubble

It will be assumed in this discussion that the bubble is spherical. It is shown in Appendix D that the error introduced by the assumption is small. Now

$$Q = - \frac{dn}{dt} \quad (3.35)$$

where

n = moles of gas in bubble

If it is assumed that the gas is ideal, then

$$n = \frac{PV}{R\theta'} \quad (3.36)$$

where

P = pressure = constant

V = bubble volume = $\frac{4}{3} \pi r^3$

θ' = temperature = constant

R = Gas Law constant

Since

$$r^3 = 3V/4\pi$$

and

$$V = nR\theta'/P$$

then

$$r^2 = \left(\frac{3 nR\theta'}{P 4\pi} \right)^{2/3}$$

Therefore combining equations 3.34, 3.35, and 3.36, one obtains

$$\frac{dn}{dt} = - N_A 4\pi \left(\frac{3 nR\theta'}{P 4\pi} \right)^{2/3} \quad (3.37)$$

Separation of variables and integration yields

$$(n^{1/3} - n_0^{1/3}) = - \left(\frac{4\pi}{3}\right)^{1/3} \left(\frac{R\theta^1}{P}\right)^{2/3} \int_0^t N_A(t) dt \quad (3.38)$$

where the functional notation on N_A is used to emphasize that it may be a function of time. The initial number of moles is n_0 . In Chapter V, which contains the presentation of the results, equation 3.38 is discussed in the light of N_A for the various absorption models.

Addendum. It was implied previously that equations 3.2 and 3.3 with the boundary conditions 3.4, 3.5, and 3.6 may not be an accurate description of the absorption process. One item not considered was the chemical reaction products. As they are formed in the film they will diffuse into the liquid bulk. The effect of this on the diffusion of CO_2 and MEA is not understood. Although it will not be generally true for all gas absorption systems, the products of the reaction of CO_2 with MEA are more dense than the reactants. Consequently, the resultant density gradients will induce liquid bulk flow perpendicular to the interface which in turn will affect the net diffusive flow of CO_2 and MEA. Therefore although the liquid film was assumed stagnant to insure that mass transport would be by molecular diffusivity only, there are still the density induced currents to consider, an effect which seems to be inherent in the process. No doubt the currents serve to enhance the absorption process. And the

phenomenon is similar to the frequently used concept of eddy diffusivity for mass or heat transfer into turbulent liquids. To account for the density effect one only has to modify equations 3.2 and 3.3 to read

$$\frac{\partial A}{\partial t} = D_A \frac{\partial^2 A}{\partial x^2} + v \frac{\partial A}{\partial x} - k'_{AB} \quad (3.39)$$

$$\frac{\partial B}{\partial t} = D_B \frac{\partial^2 B}{\partial x^2} + v \frac{\partial B}{\partial x} - k'_{AB} \quad (3.40)$$

where

v = velocity of fluid perpendicular to
interface

It should be obvious that the equations have become considerably more complicated. It is difficult to attach any quantitative meaning to v . Its exact expression would obviously involve knowledge of the hydrodynamics of a heavy fluid moving through a light fluid.

Another complication not considered up to now is the nature of the stable film that may exist about a bubble. As the bubble becomes smaller, one of two things must happen. One is that the film thickness may remain the same in which case the actual volume of the film must decrease. If this happens, there will be some liquid motion associated with the removal of the excess liquid. The author is not sure how to postulate a mechanism by which this may be done and

he is not sure whether the liquid motion will affect the absorption rate. The other possibility is that the film's volume remains intact in which case the film thickness would have to increase. Intuitively the author feels that the latter is most unlikely. It is easy to conceive of a situation where the film's thickness would be almost as much as the bubble's radius.

For a solid sphere Tomotika (see reference (23)) has shown that

$$\frac{V x_f^2}{r \nu} = \text{constant} \quad (3.41)$$

where

V = velocity of fluid at infinity flowing
past the bubble

x_f = film thickness about sphere

r = radius of sphere

ν = kinematic viscosity of fluid

If a gas bubble is not too large it might be assumed to behave similarly to a solid sphere (this assumption is subject to debate). In the present work the fluid flows past a gas bubble so that the bubble remains stationary. But as the bubble size diminishes it migrates to a region of lower fluid velocity. So as r decreases so does V and it is quite possible that the ratio V/r is a constant. The

conclusion is then reached that x_f will remain constant.

There has been considerable speculation concerning the interfacial gas concentration, A_1 . It was thought for some time that A_1 would be something less than the equilibrium value. Such a conjecture leads immediately to the concept of an interfacial resistance to mass transfer. It would seem that the interfacial resistance would be connected somehow to the interfacial tension. There is some disagreement among the various investigators on this point.

Nijsing, et al (32), state that there is no interfacial resistance. Raimondi and Toor (39) and Scriven and Pigford (40) conclude that there is no interfacial resistance per se. If there is resistance, it is because of the collection of impurities on the gas-liquid interface. A source of these impurities could well be the products of the reaction between the gas and the liquid. Chiang and Toor (4) also state there is no interfacial resistance.

On the other hand, Epstein (10) from theoretical consideration concludes that surface tension will influence mass transfer. Garner (13) says that interfacial tension "seems" to be important. But Kishenevskii (21) points out that Pozin (no reference) showed that surface tension does not affect absorption. Finally Lindland and Terjisen (27) remark that interfacial resistance has no connection with interfacial tension in liquid-liquid extraction.

An investigation by McKee (29) was recently made to see whether a change in surface tension with time could be detected when MEA absorbs CO_2 . A DuNouy Ring Tensiometer of fairly high sensitivity was used. No change could be observed. Atadan (1) determined that for total pressures near one atmosphere the absorption rate is independent of CO_2 partial pressure. This was later confirmed by Groves and Hawkins (17).

It will be concluded from the foregoing that for the CO_2 -MEA system equilibrium exists at the interface, but that A_1 may be less than the equilibrium value for pure water. There will be other species present at interface which will decrease the water concentration. As a consequence less CO_2 can be absorbed. In the present study, however, A_1 will be taken as the equilibrium concentration of CO_2 in pure water and it will be assumed that A_1 remains constant.

CHAPTER IV

EXPERIMENTAL APPARATUS AND PROCEDURE

Experimental apparatus. The experimental apparatus used in this investigation was rather simple. A flow diagram of the setup is shown in Figure 8. As can be seen the apparatus consisted of the Plexiglas absorption cell, movie camera, lens, photoflood, electric timer, powerstat, pump, manometer, rotameter, cylinder of carbon dioxide, and connecting tubing. The pump was an Eastern Industries Model D-H centrifugal pump of stainless steel (type #316) construction. It produced a head of about 17 feet of water at a flow rate of one gallon per minute.

All connecting tubing in contact with MEA had to be either glass, stainless steel or Tygon tubing. The rotameter's float was of stainless steel, also. The carbon dioxide valve located just below the absorption cell comprised a glass stopcock while the MEA valve, just downstream from the rotameter, comprised a stainless steel needle valve which allowed close control on the flow rate. The bubble generating tube was a glass capillary tube of 0.041-inch inside diameter. The MEA reservoir was a ten-liter glass jug. In the line between the rotameter and the absorption cell was placed a small wad of glass wool which effectively

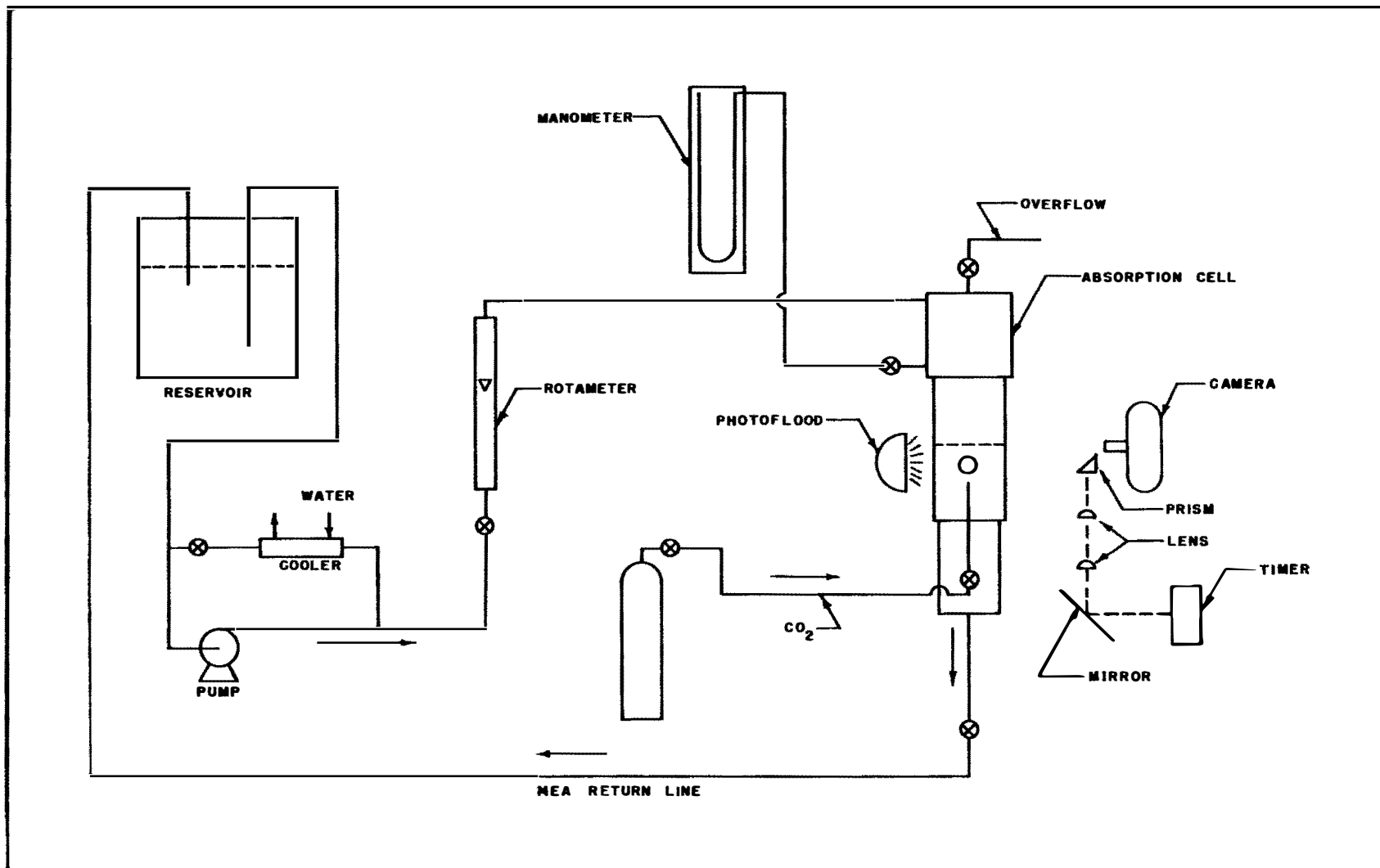


FIGURE 8. SCHEMATIC DIAGRAM OF EXPERIMENTAL APPARATUS

removed any dirt or lint in the liquid.

Noted on the diagram is a by-pass line running from the exhaust to the intake of the pump. This was necessary since the pump produced too much head for the fittings used. The fittings generally consisted of Tygon tubing slipped over glass or steel tubes and the connections were made tight with hose clamps. Such arrangements are not the most satisfactory as far as leaks are concerned, but they were expedient and economical. Certainly the best procedure would have been to use all stainless tubing, but this is rather expensive and further it would make the whole apparatus rigid. It then would become difficult to move the various components around, which was frequently necessary. A heat exchanger was installed on the by-pass line in order to remove the frictional heat generated by the pump. During the summer when the cooling water became warmer it was necessary to immerse the reservoir in an ice bath.

A detailed diagram of the reaction cell is given in Figure 9. The theoretical aspects of the cell have already been discussed in Chapter I. The cell originally consisted of only the lower rectangular portion, but it was felt that better flow characteristics could be obtained if it were made longer. Therefore the upper cylindrical portion was added. The cylindrical portion served as a calming section, and it worked very well.

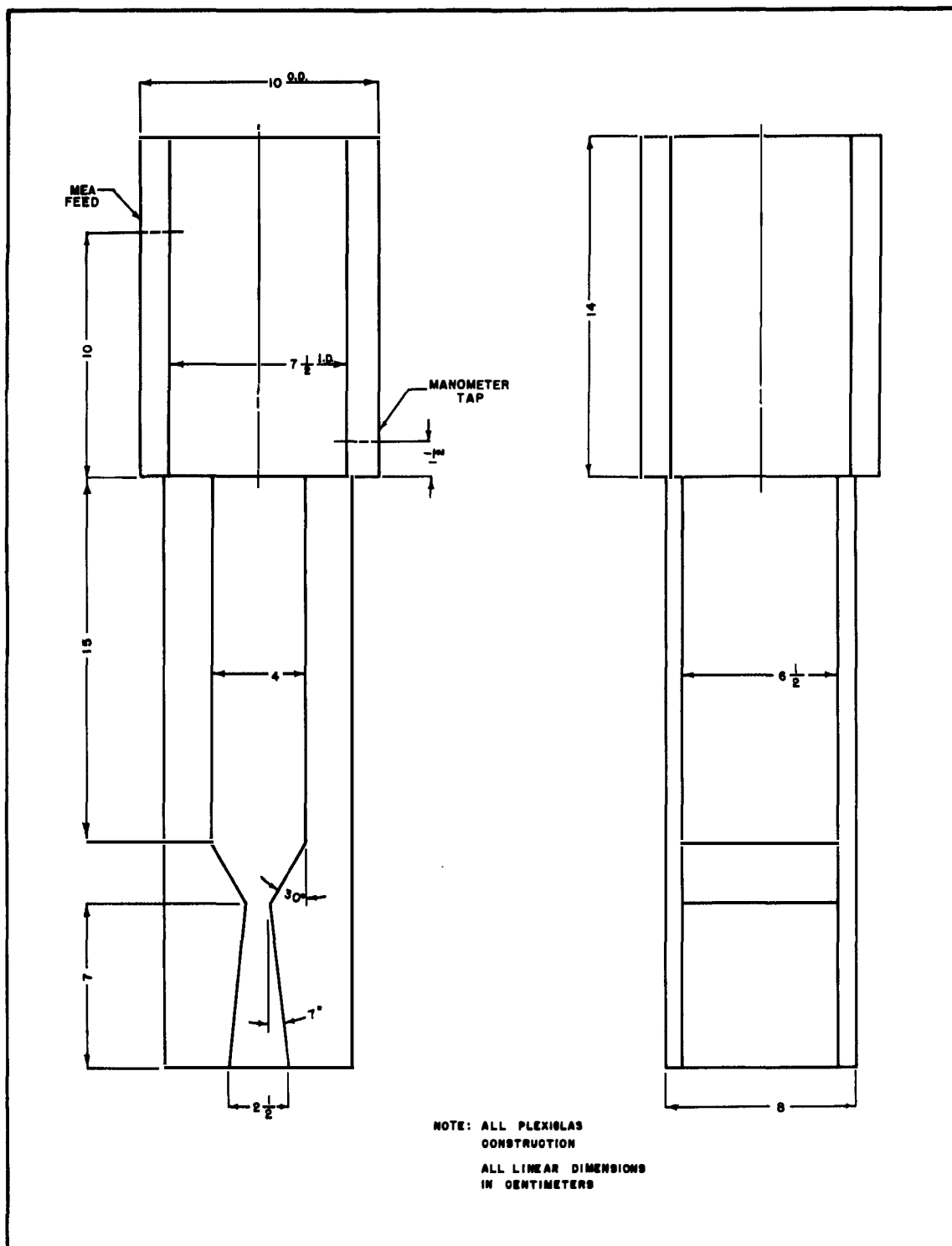


FIGURE 9 DIAGRAM OF ABSORPTION CELL

The lower portion of the cell was cut out on a milling machine and thus the converging and diverging sections were very accurately formed. It was not necessary that the converging angle be exactly 30° nor the diverging angle be 7° but it was necessary that the cell be symmetrical. Therefore a single slab of Plexiglas was milled to the desired contour and then it was cut in half to form the two sides of the cell. The front and back of the cell, that is, the sides through which the movies were taken, were 1/4-inch slabs of clear Plexiglas. The edges at the throat and at the beginning of the converging section were rather sharp. Perhaps better performance could have been obtained if the edges at the throat had been rounded off to some extent. Even though flow was laminar the sharp edges may have introduced some local turbulence.

The optical system employed warrants a few comments. The lens used was chosen by trial and error. The prism used was a totally reflecting right angle prism. The prism and the lens were not of especially high optical quality. Not shown on the flow diagram is a grid located behind the bubble. The grid was simply a tracing of a sheet of graph paper in black India ink. A six-hour photoflood was projected onto the grid and the light was reflected through a prism and two lenses into the lens of the camera. Adjustment of the lenses would make the image of the grid fall onto the plane of the

bubble. The net effect was that the bubble was photographed against the grid backdrop.

The electric timer was graduated in one-hundredths of a second and time could be estimated to the nearest one-two hundredth of a second.

The movie camera was a 16 mm Traid-70 Camera, a modified Bell and Howell unit. The camera was driven by a variable speed electric motor which was connected to a power-stat. The motor was usually run at 90 per cent of line voltage (110 A.C.). The film speed was 1.8 feet per second or 72 frames per second. The camera was equipped with a 1-inch f/1.9 Taylor-Hobson lens and could focus to a minimum distance of 2-1/2 feet. However, by placing a spacer between the lens and shutter it could be focused down to distances of six inches and at the same time give greater magnification. The film used was 16 mm Kodak tri-X Negative in 100-foot rolls.

Experimental procedure. The test solution was prepared using distilled water and 99 per cent pure monoethanolamine prepared by the Olin-Mathieson Chemical Company. The camera was then set up on a tripod in front of the cell. A reflex attachment was available which allowed focusing through the lens but it had to be removed from the camera before the film was loaded. Thus it was necessary to focus

the camera carefully and then lock the camera in place for no adjustments could be made once the film was loaded. The camera was focused with the absorption cell filled with the MEA solution. Generally the lens was set at $f/4.0$. A larger lens opening overexposed the film and did not produce as sharp an image. No improvement could be detected on stopping the lens down below $f/4.0$. After the camera was set up and loaded, the pump was started and the solution circulated through the apparatus. A thermometer was placed in the reservoir and when it indicated that the solution was at the desired temperature the test was started. First, a couple of test bubbles were generated to see whether the MEA flow rate was correctly set. The MEA flow was set so that the bubble would leave the capillary tube, rise up slowly toward the throat and remain "suspended" at the throat for a few moments. The bubble would be on the verge of escaping past the throat when it would start to move back down the cell in the direction of flow because of its decreasing size. Two or three such bubbles were generated to make sure that experimental conditions were satisfactory. The clock and lights were turned on and another bubble generated. Just before it left the capillary tube the camera was started and left running until the bubble was completely absorbed or passed from the field of view. The life of a bubble was on the order of one second. Occasionally a bubble escaped up

the cell even though several test bubbles indicated that the MEA flow was properly set.

The photographing of the life on one bubble constituted a "take," but occasionally two or more bubbles were photographed on one take. The bubbles would still be generated individually, however. The take was recorded by a small number placed on the mirror reflecting the clock face. The number appeared on the film in the center of the clock face.

For each take the following information was recorded: rotameter reading, manometer reading, MEA temperature, lens setting, barometer reading, and powerstat reading. Also, a 100-ml sample of the MEA was taken. Of the above readings the only important ones are the manometer, barometer, and MEA thermometer readings. Although the rotameter was calibrated with water its main use was to help in adjusting the MEA flow. To increase the CO₂ concentration carbon dioxide was bubbled through the MEA in the absorption cell while the MEA circulated through the apparatus. As the carbon dioxide reacts with the MEA heat is liberated so that it was necessary to cool the solution.

After a suitable period of bubbling the carbon dioxide was cut off and when the MEA had cooled down to the desired temperature another take was made. The procedure was repeated until all the film was used, generally a little over 100 feet.

Only one initial MEA concentration was used for each reel of film.

Analysis of experimental data. The film was developed by the author as per instructions given by the manufacturer. A 100-foot stainless steel reel and shallow stainless steel pans were used for developing. Film agitation was by hand. The film was dried in a closed room on a creel. A Bell and Howell 16 mm movie projector was used for examining the film. The projector could be stopped on any frame so that it was possible to analyze the film frame by frame. A typical strip of film is shown in Figure 10. At first it was thought that the grid might be used to measure the size of the bubbles, but it was found easier to use a pair of drafting dividers and scale. The measurements taken from the film for various recorded times were the bubble's horizontal diameter, i.e., the diameter perpendicular to the direction of flow, and the vertical diameter parallel to the direction of flow. Usually measurements were made from frames corresponding to time increments of .05 or .10 of a second.

The 100-ml solution sample drawn off at each take was analyzed for carbon dioxide and MEA concentration. The MEA analysis was obtained by titration with half normal sulfuric acid using methyl orange as indicator. This procedure gives the total amine concentration, reacted and unreacted. The



Time = .039 sec.



Time = 0.058 sec.



Time = 0.076 sec.



Time = 0.093 sec.



Time = 0.107 sec.



Time = 0.114 sec.

Figure 10. Typical frames from a single take.

carbon dioxide analysis was obtained by the absorption of carbon dioxide, evolved upon the addition of concentrated sulfuric acid, in a tared bottle containing ascarite.

All of the above information and original data for this investigation are recorded in Original Record of Research Notebooks, pages 23751-23800, pages 10551-10600, and pages 15628-15650, on file in the Department of Chemical Engineering, University of Tennessee.

CHAPTER V

EXPERIMENTAL RESULTS

The masses of the bubbles were computed assuming that the CO₂ gas was ideal and that the bubbles were oblate spheroids. The details of the calculations involved are given in Appendix E. A typical plot of bubble mass versus time is given in Figure 11. Zero time is somewhat arbitrary in that time was measured from the time of the first measurements of the bubble's dimensions. As the bubble breaks away from the orifice there is a short period during which the bubble's configuration oscillates between oblate and prolate spheroids. The motion is soon damped out and the bubble takes an oblate spheroidal shape with the long axis horizontal (perpendicular to the MEA flow). At this point measurements were begun. The mass versus time data are recorded in Appendix E.

Though it was hoped that the bubble would remain stationary while it was being absorbed, nevertheless there was some movement. As the bubble became smaller it moved down the column into a lower velocity region. However the experimental setup could be adjusted so that the bubble remained in the field of view of the camera until it became of negligible size. Simultaneously with the above motion the bubble oscillated toward and away from the camera. Consequently the apparent size of the bubble would fluctuate also. In

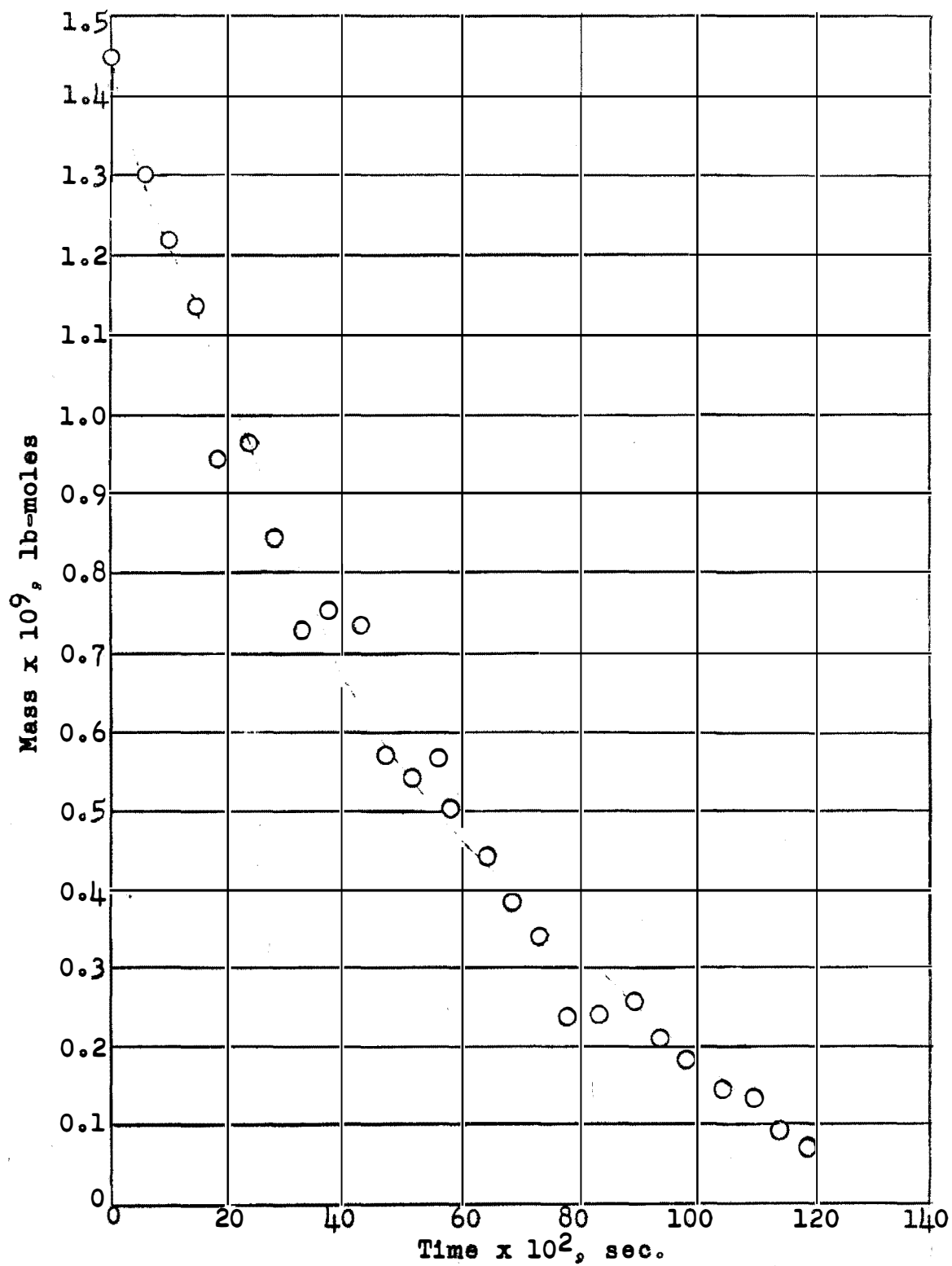


Figure 11. Typical mass-time plot, Reel 3.

Appendix D it is shown that the resulting error of this motion is on the order of 2 per cent or less. Also discussed there is the error inherent in the optical characteristics of a lens, and this error proves to be quite small. The scatter in the data shown in Figure 11 is probably the result of either the above errors or the fact that the bubble's shape is not always that of an oblate spheroid.

In Figure 12 is shown a plot of mass to the one-third power versus time. The plot was made on the basis of equation 3.38,

$$(n^{1/3} - n_0^{1/3}) = - \left(\frac{4\gamma}{3}\right)^{1/3} \left(\frac{R_0}{P}\right)^{2/3} \int_0^T N_A(t) dt \quad (3.38)$$

which, if it is assumed that N_A is not a function of time, takes the general form

$$n^{1/3} = a + bT \quad (5.1)$$

where a and b are parameters that depend on P , T , and N_A . All the experimental data were correlated by equation 5.1 using the method of least squares. In every case a straight line was obtained but in some instances the data were more scattered than in others. In general it was found that less scatter was obtained at higher MEA normalities. The viscosity increases with MEA concentration so that with an increase in MEA concentration lower MEA velocities were

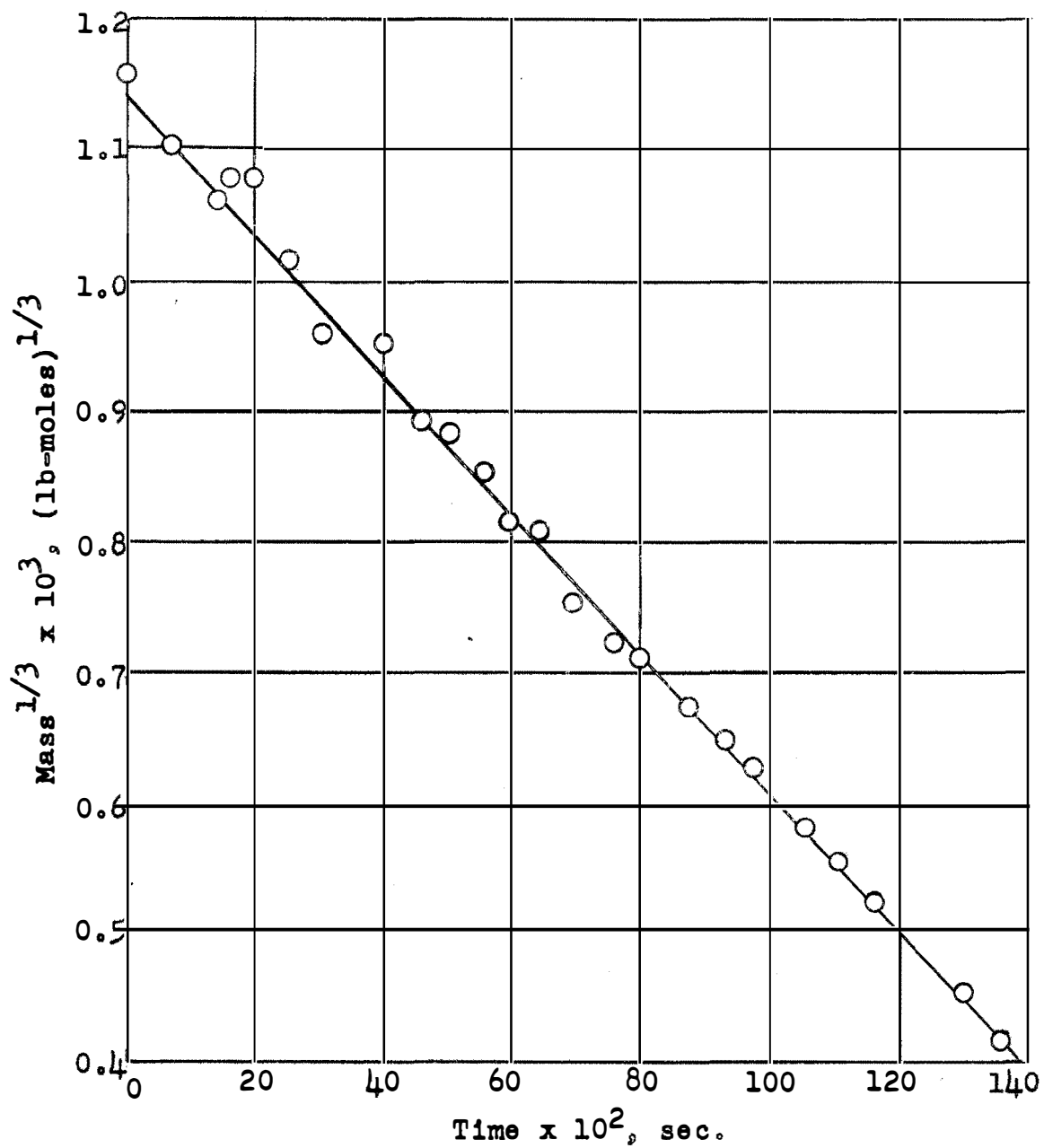


Figure 12. Typical correlation of data, Reel 6.

necessary to hold the bubble stationary. Therefore, at high MEA concentration the flow was more smooth and the bubbles did not oscillate as much. In Figure 13 is presented another plot of $n^{1/3}$ versus T . Figures 12 and 13 represent, respectively, the best and worst scatter of data obtained. It was found that the MEA flow for optimum results was that which allowed the bubble, on first forming, to rise slowly up to the throat. There it would remain motionless for a moment, and then because of its decreasing size would start back down the channel. During this period the bubble would exhibit little horizontal motion. If the MEA flow were too high the bubble would oscillate greatly while on the other hand if the flow were too low the bubble would escape up past the throat. The optimum MEA flow was rather critical, and in order to determine it several test bubbles were first generated before any pictures were taken. In spite of precautions taken, quite a few bad takes were obtained. One of the most frequent troubles was that of the bubble escaping up past the throat. The only explanation for this seems to be a small decrease in the rather critical MEA flow as a result of a decrease in pump speed. The pump speed probably decreased during a take because of a drop in line voltage which was most likely due to operation of the photoflood lamps and camera motor.

The fact that the data can be correlated by equation

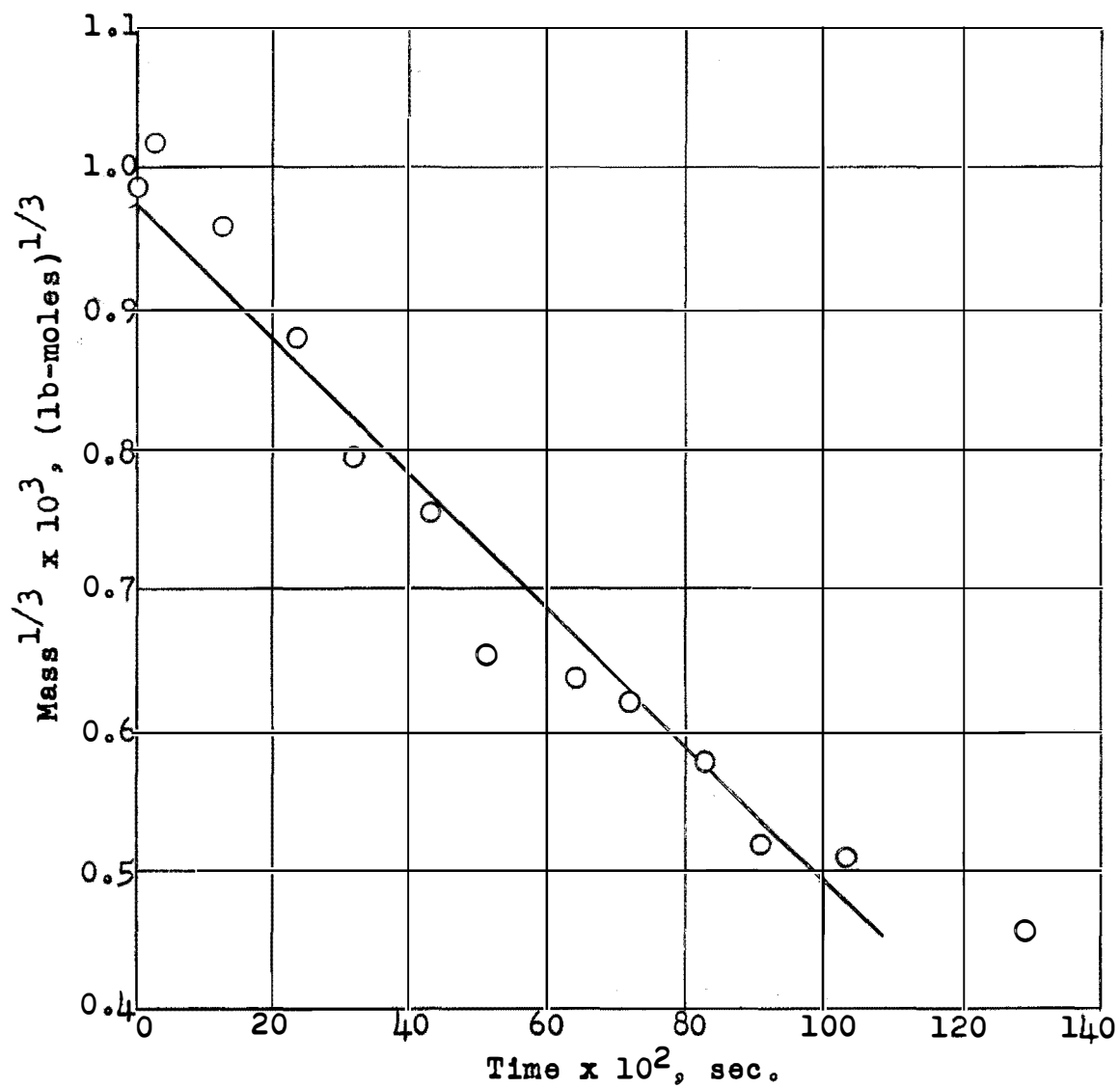


Figure 13. Typical correlation of data, Reel 3.

5.1 does not reveal anything about the absorption mechanism. At this point all one can say is that the absorption rate is constant during the life of a bubble. But such an observation can fit any one of a number of theories. One of the obvious possibilities is the steady-state laminar film model (Lewis-Whitman two film theory). But on the other hand a surface renewal model involving unsteady-state absorption by small elements of fluid could also be applicable. Recalling the discussion of Chapter III about the concepts of the model one can write

$$N_{ave} = \frac{1}{T'} \int_0^{T'} N_A(t) dt \quad (5.2)$$

where N_{ave} is the average absorption rate of a small element of fluid during the exposure time T' . In this case N_{ave} would be used in place of N_A in equation 3.38, and if T' of equation 5.2 is not a function of time then equation 5.1 would be obtained. Several investigators (22,26) have proposed that T' is about the time it takes the bubble to move one diameter. Therefore, T' would be expected to change during the life of the bubble, and thus be a function of t . Even if this were not true, T' should be a function of the agitation in the liquid. Atadan (1) and Mottern (31) have observed, however, that agitation does not influence the absorption rate of CO_2 by MEA, while Hutchinson and

Sherwood (20) have observed similar effects for other systems.

The results of the above four investigators were based on the absorption across a plane interface of known area. The argument can be extended to the present investigation, however, by considering the Reynolds number which is a criterion of the hydrodynamics of the MEA. By definition

$$N_{Re} = \frac{D V \rho}{\mu} \quad (5.3)$$

where

N_{Re} = Reynolds number

D = bubble diameter

V = MEA velocity

ρ = MEA density

μ = MEA viscosity

During the absorption process the velocity, V , remains constant, but D becomes small. Thus the Reynolds number decreases. Moreover, as the bubble's size decreases it moves down the column into a region of lower velocity, which makes the Reynolds number decrease even more.

The MEA rotameter was calibrated with water, but because of the limited amount of solution used, it could not be calibrated for each MEA normality. Nevertheless the calibration will be sufficiently accurate to determine N_{Re} for the present purposes. As an example, for Reel 7 the MEA

normality is 1.06. The density and viscosity are 1 gm/ml and 1 cp., respectively. The flow rate for Take 3 was 103 ml/sec. Initially the bubble's diameter was 0.127 inch and the diameter after 1.31 seconds was 0.064 inch. Calculation reveals that

$$N_{Re} = 510$$

$$t = 0$$

$$N_{Re} = 255$$

$$t = 1.31 \text{ sec}$$

In both cases the bubble was at the same vertical position in the tube so that the effect of vertical motion was not considered. During the take the bubble moved up and then back down the channel. The bubble can move vertically about 1 cm. For this distance it is easy to show that the ratio of N_{Re} at the throat to the N_{Re} 1 cm downstream is

$$1 + 2 \sin \theta$$

where $\theta=7^\circ$ is the angle the walls in the diverging section make with the vertical. The above decrease by a factor of two in N_{Re} is typical of the data recorded.

Discarding for the moment the concept of fluid elements moving from the top to the bottom of the bubble the residence time for the surface renewal theory should be a function of the hydrodynamics of the liquid. Thus a decrease in N_{Re} would mean an increase in residence time. The concept is analogous to the Prandtl mixing length in convectional

heat transfer.

The above remarks imply that, barring surface phenomena, the absorption mechanism involves a stagnant film surrounding the bubble. Consequently, the absorption rate can be represented functionally as

$$N_A = f(A, B, x_f, A_1, k', B_0) \quad (5.4)$$

the exact nature of the function depending on the solution of equations 3.2 and 3.3. It should be pointed out that it is quite possible that the absorption rate will vary over the surface of the bubble because of the variation of x_f about the bubble. Nevertheless the absorption rate stipulated here (N_A) is that which was measured in the laboratory, and thus is the rate averaged over the surface of the bubble. Likewise the film thickness used in equation 5.4 must be some average thickness.

In the present investigation the observed absorption rates were correlated in various ways in an attempt to find the functional relationship of equation 5.4. Figures 14 through 18 summarize the experimental portion of this investigation. There the rates are plotted as a function of total CO_2 concentration, C (or, degree of carbonation), for initial MEA normalities of 1.49, 1.95, 2.97, 1.06, and 6.06 respectively. The data are very scattered. The rates were calculated from the slope (b) of equation 5.1. From equation

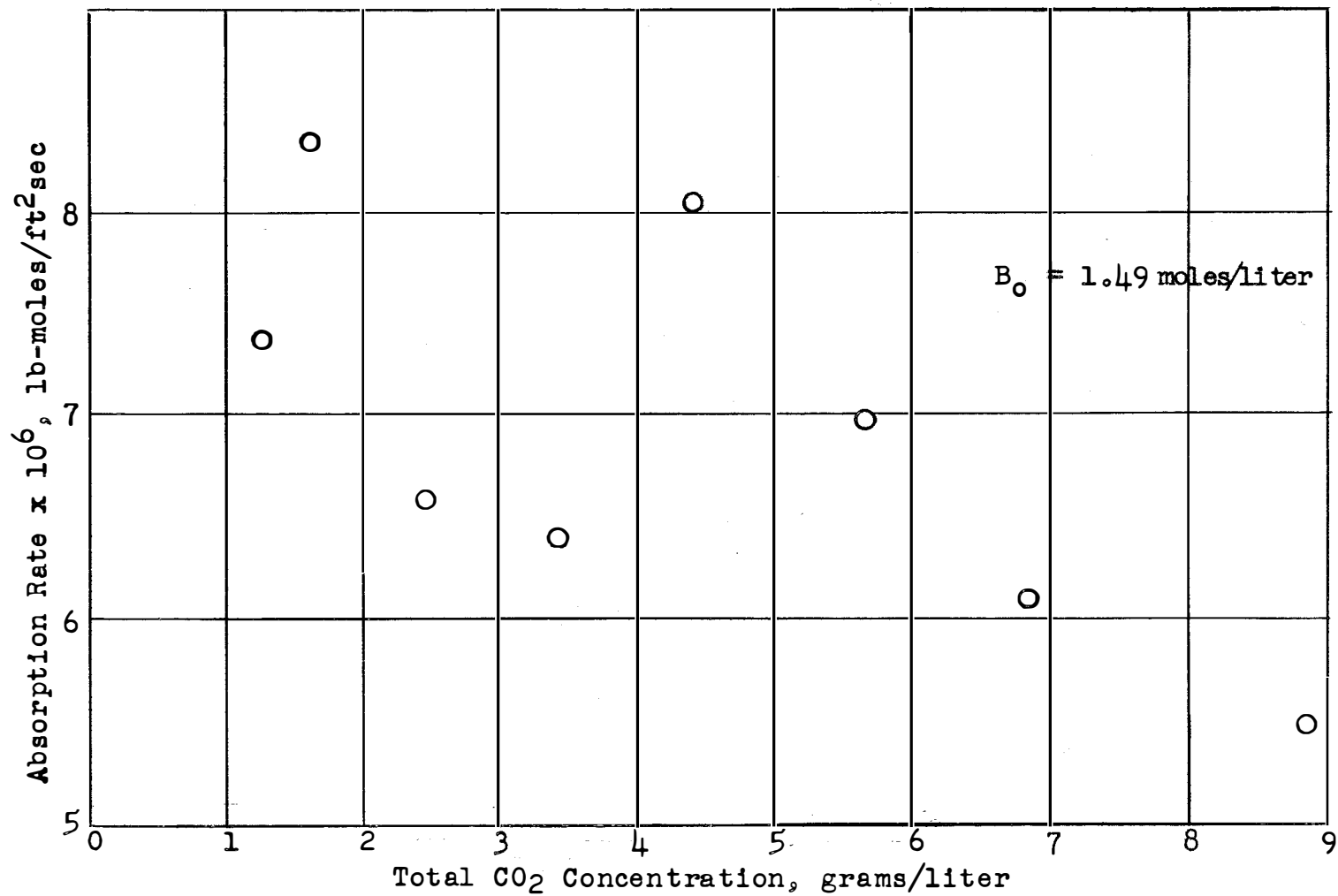


Figure 14. Rate versus CO₂ concentration, Reel 3.

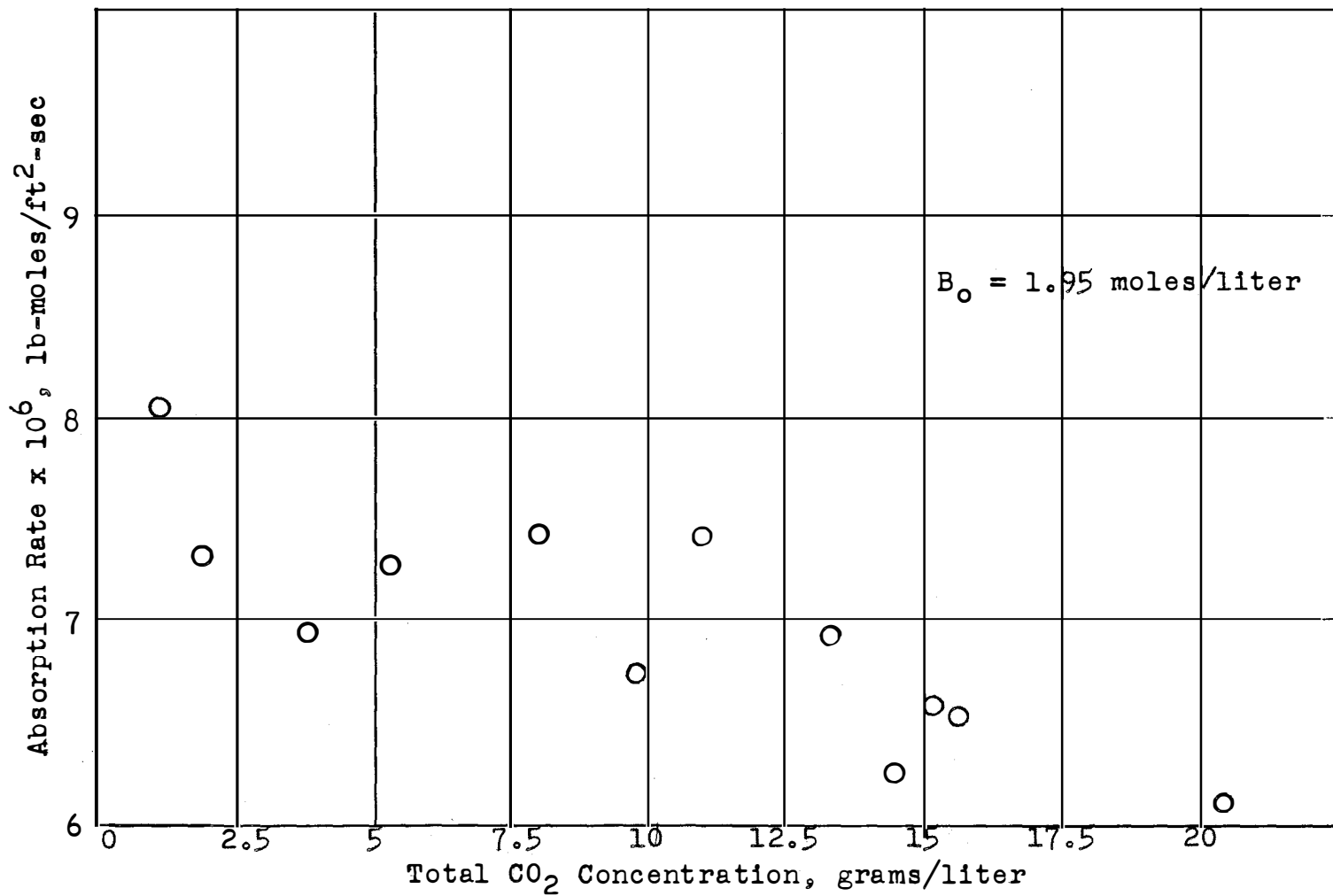


Figure 15. Rate versus CO₂ concentration, Reel 4.

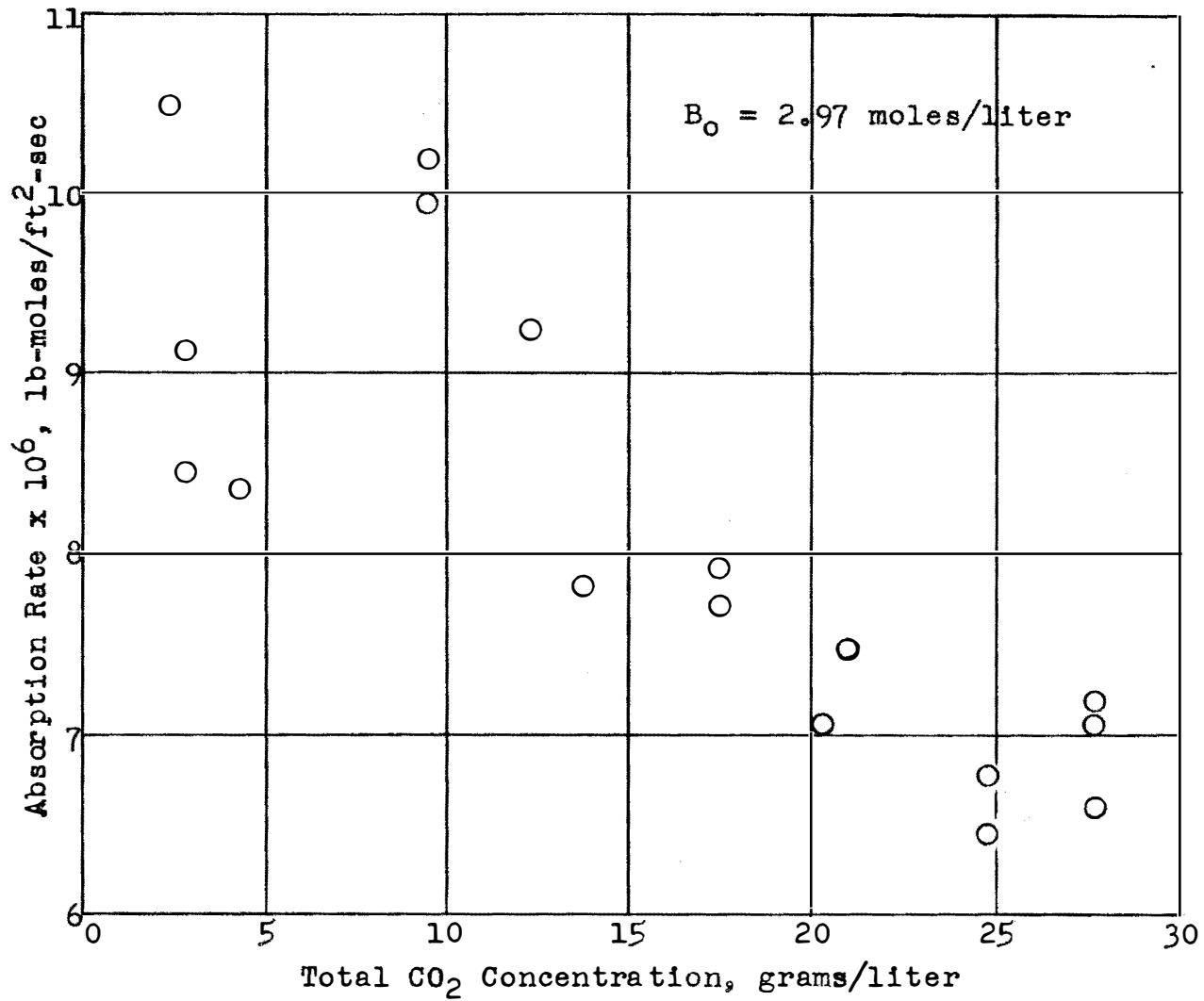


Figure 16. Rate versus CO₂ concentration, Reel 6.

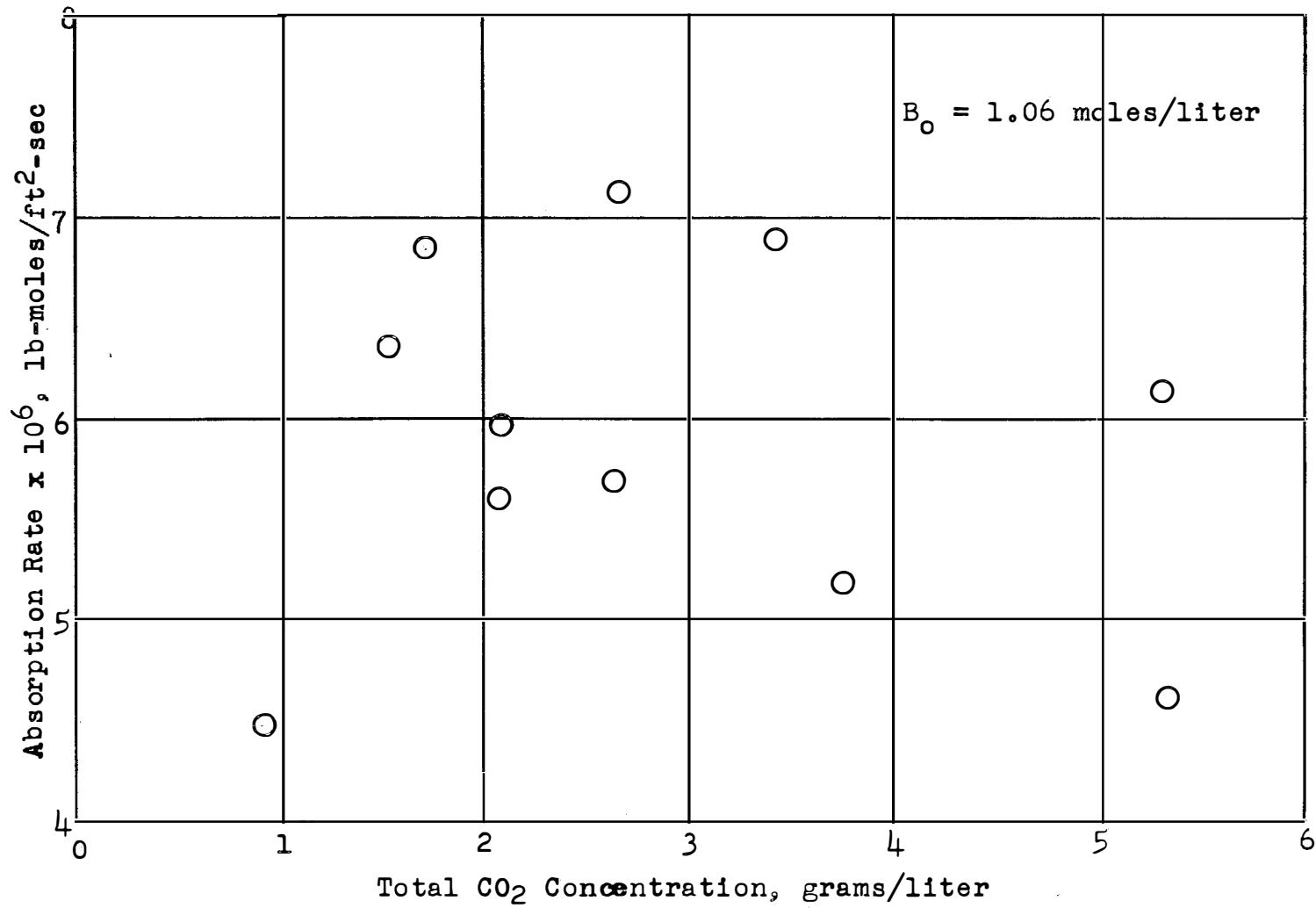


Figure 17. Rate versus CO₂ concentration, Reel 7.

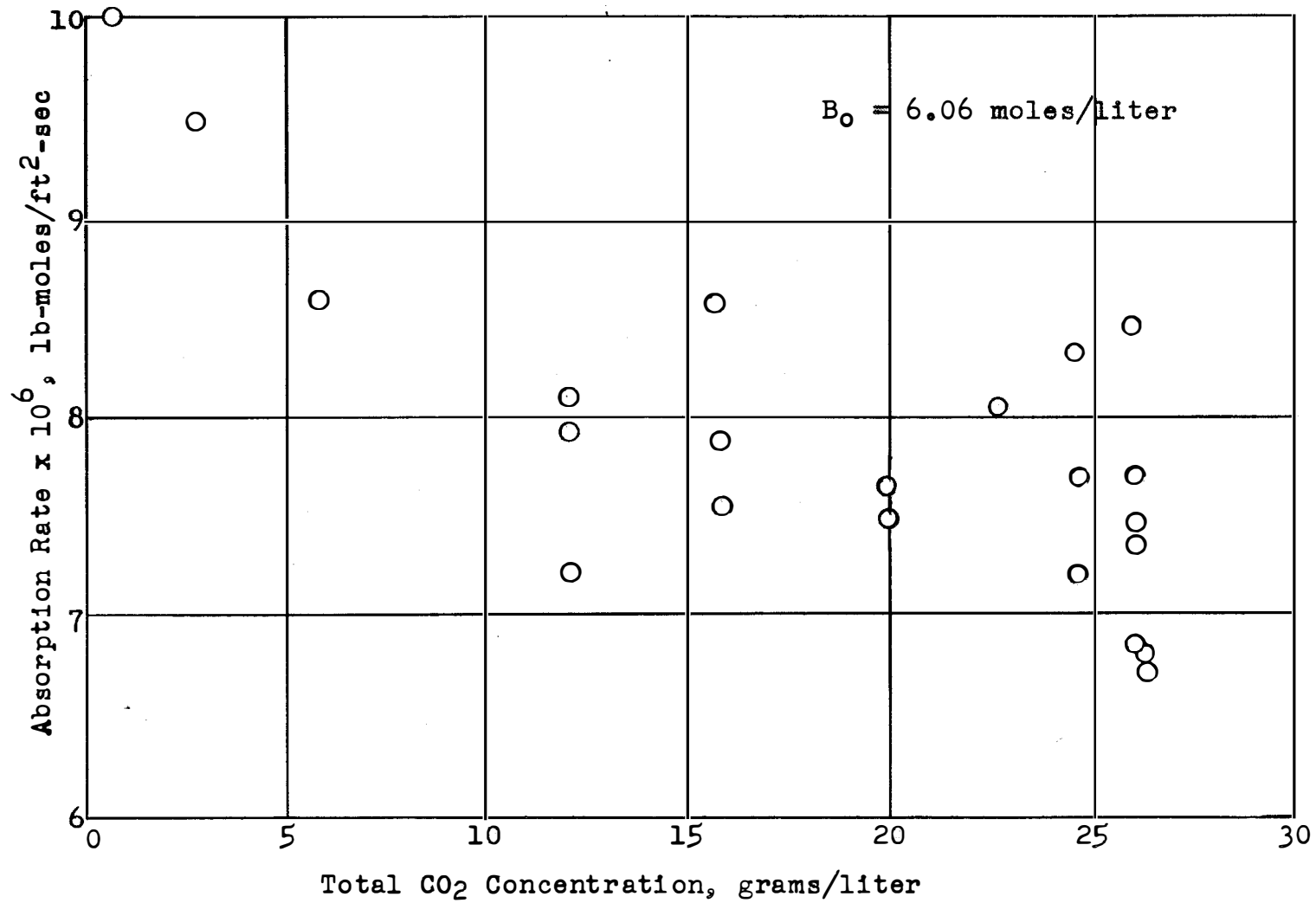


Figure 18. Rate versus CO₂ concentration, Reel 8.

3.38 it can be seen that

$$N_A = -b (3/4\gamma)^{1/3} (P/R\theta')^{2/3}$$

It was hoped that some clue on the absorption mechanism could be obtained from the above mentioned figures.

Of some value perhaps is a comparison between the measured rate and that predicted by theory. For discussion, the results for 1.95N MEA (Figure 15) will be used. At zero CO_2 concentration the experimental rate is 8×10^{-6} lb-moles/ft²-sec or 4×10^{-6} gm-moles/cm²-sec. The latter figure has already been recorded on Figure 7, so that an interpretation of the digital computer results could be made. Further comparison can be made with approximate solutions to the differential equations.

Hatta's theory (equation 3.25) states that

$$N_A = \frac{A_1 + (D_B/D_A) B}{x_f/D_A} \quad (3.25)$$

Substitution of the appropriate values gives

$$N_A = 20.5 \times 10^{-6} \text{ lb-moles/ft}^2\text{-sec for } x_f = 0.01 \text{ cm}$$

$$N_A = 6.48 \times 10^{-4} \text{ lb-moles/ft}^2\text{-sec for } x_f = 0.316 \times 10^{-3} \text{ cm}$$

Another approximation is to assume that the process is a first order chemical reaction and at steady-state in the film. Thus, from Appendix A

$$N_A = A_1 \sqrt{kD_A} \frac{\cosh(\sqrt{k/D_A} x_f)}{\sinh(\sqrt{k/D_A} x_f)} \quad (\text{A.82})$$

which gives ultimately

$$N_A = 2.83 \times 10^{-5} \text{ lb-moles/ft}^2\text{-sec for } x_f = 0.01 \text{ cm}$$

$$N_A = 2.83 \times 10^{-5} \text{ lb-moles/ft}^2\text{-sec for } x_f = 0.316 \times 10^{-3} \text{ cm}$$

The true test for the proposed theory should come from figures 14 through 18. Equation 3.25 (Hatta theory) predicts that N_A should vary as the first power of the CO_2 concentration or really $B_0 - B$ where B_0 is the MEA concentration at zero CO_2 concentration. On the other hand, equation A.82 (first order reaction) predicts that N_A should vary as $(B_0 - B)^{\frac{1}{2}}$. But the data as can be seen were disappointingly scattered, and the scatter is not the result of any temperature effects. Reel 3 (Figure 14) was made at a constant temperature of 27°C . The scatter is just as bad as for Reel 8 (Figure 18) when the temperature was varied as much as one degree. Notice in Reel 8 at a CO_2 concentration of 25.85 g/l the rates differ by 1.65, or 25 per cent of the lower value. The temperatures were the same. Figures 19, 20, and 21 show the dependence of the rate on the free MEA concentration to the one-half power assuming that carbon dioxide and monoethanolamine react in a one to one ratio. Reels 4, 6, and 8 are probably the best data taken in this investigation. It appears that the rate does not vary

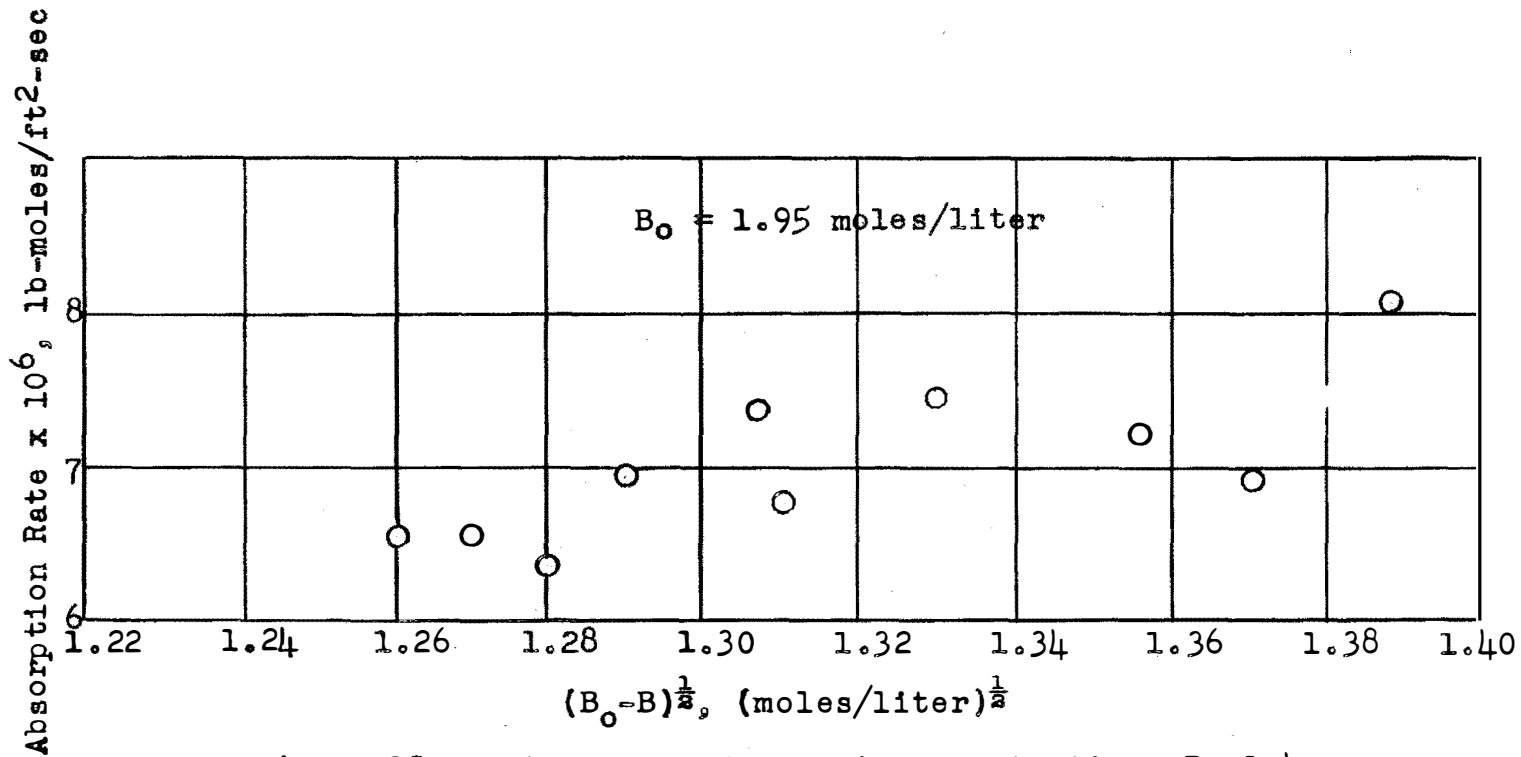


Figure 19. Rate versus free MEA concentration, Reel 4.

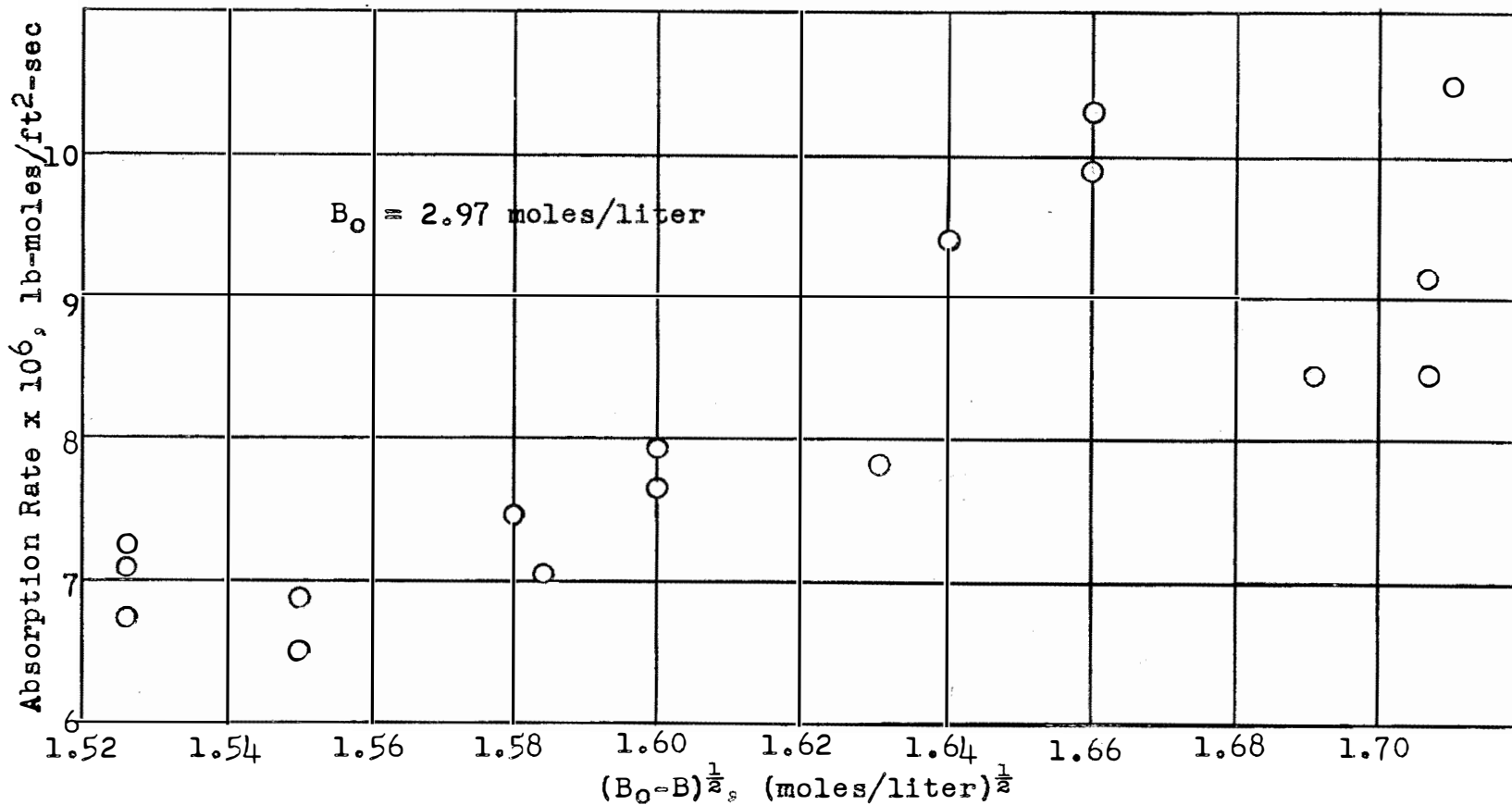


Figure 20. Rate versus free MEA concentration, Reel 6.

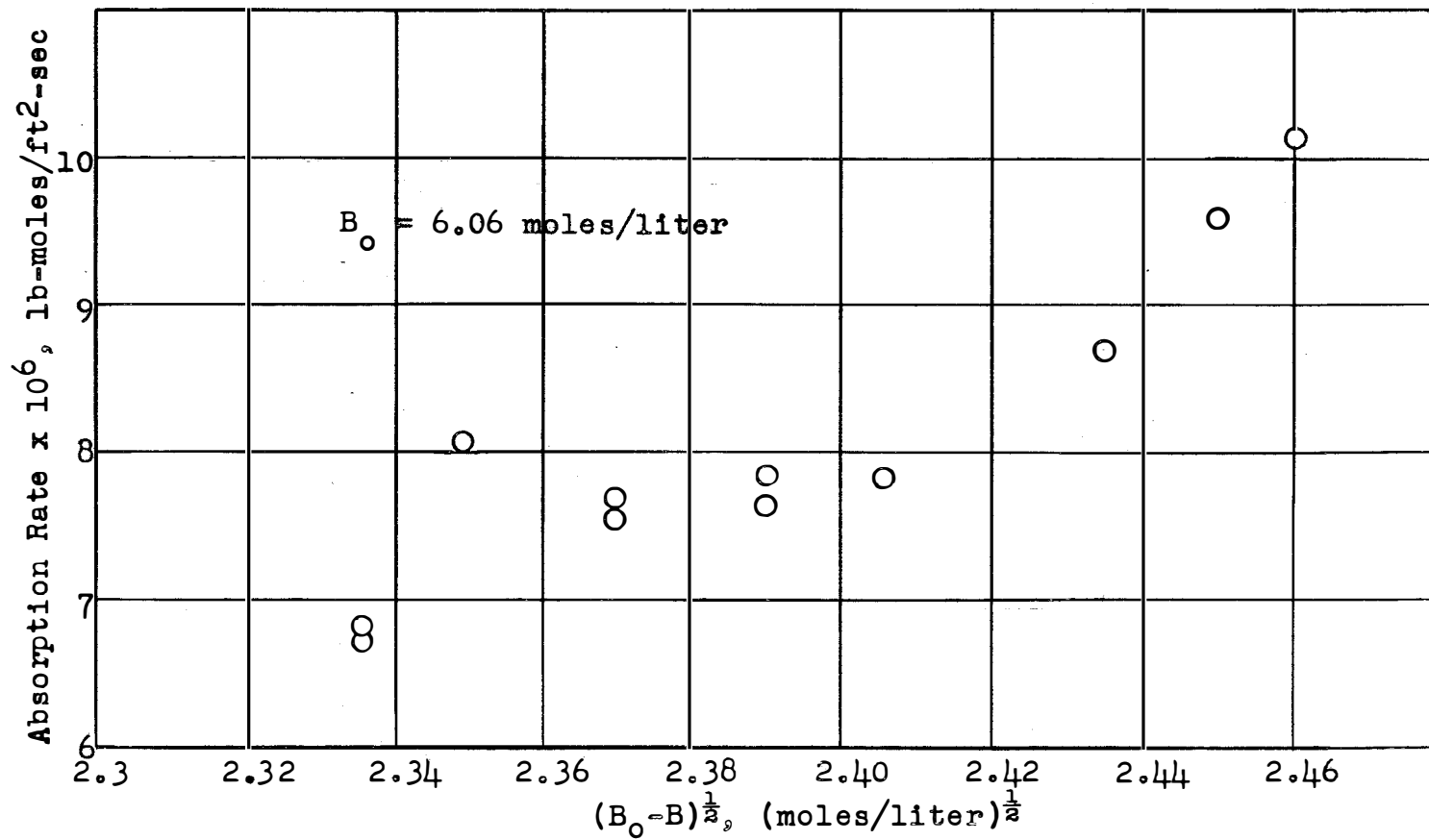


Figure 21. Absorption rate versus free MEA concentration, Reel 8.

linearly with the free MEA concentration as suggested by equation 3.25. Indeed, notice that the curves for Reels 4 and 6 seem to exhibit a maximum as in Figures 14 and 15. Reel 8 does not have a maximum. Only the data for 25°C are plotted in Figures 18, 19, and 20.

Figure 22 shows a plot of the rate versus temperature from Reel 8.

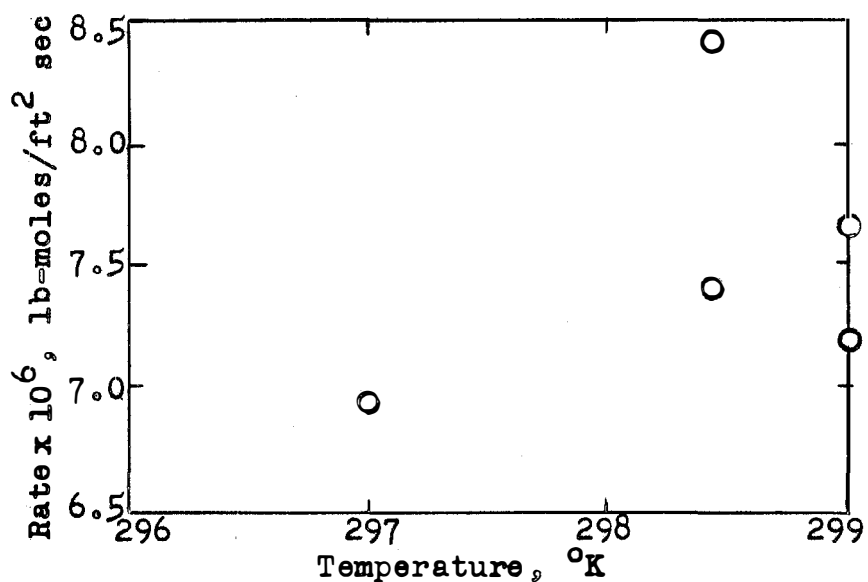


Figure 22. Rate versus temperature, Reel 8.

All that one can say is that the rate appears to increase with temperature as would be expected. The diffusivity increases with temperature. It is not clear how the rate should depend on diffusivity, because it is not clear what is meant by the diffusivity of CO₂. Is the CO₂ diffusing

through water alone, through water and MEA, or through water, MEA and reaction products? In the last two cases the diffusivity would depend not only on temperature but on MEA and reaction product concentrations, for each of these species will change the viscosity of the medium through which the CO_2 is diffusing. Comstock (5) shows that the viscosity increases linearly with CO_2 concentration. He presents data for only two MEA normalities, 2.00 and 7.86. From equation A.82

$$N_A \propto \sqrt{k D} \quad (5.5)$$

but

$$k = k' (B_0 - C) \quad (5.6)$$

and according to the best data available for liquids (45)

$$D\mu = \text{constant} = G \quad (5.7)$$

at constant temperature. The viscosity can be represented by

$$\mu = h + j C \quad (5.8)$$

where h and j are constants, and for six normal MEA

$$\mu = 3 + 1.25 C \quad (5.9)$$

The number 1.25 is only an educated guess based on Comstock's work. Combining equations 5.5, 5.7, and 5.9, one finds that

$$N_A \propto \left(\frac{B_0 - C}{3 + 1.25C} \right)^{\frac{1}{2}} \quad (5.10)$$

Figure 23 gives a plot according to equation 5.10 for Reel 8 ($B_0 = 6.06$). Again the temporary leveling off or plateau, as in Figure 17, persists. The analysis did not help much in correlating the data.

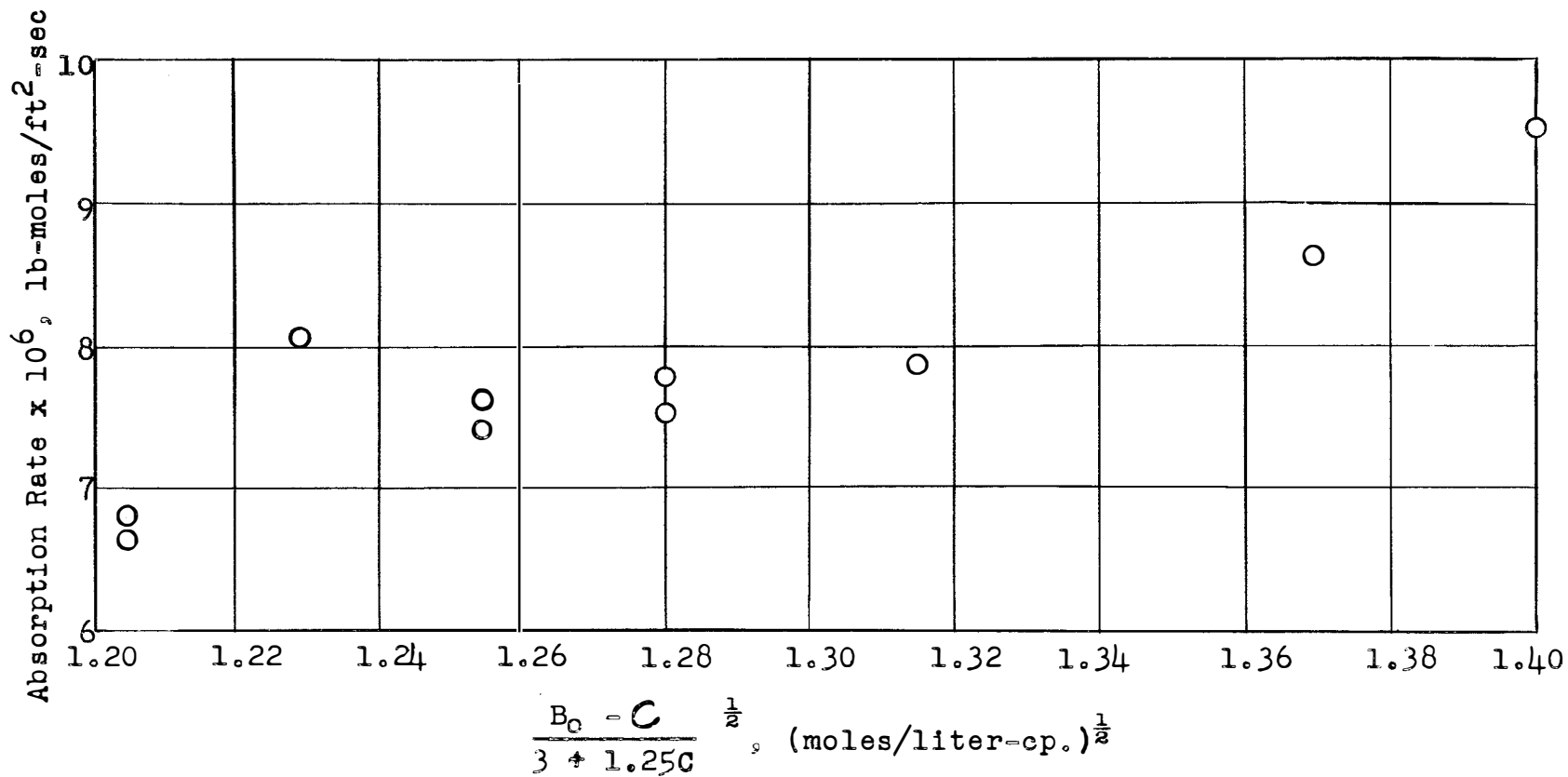


Figure 23. Correlation of rate data as suggested by equation 5.10, Reel 8.

CHAPTER VI

CONCLUSIONS AND RECOMMENDATIONS

An experimental technique was developed for determining the absorption rates of single gas bubbles suspended in a downward flowing liquid. From motion pictures of individual bubbles the mass of the bubbles was determined as a function of absorption time. The experimental data were found to correlate linearly on plotting the bubble mass to the one-third power against absorption time. The correlation is in agreement with the theoretical equation based on the assumptions that the bubbles are spherical and that the absorption rate per unit area of bubble surface is constant and uniform over the whole surface. The absorption rates were calculated from the slopes of the straight lines.

Theoretical analyses of several absorption mechanisms were made in an effort to find a model that explained the experimental data. In general the theoretical model involved a small element of fluid of finite thickness next to the gas-liquid interface across which the gas was absorbed. For this situation pure physical absorption and absorption with simultaneous chemical reaction -- zero, first and second order -- were considered. For the second order chemical reaction case the solution of two simultaneous second order non-linear partial differential equations is required. The

unsteady-state case was solved on both digital and analogue computers, and the steady-state solution was found on an analogue computer. (See Appendices B and C for details.) The zero and first order reaction cases were solved analytically (Appendix A) and an analogue solution of the latter was also obtained (Appendix C).

It is recognized that each and every fluid element at the gas-liquid interface may retain its geometrical shape and position (laminar film model), or each element may be periodically replaced (surface renewal model). A study of the above possible models indicates that the absorption mechanism is best explained by steady-state physical absorption and simultaneous second-order chemical reaction in a stagnant film of constant thickness surrounding the bubble. The digital computer results indicate that the time required to reach steady-state for thin films is much shorter than surface renewal time, which fact supports the above proposal. For this steady-state mechanism an analogue solution of the two simultaneous non-linear total differential equations was found for various film thicknesses. For two normal MEA:

$$x_f = 3.16 \times 10^{-4} \text{ cm,} \quad NA = 1 \times 10^{-5} \text{ gm-moles/cm}^2\text{-sec}$$

$$x_f = 5 \times 10^{-3} \text{ cm,} \quad NA = 4 \times 10^{-6} \text{ gm-moles/cm}^2\text{-sec}$$

$$x_f = 1 \times 10^{-2} \text{ cm,} \quad NA = 1 \times 10^{-6} \text{ gm-moles/cm}^2\text{-sec}$$

The experimental value was 4×10^{-6} gm-moles/cm²-sec. Therefore

a film thickness of 5×10^{-3} cm would appear to explain the experimental results. However, not too much significance can be given to this exact value because of the uncertainty of the proper values of CO_2 and MEA diffusivities. Also, the kinetics of the CO_2 -MEA reaction is not completely understood.

A satisfactory correlation of absorption rate as a function of total CO_2 concentration in the liquid was not found. The data were too scattered to permit reasonable interpretation.

RECOMMENDATIONS

1. Additional steady-state solutions should be run on the analogue computer at other MEA normalities. When the theoretical absorption rates are equal to the experimental values obtained in the present investigation the same film thickness may not be the same as reported herein. It is conceivable that the film thickness will be a function of liquid viscosity and hence MEA concentration.
2. Experimental data on the diffusivities of CO_2 and MEA in aqueous MEA solutions are much needed.
3. The kinetics and the dependence of the reaction rate constant for the CO_2 -MEA reaction should be studied in more detail.

4. Additional rate data at high CO₂ pressures (3 to 5 atmospheres) might be useful in clarifying the absorption mechanism.

NOMENCLATURE

NOMENCLATURE

A	= gas component absorbed by liquid; also its concentration; also bubble area
A_1	= concentration of A at interface
\bar{A}	= Laplace transform of A
AB	= true bubble diameter
$A'B'$	= apparent bubble diameter
B	= liquid component which reacts with absorbed gas, and its concentration
B_0	= initial concentration of B
C	= total CO_2 concentration (physically absorbed and chemically combined)
C_1, C_2	= constants of integration
D_1	= diffusivity of component 1
F, F'	= correction factors for bubble shape
H	= Henry's Law constant
I_1	= photographic image of point 1
ΔI	= parallax error
K_1	= $k^1 B_0 x_f^2 / D_A$
K_2	= D_B / D_A
K_3	= $k^1 A_1 x_f^2 / D_A$
N_A	= absorption or diffusion rate per unit area
N_{Re}	= Reynolds number
Q	= gross or total absorption rate
R	= gas law constant

T' ; T	= fluid element residence time; time
V	= bubble volume; also bulk liquid velocity
X	= dimensionless distance
a	= parameter; also bubble radius or semi-axis
b	= " " " " " "
h	= viscosity parameter; distance between film and lens
j	= viscosity parameter
k	= first order reaction rate constant
k'	= second " " " "
k''	= third " " " "
n	= bubble mass
p	= pressure (also P is used)
r	= bubble radius
t	= time
v	= point fluid velocity
x	= distance
x_f	= laminar film thickness
α	= dimensionless concentration, A/A_1
β	= " " " , B/B_0
θ	= temperature
θ'	= absolute temperature
μ	= liquid viscosity
ν	= kinematic viscosity
ρ	= liquid density
τ	= dimensionless time, D_{At}/x_f^2

LIST OF REFERENCES

LIST OF REFERENCES

1. Atadan, E. M., "Absorption of Carbon Dioxide by Aqueous Monoethanolamine Solutions," University of Tennessee Thesis (Ph.D.) 1954.
2. Calderbank, P. H. and I. J. O. Korchinski, "Circulation in Liquid Drops," Chem. Eng. Sci. 6, 65 (1956).
3. Carslaw, H. S. and J. C. Jaeger. Conduction of Heat in Solids. Oxford: Oxford Clarendon Press, 1947.
4. Chiang, S. H. and H. L. Toor, "Interfacial Resistance in the Absorption of Oxygen by Water," A.I.Ch.E. Jour. 5, 165 (1959).
5. Comstock, C.S., Yale University Thesis (Ph.D.) 1935.
6. Danckwerts, P. V., "Significance of Liquid Film Coefficients in Gas Absorption," Ind. Eng. Chem. 43, 1460 (1951).
7. _____, "Gas Absorption Accompanied by Chemical Reaction," A.I.Ch.E. Jour. 1, 413 (1955).
8. Danckwerts, P. V. and A. M. Kennedy, "Gas Absorption with Chemical Reaction," Trans. Inst. Chem. Engrs. 54, 325 (1954).
9. Emmert, R. E., University of Delaware Thesis (Ph.D.) 1954.
10. Epstein, P. S. and M. S. Plesset, "On the Stability of Gas Bubbles in Liquid-Gas Solutions," J. Chem. Phys. 18, 1505-1509 (1950).
11. Erdelyi, A., Tables of Integral Transforms. Vol. 1. New York: McGraw-Hill Book Co., 1954.
12. Falkovskii, V. B., U. I. Prelukov, and A. V. Vetrova, "Dynamics of Chemisorption in Bubbling Columns," Zhur. Prik. Chem. 30, 1760-1763 (1957).
13. Garner, F. H., "Mechanics of Drops and Bubbles in Diffusion Processes," Chem. and Ind., No. 8 (1956).
14. Garner, F. H. and D. Hammerton, "Circulation Inside Gas Bubbles," Chem. Eng. Sci. 3, 1-11 (1954).

15. Garner, F. H. and J. J. Lane, "Mass Transfer to Drops of Liquid Suspended in a Gas Stream, Part I and II," Trans. Inst. Chem. Engrs. 37, 155-172 (1959).
16. Griffith, R. E., "Rate of Absorption of Single Bubbles of CO₂ in Aqueous MEA," University of Tennessee Thesis (M.S.) 1954.
17. Groves, D. W. and W. Mc. Hawkins, "Steady-State Absorption of Carbon Dioxide in Aqueous Monoethanolamine Solutions at Pressures Greater than Atmospheric," University of Tennessee Thesis (B.S.) 1959.
18. Hammerton, D. and F. H. Garner, "Gas Absorption from Single Bubbles," Trans. Inst. Chem. Engrs. 32, 518-523 (1954).
19. Higbie, R., Trans. Am. Inst. Chem. Engrs. 31, 365 (1935).
20. Hutchinson, M. H. and T. K. Sherwood, "Liquid Film in Gas Absorption," Ind. Eng. Chem. 29, 836 (1937).
21. Kishinevskii, M. Kh., "Two Approaches to the Theoretical Analysis of Absorption Processes," Zhur. Prik. Chem. 28, 927-933 (1955).
22. Kishinevskii, M. Kh. and L. A. Mochalova, "Mechanism of Bubble Absorption," J. App. Chem. 29, 170-175 (1956).
23. Knudsen, J. G. and D. L. Katz, "Fluid Dynamics and Heat Transfer," University of Michigan Eng. Res. Bull. 37 (1953).
24. Ledig, P. G. and E. R. Weaver, "A Method for Studying the Rapid Absorption of Gases by Liquids," J. Am. Chem. Soc. 46, 650 (1924).
25. Lewis, W. K. and W. G. Whitman, "Principles of Gas Absorption," Ind. Eng. Chem. 16, 1215 (1924).
26. Lightfoot, E. N., "Steady-State Absorption of a Sparingly Soluble Gas in an Agitated Tank with Simultaneous Irreversible First-Order Reaction," A.I.Ch.E. Jour. 4, 499 (1958).
27. Lindland, K. P. and S. G. Terjersen, "The Effect of a Surface-Active Agent on Mass Transfer in Falling Drop Extraction," Chem. Eng. Sci. 5, 1-12 (1956).

28. Mickley, H. S., T. K. Sherwood, and C. E. Reed. Applied Mathematics in Chemical Engineering. New York: McGraw Hill Book Company, 1957.
29. McKee, R. J., "Surface Tension by the Ring Method in a Non-Equilibrium Liquid-Gas System," University of Tennessee Thesis (B.S.) 1959.
30. Mochalova, L. A. and M. Kh. Kishinevskii, "Concerning the Kinetic Mechanisms for Absorption by the Bubble Method," J. App. Chem. 31, 533-542 (1958).
31. Mottern, J. W., "Steady-State Absorption of Carbon Dioxide by Monoethanolamine Solutions," University of Tennessee Thesis (M.S.) 1957.
32. Nijsing, R. A. T. O., R. N. Hendriksz, and H. Kramers, "Absorption of CO₂ in Jets and Falling Films of Electrolyte Solutions with and without Chemical Reaction," Chem. Eng. Sci. 10, 88 (1959).
33. Pai, Shih-I. "Viscous Flow Theory," Laminar Flow. Vol. I, p. 244. Princeton, N.J.: D. Van Nostrand Co., Inc., 1956.
34. Peaceman, D. W., "Liquid Side Resistance in Gas Absorption with and without Chemical Reaction," Massachusetts Institute of Technology Thesis (Ph.D.) 1951.
35. Peebles, F. N. and H. J. Garber, "Studies of the Motion of Gas Bubbles in Liquids," Chem. Engr. Prog. 49, 88 (1953).
36. Perry, R. H. and R. L. Pigford, "Kinetics of Gas-Liquid Reactions," Ind. Eng. Chem. 45, 1247 (1953).
37. Pilt, I. G., "Kinetics of Gas Absorption," Zh. Priklad. Chem. 31, 54-60 (1958).
38. Potter, O. E., "Chemical Reactions in the Laminar Boundary Layer-Instantaneous Reaction," Trans. Inst. Chem. Engrs. 36, 415 (1958).
39. Raimondi, P. and H. L. Toor, "Interfacial Resistance in Gas Absorption," A.I.Ch.E. Jour. 5, 86-92 (1959).
40. Scriven, L. E. and R. L. Pigford, "On Phase Equilibrium at the Gas-Liquid Interface During Absorption,"

A.I.Ch.E. Jour. 4, 439 (1958).

41. Sherwood, T. K. and R. L. Pigford. Absorption and Ex-
traction. New York: McGraw Hill Book Company, 1952.
42. Toor, H. L. and S. H. Chiang, "Diffusion-Controlled
Chemical Reactions," A.I.Ch.E. Jour. 5, 339 (1959).
43. Toor, H. L. and J. M. Marchello, "Film Penetration Model
for Heat and Mass Transfer," A.I.Ch.E. Jour. 4, 97
(1958).
44. Whitman, W. G. and W. K. Lewis, "Principles of Gas Ab-
sorption," Ind. Eng. Chem. 16, 1215 (1924).
45. Wilke, C. R., "Estimation of Liquid Diffusion Coeffi-
cients," Chem. Eng. Prog. 45, 218 (1949).
46. Worthing, A. G. and J. Geffner. Treatment of Experi-
mental Data. New York: John Wiley and Sons, Inc.,
1943.

APPENDICES

APPENDIX A

SOLUTIONS OF EQUATIONS 3.2 AND 3.3

SOLUTIONS OF EQUATIONS 3.2 AND 3.3

It was mentioned in Chapter III that equations 3.2 and 3.3 cannot be solved analytically. However, they can be solved for particular simplifying cases.

I. Zero Order Reaction.

A. Unsteady state.

The differential equation now becomes

$$\frac{\partial A}{\partial t} = D_A \frac{\partial^2 A}{\partial x^2} - k^n \quad (\text{A.1})$$

where k^n = the zero order reaction rate constant. The boundary conditions remain unchanged, that is

$$\begin{aligned} A(x, 0) &= 0 \\ A(0, t) &= A_1 \\ A(x_f, t) &= 0 \end{aligned} \quad (\text{A.2})$$

It is convenient to make the variable substitution

$$A' = A + k^n t$$

So that

$$D_A \frac{\partial^2 A'}{\partial x^2} = \frac{\partial A'}{\partial t} \quad (\text{A.3})$$

and the boundary conditions become

$$A'(x, 0) = 0$$

$$A'(0, t) = A_1 + k^n t \quad (\text{A.4})$$

$$A'(x_f, t) = k^n t$$

which are time dependent. The primes will be dropped from the k for convenience. Because of this time dependence, it is necessary to use Duhamel's Theorem (5) to obtain a solution. The mechanics of the solution are given in section II.A. of this appendix where the solution is worked out for the first order reaction case. Thus Duhamel's Theorem states (c.f. equation A.25) that

$$A' = \frac{\partial}{\partial t} \int_0^t V(x, \gamma) [A_1 + 2k(t-\gamma)] d\gamma \quad (\text{A.5})$$

where $V(x, t)$ is given by equation A.49. Consequently the solution to equation A.1 can be written down immediately:

$$A' = \frac{\partial}{\partial t} \int_0^t \frac{x_f - x}{x_f} [A_1 + 2k(t-\gamma)] d\gamma - \frac{2A_1}{\pi} \int_0^t \sum_{n=1} \frac{1}{n} e^{-\frac{n^2 x^2 D_A \gamma}{x_f^2}} \sin \frac{n\pi x}{x_f} d\gamma - \frac{4k}{\pi} \sum_{n=1} \frac{1}{n} \sin \frac{n\pi x}{x_f} \int_0^t (t-\gamma) e^{-\frac{n^2 \pi^2 D_A \gamma}{x_f^2}} d\gamma \quad (\text{A.6})$$

Carrying out the integration and subsequent differentiation one obtains

$$A' = \frac{x_f - x}{x_f} [A_1 + kt] - \frac{2A_1}{\pi} \sum_{n=1} \frac{1}{n} \sin \frac{n\pi x}{x_f} e^{-\frac{n^2 \pi^2 D_A}{x_f^2} t} -$$

$$\frac{4k}{\pi} \sum_{n=1} \frac{1}{n} \sin \frac{n\pi x}{x_f} \cdot \frac{x_f^2}{n^2 \pi^2 D_A} \left[1 + \frac{n^2 \pi^2 D_A}{x_f^2} t e^{-\frac{n^2 \pi^2 D_A}{x_f^2} t} - \right.$$

$$\left. e^{-\frac{n^2 \pi^2 D_A}{x_f^2} t} \right] + \frac{4k}{\pi} \sum_{n=1} \frac{1}{n} \sin \frac{n\pi x}{x_f} \left[t e^{-\frac{n^2 \pi^2 D_A}{x_f^2} t} \right] \quad (A.7)$$

Since $\partial A / \partial x = \partial A' / \partial x$, then

$$\left. \frac{\partial A}{\partial x} \right]_{x=0} = -A_1 - 2kt - \frac{2A_1}{x_f} \sum_{n=1} e^{-\frac{n^2 \pi^2 D_A}{x_f^2} t} - \frac{4k}{x_f}$$

$$\sum_{n=1} \left[\frac{x_f^2}{n^2 \pi^2 D_A} - \frac{x_f^2}{n^2 \pi^2} e^{-\frac{n^2 \pi^2 D_A}{x_f^2} t} \right] \quad (A.8)$$

Thus

$$N_A = -D_A \left. \frac{\partial A}{\partial x} \right]_{x=0} = D_A \left[A_1 + 2kt + \frac{2A_1}{x_f} \sum_{n=1} e^{-\frac{n^2 \pi^2 D_A}{x_f^2} t} + \right.$$

$$\left. \frac{4k}{x_f} \sum_{n=1} \frac{x_f^2}{n^2 \pi^2 D_A} (1 - e^{-\frac{n^2 \pi^2 D_A}{x_f^2} t}) \right] \quad (A.9)$$

I. Zero Order Reaction (continued)

B. Steady state.

The differential equation now is

$$D_A \frac{d^2 A}{dx^2} - k = 0 \quad (\text{A.10})$$

The boundary conditions are

$$\begin{aligned} A(0) &= A_1 \\ A(x_f) &= 0 \end{aligned} \quad (\text{A.11})$$

Integration of A.10 gives

$$\frac{dA}{dx} = \frac{k}{D_A} x + C_1 \quad (\text{A.12})$$

$$A = \frac{k}{D_A} x^2 + C_1 x + C_2 \quad (\text{A.13})$$

From A.11, the constants of integration are

$$C_2 = A_1 \quad (\text{A.14})$$

$$C_1 = - \frac{\frac{k}{D_A} x_f^2 + A_1}{x_f} \quad (\text{A.15})$$

Therefore

$$A = \frac{k}{D_A} x^2 - \frac{\frac{k}{D_A} x_f^2 + A_1}{x_f} x + A_1 \quad (\text{A.16})$$

and

$$\left. \frac{dA}{dx} \right]_{x=0} = - \frac{\frac{k}{D_A} x_f^2 + A_1}{x_f} \quad (\text{A.17})$$

Thus

$$N = - D_A \frac{dA}{dx} = - \frac{k x_f^2 + D_A A_1}{x_f} \quad (\text{A.18})$$

The above solutions are only of academic interest in that they have little application to the present investigation because the CO_2 -MEA reaction is either a first or second order reaction.

II. First Order Reaction.

A. Unsteady state.

1. Series solution.

The differential equation is

$$D_A \frac{\partial^2 A}{\partial x^2} - \frac{\partial A}{\partial t} = k A \quad (\text{A.19})$$

with boundary and initial conditions

$$\begin{aligned} A(x, 0) &= 0 \\ A(0, t) &= A_1 \\ A(x_f, t) &= 0 \end{aligned} \quad (\text{A.20})$$

and

$$k = k' B_0$$

In the following the subscript A will be dropped from D . Let

$$A = U \exp(-kt) \quad (\text{A.21})$$

then A.19 and A.20 become respectively

$$D \frac{\partial^2 U}{\partial x^2} = \frac{\partial U}{\partial t} \quad (\text{A.22})$$

and

$$\begin{aligned} U(x, 0) &= 0 \\ U(0, t) &= A_1 \exp(kt) \\ U(x_f, t) &= 0 \end{aligned} \quad (\text{A.23})$$

Since A.23 involves time dependent boundary conditions the solution of A.22 must be obtained in a special manner. One way is with the help of Duhamel's Theorem (5) one form of which states that if V is a solution of A.20 with boundary conditions

$$\begin{aligned} V(x, 0) &= 0 \\ V(0, t) &= 1 \\ V(x_f, t) &= 0 \end{aligned} \quad (\text{A.24})$$

then

$$U = \frac{\partial}{\partial t} \int_0^t A_1 \exp(k(t - \tau)) V(x, \tau) d\tau \quad (\text{A.25})$$

Let

$$V = R + W \quad (\text{A.26})$$

where R satisfies the equations

$$\frac{d^2 R}{dx^2} = 0 \quad (\text{A.27})$$

$$R(x_f) = 0 \quad (\text{A.28})$$

$$R(0) = 1$$

and W satisfies the equations

$$\frac{\partial W}{\partial t} = D \frac{\partial^2 W}{\partial x^2} \quad (\text{A.29})$$

$$W(x, 0) = -R$$

$$W(0, t) = 0 \quad (\text{A.30})$$

$$W(x_f, t) = 0$$

The solution to A.27 and A.28 is

$$R = \frac{x_f - x}{x_f} \quad (\text{A.31})$$

For W assume that

$$W = X(x) T(t) \quad (\text{A.32})$$

Therefore from A.29

$$X T' = D X'' T \quad (\text{A.33})$$

or

$$\frac{\tau'}{\tau} = D \frac{x''}{x} = -\beta^2 \quad (\text{A.34})$$

Thus

$$\frac{\tau'}{\tau} = -\beta^2 \quad (\text{A.35})$$

and

$$D \frac{x''}{x} = -\beta^2 \quad (\text{A.36})$$

The solution to A.35 is

$$\tau = \exp(-\beta^2 t) \quad (\text{A.37})$$

and for A.36

$$x = C_1 \cos \frac{\beta}{\sqrt{D}} x + C_2 \sin \frac{\beta}{\sqrt{D}} x \quad (\text{A.38})$$

Or, from A.32

$$W = \exp(-\beta^2 t) \left[C_1 \cos \frac{\beta}{\sqrt{D}} x + C_2 \sin \frac{\beta}{\sqrt{D}} x \right] \quad (\text{A.39})$$

Since, from equation A.30,

$$W(0, t) = 0$$

and

$$C_1 = 0 \quad (\text{A.40})$$

then

$$W(x_f, t) = 0 = C_2 \sin \frac{\beta}{\sqrt{D}} x_f \quad (\text{A.41})$$

Therefore

$$\frac{\beta}{\sqrt{D}} x_f = n\pi, \quad n=0,1,2,3,\dots \quad (\text{A.42})$$

or

$$\beta = \frac{n\pi\sqrt{D}}{x_f} \quad (\text{A.43})$$

Thus

$$W(x,t) = \exp\left(-\frac{n^2\pi^2 D}{x_f^2} t\right) C_1 \sin \frac{n\pi}{x_f} x \quad (\text{A.44})$$

and, at $t=0$

$$W(x,0) = -\frac{x_f - x}{x_f} = \sum_{n=0} C_n \sin \frac{n\pi}{x_f} x \quad (\text{A.45})$$

which can be recognized as a Fourier Series if

$$C_n = \frac{2}{x_f} \int_0^{x_f} \left(\frac{x - x_f}{x_f}\right) \sin \frac{n\pi}{x_f} x \, dx \quad (\text{A.46})$$

It should be noted that $C_0 = 0$.

From A.46 one obtains

$$C_n = -\frac{2}{n\pi}, \quad n=1,2,3,\dots \quad (\text{A.47})$$

Consequently

$$W = -\sum_{n=1} \frac{2}{n\pi} \exp\left(-\frac{n^2\pi^2 D}{x_f^2} t\right) \sin \frac{n\pi}{x_f} x \quad (\text{A.48})$$

Therefore substitution of equations A.48 and A.31 into equation A.26 gives

$$V = \frac{x_f - x}{x_f} - \frac{2}{\pi} \sum_{n=1}^{\infty} \frac{1}{n} \exp\left(-\frac{n^2 \pi^2 D}{x_f^2} t\right) \sin \frac{n\pi x}{x_f} \quad (\text{A.49})$$

This in turn must be substituted into equation A.25 to obtain U, that is

$$U = \frac{\partial}{\partial t} \int_0^t A_1 \exp(k[t-\tau]) \left[\frac{x_f - x}{x_f} - \frac{2}{\pi} \sum_{n=1}^{\infty} \frac{\exp\left(-\frac{n^2 \pi^2 D \tau}{x_f^2}\right)}{n} \sin \frac{n\pi x}{x_f} \right] d\tau \quad (\text{A.50})$$

which gives

$$U = \frac{\partial}{\partial t} \left\{ \frac{A_1}{k} \left(\frac{x_f - x}{x_f} \right) \left[\exp(kt) - 1 \right] - \frac{2A_1 \exp(kt)}{\pi} \sum_{n=1}^{\infty} \frac{1}{n} \sin \frac{n\pi x}{x_f} \frac{1 - \exp\left(-\left[\frac{n^2 \pi^2 D}{x_f^2} + k\right] t\right)}{\frac{n^2 \pi^2 D}{x_f^2} + k} \right\} \quad (\text{A.51})$$

Now by A.21 one obtains for A after differentiating

$$A = A_1 \left(\frac{x_f - x}{x_f} \right) - \frac{2A_1}{\pi} \sum_{n=1}^{\infty} \frac{1}{n} \sin \frac{n\pi x}{x_f} \left(\frac{x_f^2}{n^2 \pi^2 D + x_f^2 k} \right) \cdot$$

$$\left[k + \frac{n^2 \pi^2 D}{x_f^2} \exp\left(-\left[\frac{n^2 \pi^2 D}{x_f^2} + k\right] t\right) \right] \quad (\text{A.52})$$

The next step is to find the absorption rate by Fick's Law.

Thus

$$\frac{\partial A}{\partial x} = -\frac{A_1}{x_f} - \frac{2A_1}{\pi} \sum_{n=1} \frac{\pi}{x_f} \cos \frac{n\pi x}{x_f} \left(\frac{x_f^2}{n^2 \pi^2 D + x_f^2 k} \right) \left[k + \frac{n^2 \pi^2 D}{x_f^2} \exp\left(-\left[\frac{n^2 \pi^2 D}{x_f^2} + k\right] t\right) \right] \quad (\text{A.53})$$

and at $x=0$

$$\left. \frac{\partial A}{\partial x} \right|_{x=0} = -\frac{A_1}{x_f} - \frac{2A_1}{x_f} \sum_{n=1} \frac{x_f^2}{n^2 \pi^2 D + x_f^2 k} \left[k + \frac{n^2 \pi^2 D}{x_f^2} \exp\left(-\left[\frac{n^2 \pi^2 D}{x_f^2} + k\right] t\right) \right] \quad (\text{A.54})$$

from which on application of Fick's Law

$$N_A = \frac{DA_1}{x_f} \left[1 + 2 \sum_{n=1} \frac{x_f^2}{n^2 \pi^2 D + x_f^2 k} \left[k + \frac{n^2 \pi^2 D}{x_f^2} \exp\left(-\left[\frac{n^2 \pi^2 D}{x_f^2} + k\right] t\right) \right] \right] \quad (\text{A.55})$$

Of interest is the amount absorbed after a time T has

elapsed. Consequently

$$\int_0^T N_A dt = \frac{DA_1}{x_f} T + 2 \sum_{n=1} \frac{k T x_f^2}{n^2 \pi^2 D + x_f^2 k} + \left[\frac{n^2 \pi^2 D x_f^2}{(n^2 \pi^2 D + x_f^2 k)^2} \right. \\ \left. (1 - \exp \left\{ - \left[\frac{n^2 \pi^2 D}{x_f^2} + k \right] T \right\}) \right] \quad (\text{A.56})$$

1. Laplace Transform Method.

Equation A.55 is not convenient for analysis of data because of the uncertainty in the convergence of the series. Some interesting results can be obtained if equation A.19 is solved by the Laplace Transform Method. In the following $\bar{A}(x,p)$ will denote the transform of $A(x,t)$ with respect to the kernel p . Thus by definition

$$\bar{A}(x,p) = \int_0^{\infty} \exp(-pt) A(x,t) dt \quad (\text{A.57})$$

The inverse transform was found from the tables compiled by Erdelyi (11).

The transform of equation A.19 is

$$D \frac{d^2 \bar{A}}{dx^2} - p\bar{A} + A(x,0) = k \bar{A} \quad (\text{A.58})$$

There are two possibilities to consider here; $A(x,0) = 0$

or $A(x, 0) = A_0 > 0$, in which case

$$A(x_f, t) = A_0 \exp(-k t) \quad (\text{A.59})$$

If the reaction is truly first order, then A can never be zero; but keeping in mind that the results must be applied to the CO_2 -MEA system where it is possible that A can be zero, the first situation may give an approximate picture of what is taking place. Nevertheless the latter case will be solved first, and the solution for the former will be deduced as a special case of another set of boundary conditions.

Thus the transformed boundary conditions for A.58 are

$$\begin{aligned} \bar{A}(0, p) &= \frac{A_1}{p} \\ \bar{A}(x, 0) &= \frac{A_0}{p} \\ \bar{A}(x_f, p) &= \frac{A_0}{p + k} \end{aligned} \quad (\text{A.60})$$

The solution to A.58 is

$$\bar{A} = C_1 \exp(Rx) + C_2 \exp(-Rx) + \frac{A_0}{p + k} \quad (\text{A.61})$$

where

$$R^2 = \frac{p + k}{D} \quad (\text{A.62})$$

By equation A.60 the constants of integration (C_1 and C_2) may be found so that finally

$$\bar{A} = \frac{p \Delta A + A_1 k}{p(p + k)} \frac{\sinh R(x_f - x)}{\sinh R x_f} \quad (\text{A.63})$$

where

$$\Delta A = A_1 - A_0 \quad (\text{A.64})$$

Differentiation of A.63 gives

$$\frac{\partial \bar{A}}{\partial x} = - \frac{p \Delta A + A_1 k}{p(p+k)} R \frac{\cosh R(x_f - x)}{\sinh R x_f} \quad (\text{A.65})$$

or at the interface ($x=0$)

$$\left. \frac{\partial \bar{A}}{\partial x} \right]_{x=0} = - \frac{p \Delta A + A_1 k}{D_A^{\frac{1}{2}} p(p+k)^{\frac{1}{2}}} \frac{\cosh R x_f}{\sinh R x_f} \quad (\text{A.66})$$

after substitution of equation A.62.

Unfortunately the inverse of equation A.66 cannot be written explicitly. The solution involves the evaluation of the convolution integrals

$$\int_0^t \exp(-kU) \sum_{n=-\infty}^{\infty} \left[\frac{x_f^2 n^2}{D_A U^{5/2}} \exp\left(-\frac{x_f^2 n^2}{D_A U}\right) - \frac{1}{2U^{3/2}} \exp\left(-\frac{L^2 n^2}{DU}\right) \right] dU \quad (\text{A.67})$$

and

$$\int_0^t \sum_{n=-\infty}^{\infty} \left[\frac{x_f^2 n^2}{D_A U^{5/2}} \exp\left(-\frac{x_f^2 n^2}{D_A U}\right) - \frac{1}{2U^{3/2}} \exp\left(-\frac{x_f^2 n^2}{D_A U}\right) \right] dU \quad (\text{A.68})$$

which cannot be evaluated in closed form and which nevertheless

appear to diverge at the lower limit.

But the inverse of A.66 can be found for the special case of p large. Thus

$$\lim_{p \rightarrow \infty} \left. \frac{\partial \bar{A}}{\partial x} \right|_{x=0} = - \frac{p \Delta A + A_1 k}{\sqrt{D} p \sqrt{p+k}} \quad (\text{A.69})$$

Notice that p does not have to be too large for

$$\left(\frac{p+k}{D} \right)^{\frac{1}{2}} = \left(\frac{p + \frac{2}{3} \cdot 10^3}{2 \cdot 10^{-5}} \right)^{\frac{1}{2}} > \frac{1}{3} \cdot 10^4 \quad (\text{A.70})$$

(for 2 normal MEA) and

$$\frac{\cosh 10^4}{\sinh 10^4} \approx 1$$

The limit of A.69 corresponds to $t \rightarrow 0$ and thus the inverse would be applicable to short absorption time a realistic condition for the present investigation.

Taking the inverse of equation A.69 one obtains

$$\left. \frac{\partial A}{\partial x} \right|_{x=0} = - \frac{1}{\sqrt{D}} \left[\frac{\Delta A \exp(-kt)}{\pi^{\frac{1}{2}} t^{\frac{1}{2}}} + A_1 k \left\{ \frac{\exp(-kt)}{\sqrt{\pi t}} + k^{\frac{1}{2}} \text{Erf}(k^{\frac{1}{2}} t^{\frac{1}{2}}) \right\} \right] \quad (\text{A.71})$$

which gives immediately for the absorption rate

$$N_A = - D_A \left. \frac{\partial A}{\partial x} \right|_{x=0} = \sqrt{D_A} \left[\frac{\Delta A \exp(-kt)}{\sqrt{\pi t}} + A_1 k \left\{ \frac{\exp(-kt)}{\sqrt{\pi t}} + \right. \right.$$

$$\left. k^{\frac{1}{2}} \text{Erf} (\sqrt{kt}) \right] \quad (\text{A.72})$$

Recall that Erf is the error function defined thusly

$$\text{Erf } x = \frac{2}{\sqrt{\pi}} \int_0^x \exp(-u^2) du \quad (\text{A.73})$$

If now the boundary conditions to A.19 are modified to read

$$\begin{aligned} A(0, t) &= A_1 \\ A(x, 0) &= A_0 \\ A(x_f, t) &= A_0 \end{aligned} \quad (\text{A.74})$$

which precludes any reaction in the bulk of the liquid then one can obtain by an analysis similar to the above that

$$N = \sqrt{D_A} \left[\frac{\Delta A \exp(-kt)}{\sqrt{\pi t}} + A_1 \sqrt{k D} \text{Erf} (kt) \right] \quad (\text{A.75})$$

For the special and more realistic case $A_0 = 0$ one has

$$N = \sqrt{D_A} A_1 \left[\frac{\exp(-kt)}{\sqrt{\pi t}} + k^{\frac{1}{2}} \text{Erf} (kt) \right] \quad (\text{A.76})$$

For an absorption time T the average absorption rate is given by

$$N_{\text{ave}} = \frac{1}{T} \int_0^T N_A dt \quad (\text{A.77})$$

From A.76

$$\int_0^T N_A dt = A_i \sqrt{D} \int_0^T \frac{\exp(-kt)}{\sqrt{\pi t}} dt + A_i \sqrt{D_A k} \int_0^T \text{Erf} \sqrt{kt} dt \quad (\text{A.78})$$

Finally

$$N_{ave} = A_i \sqrt{D_A} \left\{ \frac{2}{\sqrt{T}} \exp(-kT) + 4k \sum_{n=1}^{\infty} (-1)^{n+1} \frac{T^{\frac{2n-1}{2}} k^{n-1}}{(2n+1)(n-1)!} \right\} + A_i \sqrt{D_A k} \left\{ \text{Erf}(\sqrt{kT}) + \sqrt{\frac{1}{kT}} \exp(-kT) - \frac{1}{2kT} \text{Erf}(\sqrt{kT}) \right\} \quad (\text{A.79})$$

II. First Order Reaction (continued)

B. Steady state.

The differential equation now becomes

$$D_A \frac{d^2 A}{dx^2} - kA = 0 \quad (\text{A.80})$$

and the boundary conditions are

$$\begin{aligned} A(0) &= A_i \\ A(x_f) &= 0 \text{ (for CO}_2\text{-MEA system)} \end{aligned} \quad (\text{A.81})$$

The solution to equation A.80 is easily obtained, thus:

$$N_A = A_i \sqrt{k D_A} \frac{\cosh(\sqrt{k/D_A} x_f)}{\sinh(\sqrt{k/D_A} x_f)} \quad (\text{A.82})$$

APPENDIX B

DETAILS OF DIGITAL MACHINE SOLUTION
OF EQUATIONS 3.2 AND 3.3

DETAILS OF DIGITAL MACHINE SOLUTION
OF EQUATIONS 3.2 AND 3.3

It is not intended here to go into the coding of the problem, but rather to present the overall calculation scheme and certain other pertinent points which will prove to be interesting. In Chapter III, equations 3.20 and 3.21 are the finite difference form of the unsteady-state equations.

$$\frac{\alpha_{m,n+1} - \alpha_{m,n}}{\Delta \tau} = \frac{\alpha_{m+1,n} - 2\alpha_{m,n} + \alpha_{m-1,n}}{(\Delta x)^2} - K_1 \alpha_{m,n} \beta_{m,n} \quad (B.1)$$

$$\frac{\beta_{m,n+1} - \beta_{m,n}}{\Delta \tau} = K_2 \frac{\beta_{m+1,n} - 2\beta_{m,n} + \beta_{m-1,n}}{(\Delta x)^2} - K_3 \alpha_{m,n} \beta_{m,n} \quad (B.2)$$

The constants K_1 , K_2 , and K_3 were defined in the text. Equations B.1 and B.2 can be solved explicitly for $\alpha_{m,n+1}$ and $\beta_{m,n+1}$ — the α and β after a time $\Delta \tau$ has passed. Thus

$$\alpha_{m,n+1} = a_1 (\alpha_{m-1,n} + \alpha_{m+1,n}) + (a_2 - a_3 \beta_{m,n}) \alpha_{m,n} \quad (B.3)$$

$$\beta_{m,n+1} = a_4 (\beta_{m-1,n} + \beta_{m+1,n}) + (a_5 - a_6 \alpha_{m,n}) \beta_{m,n} \quad (B.4)$$

where now

$$a_1 = \frac{\Delta \tau}{(\Delta x)^2}$$

$$a_2 = 1 - 2 \frac{\Delta \tau}{(\Delta x)^2}$$

$$a_3 = K_1 \Delta \tau = \frac{k B_0 x_f^2}{D_A} \Delta \tau$$

$$a_4 = K_2 \frac{\Delta \tau}{(\Delta x)^2} = \frac{D_B \Delta \tau}{D_A (\Delta x)^2}$$

$$a_5 = 1 - 2 \frac{K_2 \Delta \tau}{(\Delta x)^2} = 1 - 2 \frac{D_B \Delta \tau}{D_A (\Delta x)^2}$$

$$a_6 = K_3 \Delta \tau = \frac{k A_1 x_f^2}{D_A} \Delta \tau$$

In words one can describe the machine computation as follows: for each x increment, new α 's and β 's were computed from the old α 's and β 's by equations B.3 and B.4. The process is repeated over and over until it is decided to stop. The boundary conditions for equations B.3 and B.4 were $\alpha_{0,n} = 1$, which corresponds to $\alpha(0,T) = 1$, $\alpha_{m,0} = 0$, which corresponds to $\alpha(x,0) = 0$, $\beta_{0,n} = \beta_{1,n}$, which corresponds to $\left. \frac{\partial \beta}{\partial x} \right|_{x=0} = 0$, and $\beta_{m,0} = 1$, which corresponds to $\beta(x,0) = 1$.

For Case 1 $\Delta \tau$ was 2^{-16} and Δx was 2^{-7} . The question immediately arises as to whether these values are the optimum values. In Case 3 $\Delta \tau$ was one-half of that in Case 1

and it was found that the results remain unchanged. Consequently the lattice size must be small enough. On the other hand during the computations it appeared that the α 's and β 's were approaching steady state values very slowly, which suggested that $\Delta\gamma$ could be increased in order to decrease the computing time. The author, using a desk calculator, duplicated the computer's work by the machine for $\Delta\gamma = 2^{-14}$. After the first $\Delta\gamma$ $\alpha_1 = 1$, but after the second $\Delta\gamma$ it decreases to -2.016 and then at the end of the third time increment it has increased to 7.925 . Similar behavior was obtained at the other X values. Of course the above behavior is not realistic in terms of the physical nature of the absorption process. But when equations B.3 and B.4 are used the absorption proceeds in a syncopated fashion. During the first time increment the liquid absorbs the gas, but no chemical reaction takes place as evidenced by the fact that β does not change. The liquid absorbs more gas during the second time increment, and chemical reaction occurs between the β and the α absorbed in the previous time increment. Thus the effect of making $\Delta\gamma$ too large is that the absorption process goes on too long before chemical reaction can start. The above comments will apply to subsequent time increments and at each X .

Computations were also made for $\Delta\gamma = 2^{-15}$ and $\Delta X = 2 \times 2^{-7}$ so that $\frac{\Delta\gamma}{(\Delta X)^2}$ remained constant. The same

behavior was obtained but not nearly as extreme as before. In fact no matter what size $\Delta\gamma$ is used the effect of α first increasing then decreasing will be observed. For example, for Case 4, $\alpha_{1,1} = 0.25$, $\alpha_{1,2} = 0.249$, $\alpha_{1,3} = 0.2649$, and α continues to increase. A similar momentary dip occurs at the other X values.

The machine reported results after 256 iterations and for every eighth X increment. For Case 1, it took about 2-1/2 hours to produce 35 outputs. Since

$$\gamma = \frac{D_A}{x_f^2} t$$

then

$$\Delta t = \frac{x_f^2}{D_A} \Delta\gamma$$

and

$$\Delta\gamma = 2^{-16}$$

Substitution of $D_A = 2 \times 10^{-5}$ and $\Delta\gamma = 2^{-16}$ gives

$$\Delta t = \frac{x_f^2}{10^{-5}} \times 2^{-17}$$

as the change in real time per iteration. Thus for 2^8 iterations and 2^5 outputs the time elapsed is

$$t = x_f^2 \cdot 10^5 \cdot 2^{-4}$$

If $x_f = 10^{-4}$ the time is $5/8$ second, and for $x_f^2 = 10^{-7}$, the time is $1/600$ second.

Table II contains a typical set of outputs as produced by the machine for Case 1.

TABLE II
 CONCENTRATION GRADIENTS FROM THE DIGITAL COMPUTER
 CASE 1

<u>Xx16</u>	<u>α</u>	<u>β</u>	<u>α</u>	<u>β</u>
	<u>Output 1</u>		<u>Output 5</u>	
0	1.00000000	0.99856741	1.00000000	0.99283151
1	0.45365186	0.99922278	0.65945146	0.99389412
2	0.14385650	0.99982215	0.41690378	0.99598653
3	0.03020820	0.99997517	0.25007698	0.99778213
4	0.00406044	0.99999757	0.14105355	0.99892365
5	0.00034155	0.99999969	0.07425102	0.99952767
6	0.00001765	0.99999982	0.03625657	0.99980909
7	0.00000053	0.99999982	0.01634318	0.99992818
8	0.00000000	0.99999982	0.00677477	0.99997459
9	0.00000000	0.99999982	0.00257485	0.99999130
10	0.00000000	0.99999982	0.00089506	0.99999684
11	0.00000000	0.99999982	0.00028398	0.99999853
12	0.00000000	0.99999982	0.00008206	0.99999900
13	0.00000000	0.99999982	0.00002152	0.99999912
14	0.00000000	0.99999982	0.00000506	0.99999921
15	0.00000000	0.99999984	0.00000100	0.99999947
	<u>Output 10</u>		<u>Output 15</u>	
1	1.00000000	0.98625692	1.00000000	0.98024105
2	0.68915719	0.98752132	0.69653181	0.98164436
3	0.46955882	0.99035046	0.48301942	0.98494486
4	0.31518348	0.99331538	0.33300531	0.98866943
5	0.20765347	0.99574768	0.22788661	0.99202583
6	0.13379113	0.99747526	0.15453154	0.99469009
7	0.08400501	0.99858323	0.10364280	0.99662506
8	0.05123461	0.99924114	0.06861884	0.99793750
9	0.03026457	0.99960917	0.04475869	0.99878049
10	0.01727042	0.99980547	0.02870693	0.99929871
11	0.00949940	0.99990603	0.01806678	0.99960617
12	0.00502619	0.99995569	0.01112885	0.99978342
13	0.00255233	0.99997939	0.00667891	0.99988324
14	0.00123744	0.99999037	0.00385831	0.99993861
15	0.00055946	0.99999547	0.00205969	0.99996948
16	0.00020309	0.99999816	0.00084584	0.99998792

TABLE II (continued)

x_{16}	α	β
	<u>Output 20</u>	
1	1.00000000	0.97467791
2	0.69926577	0.97618820
3	0.48787670	0.97984361
4	0.33941890	0.98414043
5	0.23530720	0.98821396
6	0.16243410	0.99164732
7	0.11155045	0.99431616
8	0.07613081	0.99626552
9	0.05157182	0.99761927
10	0.03462486	0.99852104
11	0.02299481	0.99910142
12	0.01515675	0.99946479
13	0.00965566	0.99968767
14	0.00596401	0.99982309
15	0.00337888	0.99990652
16	0.00144561	0.99996167

APPENDIX C

ANALOGUE SOLUTION OF EQUATIONS 3.2 AND 3.3

ANALOGUE SOLUTION OF EQUATIONS 3.2 AND 3.3

A Donner 3100 analogue computer located in the Nuclear Engineering Department of the University of Tennessee was used to investigate the nature of equations 3.2 and 3.3 for several different cases. The cases considered were first order chemical reaction, second order reaction and the steady state solution of the second order case.

1. First order chemical reaction.

The equation is

$$\frac{\partial A}{\partial t} = D \frac{\partial^2 A}{\partial x^2} - k A \quad (C.1)$$

with the boundary conditions

$$\begin{aligned} A(x, 0) &= 0 \\ A(0, t) &= A_1 \\ A(x_f, t) &= 0 \end{aligned} \quad (C.2)$$

It is convenient to define a new variable

$$\alpha = \frac{A}{A_1}$$

so that equation C.1 becomes

$$\frac{\partial \alpha}{\partial t} = D \frac{\partial^2 \alpha}{\partial x^2} - k \alpha \quad (C.3)$$

and the boundary conditions are

$$\begin{aligned}\alpha(x, 0) &= 0 \\ \alpha(0, t) &= 1 \\ \alpha(x_f, t) &= 0\end{aligned}\tag{C.4}$$

Since the computer integrates with respect to only one variable one of the derivatives must be approximated in finite difference form. For this purpose it is convenient to think of the region of interest, namely $0 < x < x_f$, to be divided into N equal increments Δx wide. The variable x then can take on only discrete values $x_0, x_1, x_2, x_3, \dots, x_n, \dots, x_N$, with $\Delta x = x_{n+1} - x_n$. The parameter N is the number of increments. Thus for any $n > 0$ but $< N$ one can write

$$\frac{\partial \alpha_n}{\partial t} = \frac{D}{(\Delta x)^2} (\alpha_{n+1} - 2\alpha_n + \alpha_{n-1}) - k\alpha_n\tag{C.5}$$

There will be $N-1$ such equations for each interior point in the lattice. There is no need to write equations for the points x_0 and x_N since these are boundary points and α at these points is known and fixed. The width of the increments, Δx , is x_f/N and the greater N is the more accurate the solution.

A solution to C.3 was determined for the following conditions:

$$\begin{aligned}
 N &= 14 \\
 B_0 &= 1.87N \text{ MEA} \\
 D &= 2 \times 10^{-5} \text{ cm}^2/\text{sec} \\
 x_f &= 0.01 \text{ cm}
 \end{aligned}$$

Thus

$$\frac{D}{(x_f)^2} = \frac{DN^2}{x_f^2} = \frac{(196)(2 \times 10^{-5})}{(0.01)^2} = 39.2 \quad (\text{C.6})$$

and

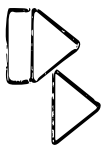
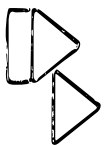
$$\frac{d\alpha_n}{dt} = 39.2 (\alpha_{n+1} + \alpha_{n-1}) - (78.4 + 6.32 \times 10^3) \alpha_n$$

It is convenient to define a new variable

$$\gamma = (78.4 + 2/3 \cdot 10^4) t \quad (\text{C.7})$$

which has the effect of slowing the solution down. Finally, equation C.5 becomes

$$\frac{d\alpha_n}{d\gamma} = 6.1 \times 10^{-3} (\alpha_{n+1} + \alpha_{n-1}) - \alpha_n \quad (\text{C.8})$$

For $N = 14$, thirteen equations must be solved simultaneously. In Figure 24 is shown a schematic diagram of a portion of the network employed in the analogue setup. In the sketch  denotes an amplifier used as an integrator and  denotes an amplifier used as a summer or in the case here it is used as a sign changer and signal

multiplier. The symbol \bigcirc denotes a coefficient multiplier. The numbers immediately above the feed lines to the amplifiers denote the factor by which the input signal is multiplied in the amplifier. The coefficient multiplier, or "pot," setting is indicated by the number below the symbol. There were

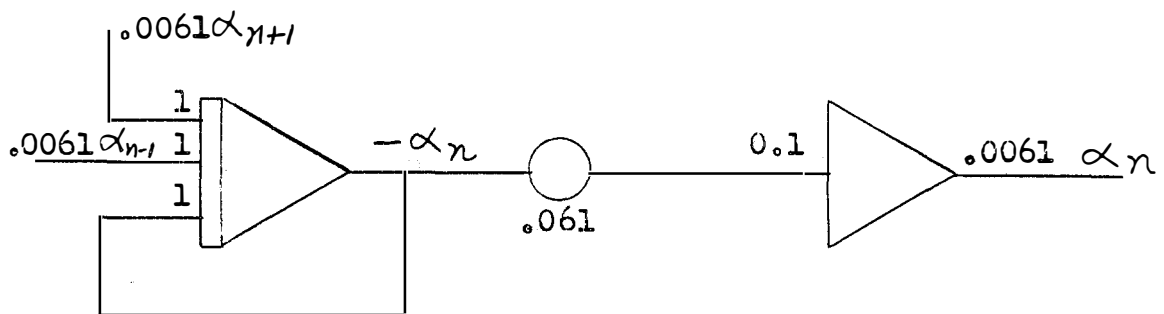


Figure 24. Schematic diagram, first order case.

thirteen such networks for each of the thirteen interior lattice points. For $n=1$ the α_0 is fed into the integrator from a constant voltage source. On the other hand, for $n=N-1$, $\alpha_N = 0$, and thus that lead does not appear. The initial conditions on all of the integrators were zero. The solutions are given as plots of α versus t for each x . A set of typical plots is given in Figure 25. The pot settings were, incidentally, set on 0.062 instead of on 0.061. The effect is to change the time scale slightly. Three solutions were run for three different pot settings: 0.062, 0.01, and 0.62. A change in the pot settings corresponds to a change in B_0 , the initial MEA concentration, because

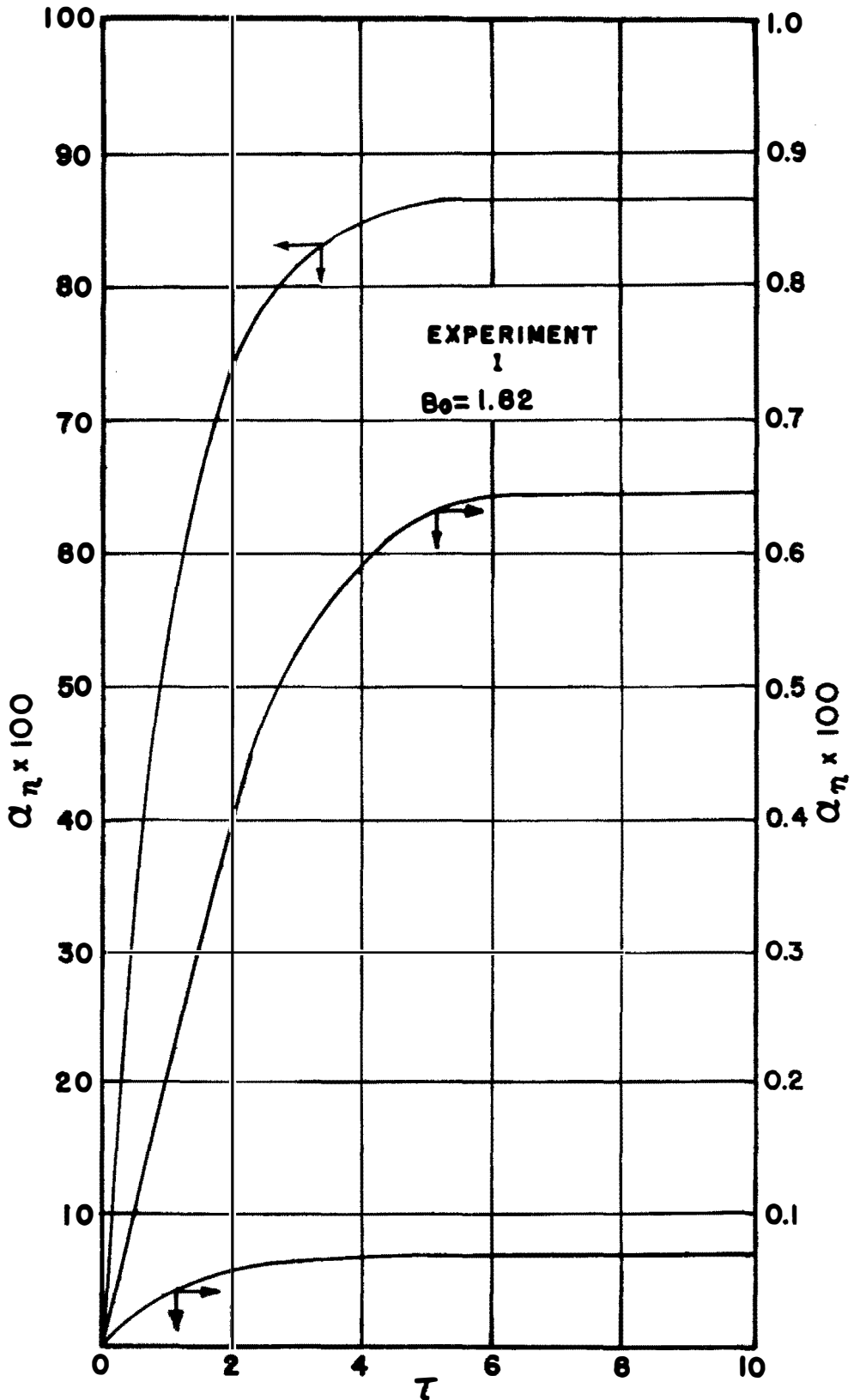


FIGURE 25 CONCENTRATION-TIME CURVES FROM ANALOGUE COMPUTER

$$\text{Pot setting} = \frac{DN^2}{x_f^2 \left[k B_0 + 2 \frac{DN^2}{x_f^2} \right]} \cdot 10 \quad (\text{C.9})$$

and all the values except B_0 in the expression on the right are taken to be constant. The pot settings 0.062, 0.01, and 0.62 correspond respectively to B_0 equal to 1.82, 11.74, and 0.17. Figures 25, 26, and 27 show the results of the three experiments. The dimensionless concentration, α , decreases very rapidly away from the interface. The results show that steady-state is reached quickly (10^{-3} seconds).

2. Second order chemical reaction.

The equations to consider here are the dimensionless forms of equations 3.2 and 3.3 given in Appendix B.

$$\frac{\partial \alpha}{\partial \gamma} = \frac{\partial^2 \alpha}{\partial x^2} - K_1 \alpha \beta \quad (\text{C'.1})$$

$$\frac{\partial \beta}{\partial \gamma} = K_2 \frac{\partial^2 \beta}{\partial x^2} - K_3 \alpha \beta \quad (\text{C'.2})$$

Recall that for $x_f = 10^{-2}$ cm

$$K_1 = \frac{k B_0 x_f^2}{D_A} = \frac{B_0}{6} \cdot 10^8 = \frac{N_0}{6} \cdot 10^5 \quad (\text{C'.3})$$

where

N_0 = initial MEA concentration in moles/liter

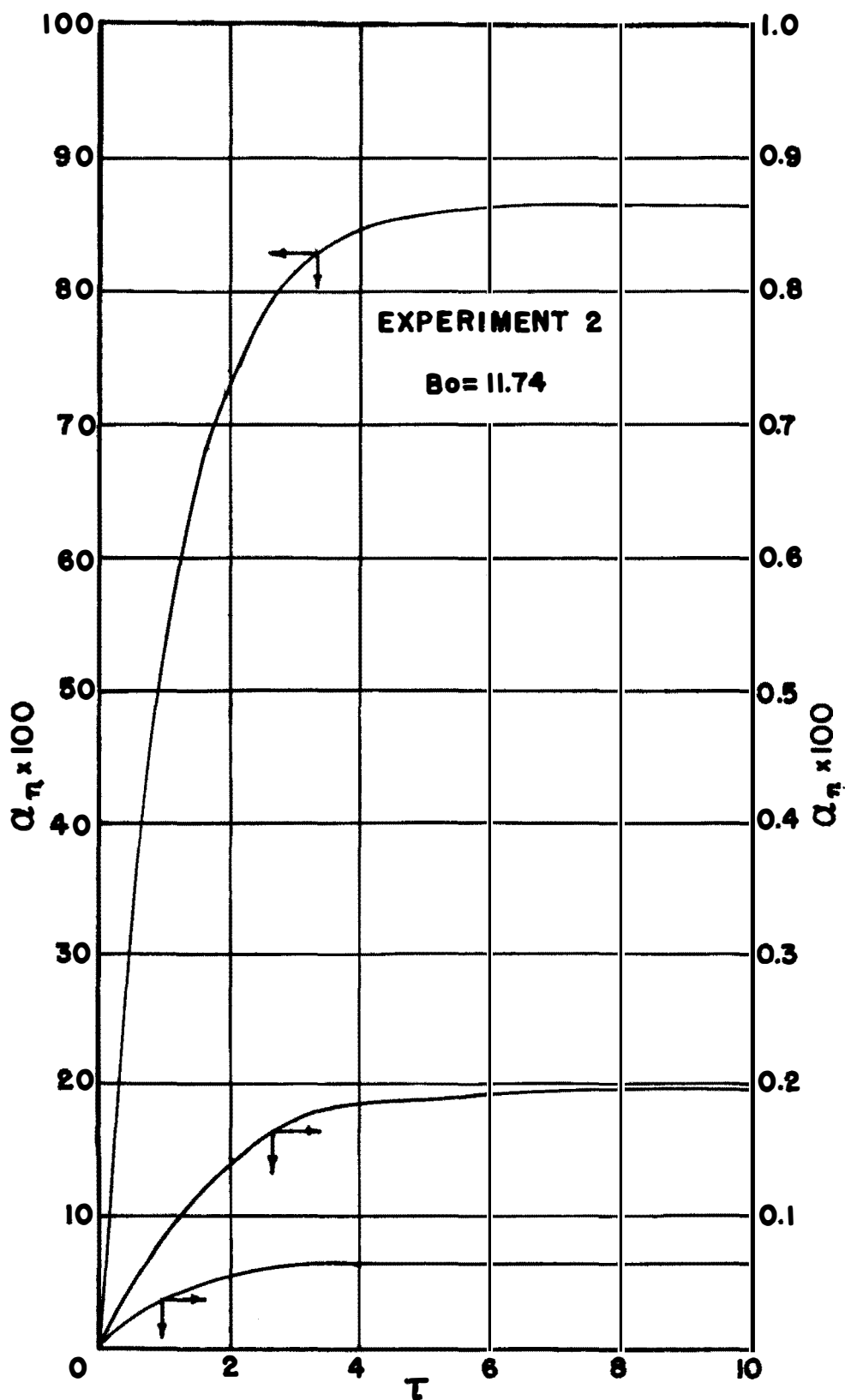


FIGURE 26 ANALOGUE RESULTS

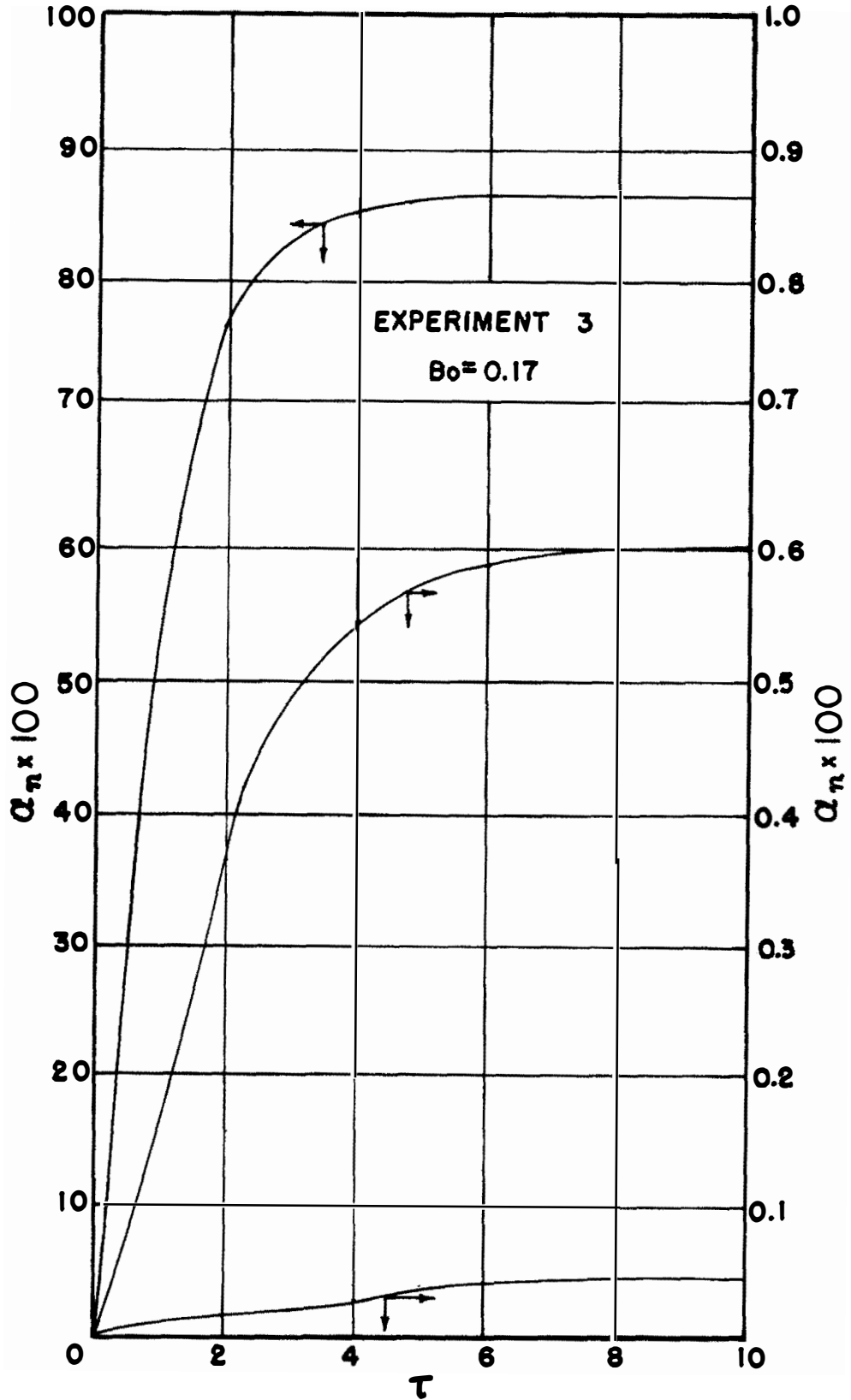


FIGURE 27 ANALOGUE RESULTS

$$K_2 = \frac{D_B}{D_A} = \frac{1}{4} \quad (C'.4)$$

and

$$K_3 = \frac{k A_1 x_f^2}{D_A} = \frac{A_1}{6} \cdot 10^8 \quad (C'.5)$$

In Appendix B, A_1 was assumed to be 3.78×10^{-5} gm moles/cm³. In the present section, A_1 was 4×10^{-5} so that $K_3 = 2/3 \times 10^3$.

Now C'.1 and C'.2 are written in finite difference form

$$\frac{\partial \alpha_n}{\partial t} = \frac{1}{(\Delta X)^2} (\alpha_{n+1} - 2\alpha_n + \alpha_{n-1}) - K_1 \alpha_n \beta_n \quad (C'.6)$$

$$\frac{\partial \beta_n}{\partial t} = \frac{K_2}{(\Delta X)^2} (\beta_{n+1} - 2\beta_n + \beta_{n-1}) - K_3 \alpha_n \beta_n \quad (C'.7)$$

with two such equations written for each interior point in the region of interest ($0 < X < 1$). Notice that a function multiplier is needed for each pair of equations. The computer used has only four multipliers so that the number of increments must be no more than five. The problem was run for the case $N=5$. The boundary conditions were

$$\begin{aligned} \alpha_0(\tau) &= 1 \\ \alpha_5(\tau) &= 0 \\ \alpha_n(0) &= 0 \end{aligned} \quad (C'.8)$$

$$\begin{aligned}\beta_0(\tau) &= \beta_1 \\ \beta_5(\tau) &= 1 \\ \beta_n(0) &= 1\end{aligned}$$

If now the substitutions

$$\alpha = \frac{\alpha'}{100} \quad (c'.9)$$

$$\beta = \frac{\beta'}{100} \quad (c'.10)$$

and

$$t = 100\tau \quad (c'.11)$$

are made, then equations 3.2 and 3.3 become

$$\frac{\partial \alpha'_n}{\partial \tau} = 0.25 \left[\alpha'_{n+1} - 2\alpha'_n + \alpha'_{n-1} \right] - \frac{10 B_0}{6} \alpha'_n \beta'_n \quad (c'.12)$$

$$\frac{\partial \beta'_n}{\partial \tau} = \frac{0.25}{4} \left[\beta'_{n+1} - 2\beta'_n + \beta'_{n-1} \right] - \frac{2}{30} \alpha'_n \beta'_n \quad (c'.13)$$

after assigning the proper values to the constants K_1 , K_2 , and K_3 . The boundary conditions are modified to the extent that

$$\alpha_0(\tau) = \beta_5(\tau) = \beta_n(0) = 100$$

Figure 28 shows the schematic diagram of the network for one pair of equations. The symbol \square denotes a function multiplier. An operating feature of the multiplier is

that its output is minus one hundredth of the product of the inputs. The coefficient potentiometers only multiply by number less than or equal to one. In equation C.8 the coefficient $10 B_0/6$ is generally greater than unity so that it was necessary to use a special network to perform this operation. It is located in the network after the function multiplier on the feedback to the α integrator.

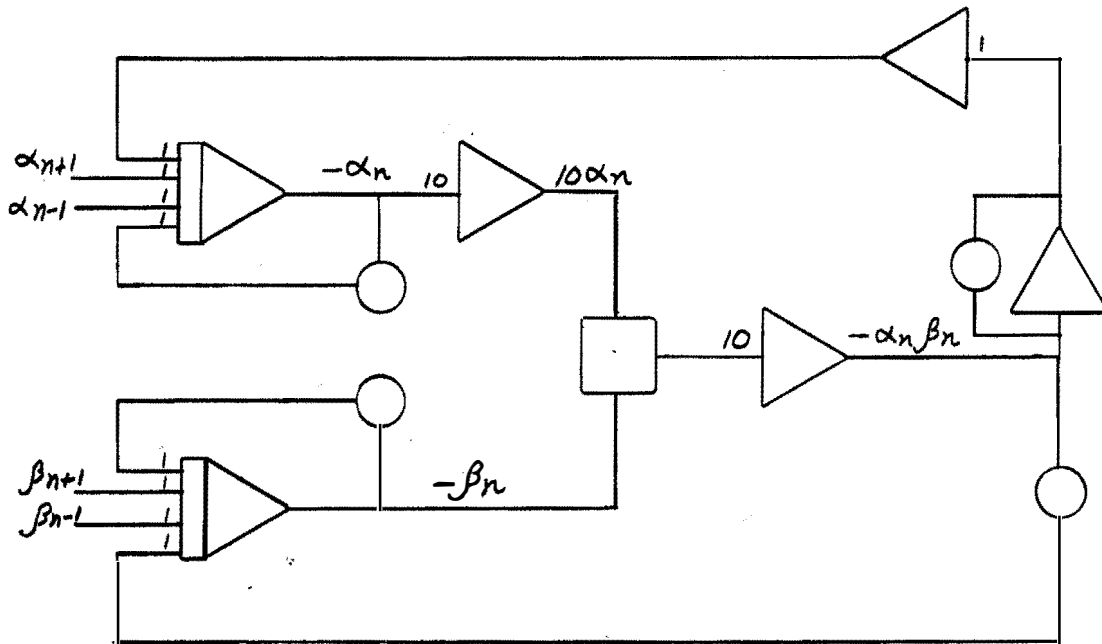


Figure 28. Schematic diagram for analogue solution, second order case.

Solutions were presented in the form of plots of α' and β' versus t at each x in the liquid. A solution was obtained for $B_0=1$. Figure 29 shows the result for $B_0 = 1$.

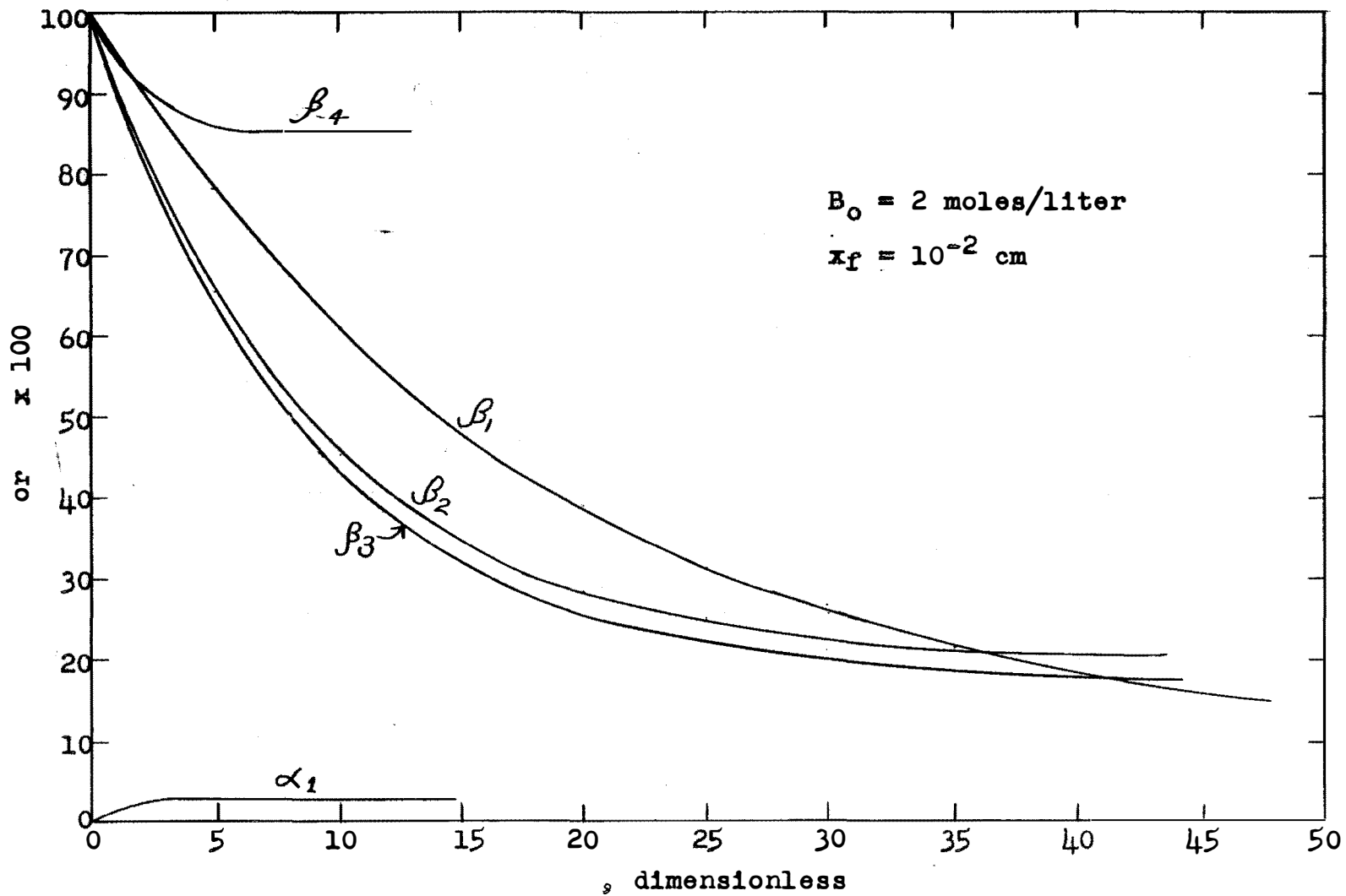


Figure 29. Analogue solution, second order case.

3. Steady-state solution of second-order reaction case.

For this analysis a Pace Analogue Computer (Model 221R) located in the Department of Chemical Engineering was used. The differential equations for steady-state absorption are

$$\frac{d^2\alpha}{dX^2} = K_1\alpha\beta \quad (C'.14)$$

$$K_2 \frac{d^2\beta}{dX^2} = K_3\alpha\beta \quad (C'.15)$$

with the following boundary conditions

$$\begin{aligned} \alpha(0) &= 1 \\ \alpha(1) &= 0 \\ \beta(1) &= 1 \\ \frac{d\beta}{dX} \Big|_{X=0} &= 0 \end{aligned} \quad (C'.16)$$

In order to obtain a solution the initial values of $d\alpha/dX$ and β must be known. Combining equations C.14 and C.15, one obtains

$$\frac{d^2\alpha}{dX^2} = \frac{K_1K_2}{K_3} \frac{d^2\beta}{dX^2} \quad (C'.17)$$

which may be integrated twice to give

$$\alpha = \frac{K_1K_2}{K_3} \beta + C_1 X + C_2 \quad (C.18)$$

where C_1 and C_2 are constants of integration. From the

boundary conditions c'.16 it is seen that

$$c_1 = \left. \frac{d\alpha}{dX} \right]_{X=0} \quad (c'.19)$$

and

$$c_2 = - \frac{K_1 K_2}{K_3} - \left. \frac{d\alpha}{dX} \right]_{X=0} \quad (c'.20)$$

Thus

$$- \left. \frac{d\alpha}{dX} \right]_{X=0} = \frac{K_1 K_2}{K_3} \left[1 - \beta_1 \right] + 1 \quad (c'.21)$$

where β_1 is the value of β at $X=0$. Equation c'.21 was included in the network so that when β_1 was set $\left. \frac{d\alpha}{dX} \right]_{X=0}$ was simultaneously computed and set. The analogue solution involves trial and error in that the proper β_1 must be found so that $\alpha(1)=0$ and $\beta(1)=1$. Once β_1 was found it was easy to compute the absorption rate. Figure 30 shows the circuit diagram.

The parameters K_1 , K_2 , and K_3 , and thus the various pot settings, depend on the values assigned to the physical factors. In this analysis only the film thickness was varied. The diffusivities, reaction rate constant and interfacial concentration of CO_2 were the same as used in Cases 1 and 4 of the digital computer analysis.

Figure 31 shows a typical set of curves for 2 normal MEA. The film thickness used included the ones used in Cases

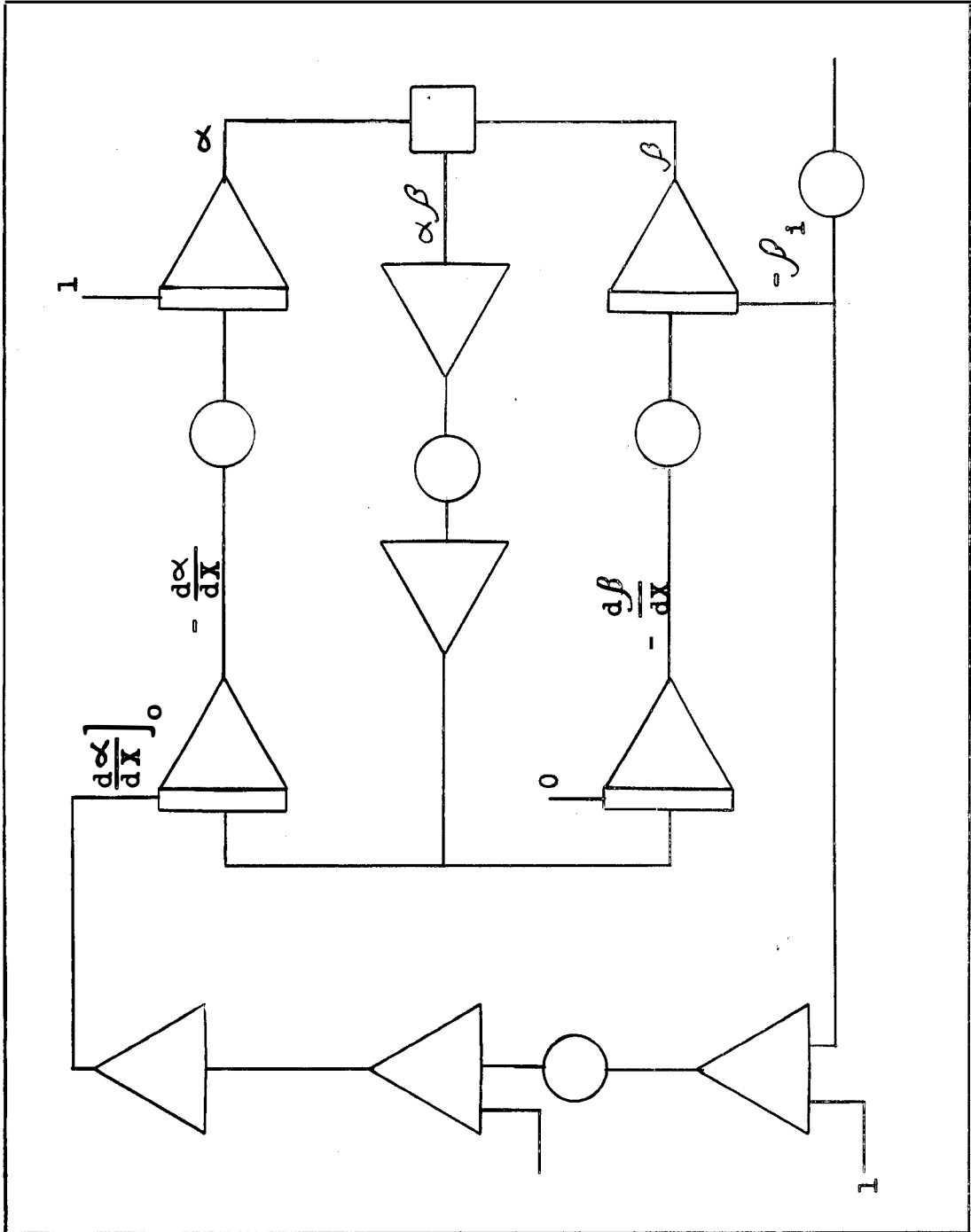


Figure 30. Computer diagram for steady-state solution.

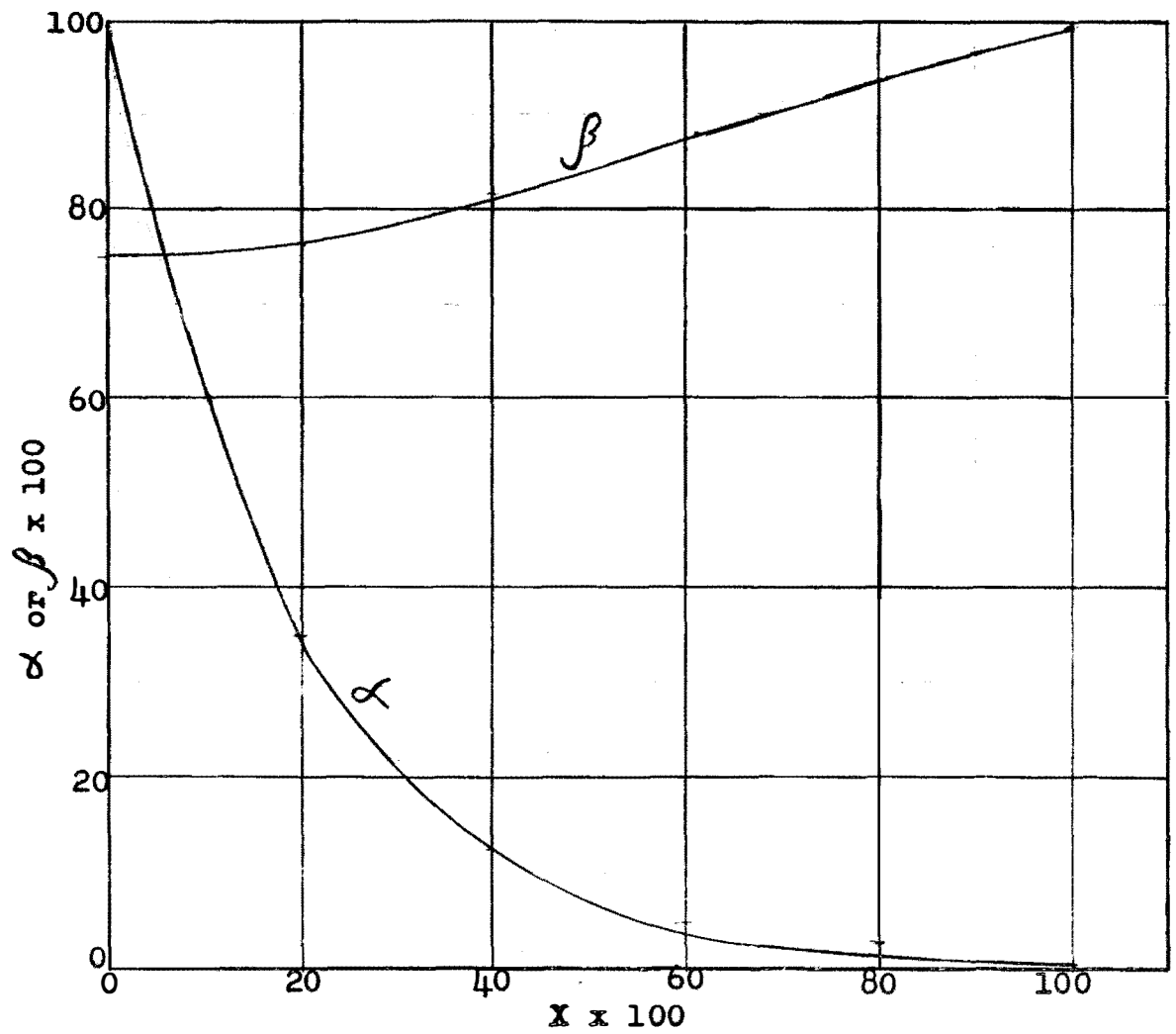


Figure 31. Steady-state concentration profiles,
 $x_f = 3.16 \times 10^{-4}$ cm.

1 and 4, mentioned above. For

$$x_f = 3.16 \times 10^{-4} \text{ cm, } N_A = 1 \times 10^{-5} \text{ gm-moles/cm}^2\text{-sec (Case 1)}$$

$$x_f = 1 \times 10^{-3} \text{ cm, } N_A = 8 \times 10^{-6} \text{ gm-moles/cm}^2\text{-sec}$$

$$x_f = 5 \times 10^{-3} \text{ cm, } N_A = 4 \times 10^{-6} \text{ gm-moles/cm}^2\text{-sec}$$

$$x_f = 1 \times 10^{-2} \text{ cm, } N_A = 1 \times 10^{-6} \text{ gm-moles/cm}^2\text{-sec (Case 4)}$$

The above results are to be compared with the experimental value of 4×10^{-6} .

For academic interest, the steady-solution was found for Cases 5, 6, and 7, run on the digital computer (See Table I for a summary of the cases). It was found that for

$$\text{Case 5, } N_A = 6.64 \times 10^{-6} \text{ gm-moles/cm}^2\text{-sec}$$

$$\text{Case 6, } N_A = 5.16 \times 10^{-6} \text{ gm-moles/cm}^2\text{-sec}$$

$$\text{Case 7, } N_A = 4.4 \times 10^{-6} \text{ gm-moles/cm}^2\text{-sec}$$

APPENDIX D

ANALYSIS OF ERRORS IN DETERMINING BUBBLE SIZE

ANALYSIS OF ERRORS IN DETERMINING BUBBLE SIZE

1. Optical error.

In the following it will be assumed that the camera's lens can be represented by a plane. Figure 31 shows a sketch of the optical paths in which conditions have been slightly exaggerated for the sake of clarity.

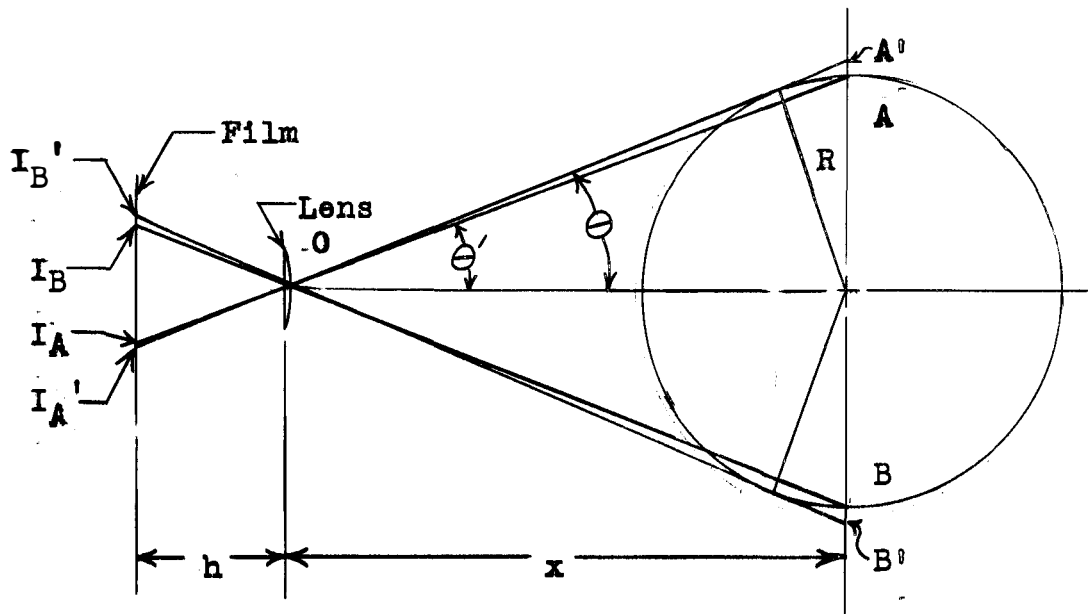


Figure 32. Optical view of bubble.

The film distance h can only be approximated since the lens is actually a system of lenses one behind the other. The other quantities are

$$AB = \text{true bubble diameter} = 2R$$

$A'B'$ = apparent bubble diameter

I_1 = image of point 1

$I_{A'B'}$ = image of apparent bubble diameter

I_{AB} = image of true bubble diameter

The lines I_B, OB' and I_A, OA' were drawn tangential to the bubble and represent the light ray paths. It can be seen that the true bubble diameter is not photographed and the error is represented by the distance

$$\overline{I_A I_{A'}} = \overline{I_B I_{B'}} = 2 \overline{I_A I_{A'}} = I \times 2$$

To determine I the small angle $\theta - \theta'$ must be determined.

Now

$$\sin \theta' = \frac{R}{\sqrt{x^2 + R^2}}, \quad \cos \theta' = \frac{x}{\sqrt{x^2 + R^2}} \quad (D.1)(D.2)$$

and

$$\sin \theta = \frac{R}{x}, \quad \cos \theta = \frac{\sqrt{x^2 - R^2}}{x} \quad (d.3)(D.4)$$

But

$$\sin (\theta - \theta') = \sin \theta \cos \theta' - \cos \theta \sin \theta' \quad (D.5)$$

so that

$$\sin (\theta - \theta') = \frac{Rx - R\sqrt{x^2 - R^2}}{x\sqrt{x^2 + R^2}} \quad (D.6)$$

Some typical values for R and x are

$$x = 5\frac{1}{2} \text{ in.}$$

$$R = 0.06 \text{ in.}$$

which makes

$$\sin (\theta - \theta') = 1.205 \times 10^{-6} \text{ radians} \quad (\text{D.7})$$

Thus

$$\Delta I = h (\theta - \theta')$$

$$h \approx 1 \text{ in.}$$

$$\Delta I = 1.2 \times 10^{-6} \text{ in.}$$

For percentage error a value for $I_{A'B'}$ = 0.04 in. will be used. It was determined directly from the film using calipers and a scale.

Therefore

$$\begin{aligned} \% \text{ Error} &= 1.2 \times 10^{-6} / 0.04 \times 100 \\ &= 0.003 \end{aligned}$$

which may be taken as insignificant.

2. Bubble motion.

While the pictures were being taken the bubbles would oscillate toward and away from the column. In so doing the apparent image would become correspondingly larger or smaller. Again with reference to Figure 31, it can be seen that

$$\frac{I_{AB}}{h} = \frac{AB}{x} \quad (\text{D.10})$$

or

$$d I_{AB} = \frac{h \cdot AB}{x^2} dx \quad (D.10)$$

$$\Delta I_{AB} = \frac{h \cdot AB}{x^2} \Delta x \quad (D.11)$$

Using the numbers from Section 1 of this appendix

$$\Delta I_{AB} \approx - \frac{(1 \text{ in.}) \cdot (2 \cdot 0.06 \text{ in.})}{(5.5)^2 \text{ in.}^2} \Delta x$$

$$\Delta I_{AB} = 0.004 \Delta x$$

During the worst cases the bubble would oscillate across the depth of field which was about 9/16 in. or 9/32 in. on each side of the midpoint.

Thus

$$\Delta I_{AB} = 0.004 \times 9/32 = 1.1 \times 10^{-3} \text{ in.}$$

The

$$\% \text{ Error} = \frac{1.1 \times 10^{-3}}{0.04} \times 100 = 2.8$$

which is significant. Remember that this is the error in the determination of the diameter of a bubble. The next step is to determine the subsequent error in the determination of the mass of the bubble. Recall that the mass of the bubble was calculated assuming that the bubble was an oblate spheroid.

If

a = horizontal radius of bubble

b = vertical radius of bubble

then the volume of a bubble is

$$v = \text{volume of bubble} = \frac{4}{3} \pi a^2 b$$

The mass of the bubble (n) will be some constant times the volume, i.e.,

$$n = k \times a^2 b$$

where

$$k = \text{constant}$$

But of interest here is

$$n^{1/3} = k^{1/3} \times a^{2/3} \times b^{1/3}$$

Differentiation gives

$$d(n^{1/3}) = k^{1/3} \left(\frac{2}{3}\right) \frac{b^{1/3} da}{a^{1/3}} + k^{1/3} \left(\frac{1}{3}\right) \frac{a^{2/3} db}{b^{2/3}} \quad (\text{D.12})$$

or

$$\Delta (n^{1/3}) \approx k^{1/3} \left[\frac{2}{3} \frac{b^{1/3}}{a^{1/3}} \Delta a + \frac{1}{3} \frac{a^{2/3}}{b^{2/3}} \Delta b \right] \quad (\text{D.13})$$

and thus

$$\frac{\Delta (n^{1/3})}{n^{1/3}} = \frac{2}{3} \frac{\Delta a}{a} + \frac{1}{3} \frac{\Delta b}{b} \quad (\text{D.14})$$

But

$$\frac{\Delta a}{a} = \frac{\Delta b}{b} \quad (\text{D.15})$$

therefore

$$\frac{\Delta (n^{1/3})}{n^{1/3}} = \frac{\Delta a}{a} = \frac{\Delta b}{b} \quad (\text{D.16})$$

which says that the error in $n^{1/3}$ is equal to the error in the horizontal or vertical diameter, that is, 2.8 per cent.

3. Oblate spheroid versus spherical geometry.

Equation 3.38 in Chapter III was derived with the assumption that the bubble was a true sphere. However, as was pointed out there, the bubble is actually an oblate spheroid. It is desired to see the error introduced into equation 3.38 by the assumption of spherical geometry.

Let A = area of oblate spheroid

A_s = area of sphere

V = volume of oblate spheroid

V_s = volume of sphere

Then, using the notation of the previous section:

$$A = 2\pi \left[a^2 + \frac{ab^2}{\sqrt{a^2-b^2}} \ln \frac{\sqrt{a^2-b^2} + a}{b} \right] \quad (D.17)$$

$$A_s = 4\pi a^2 \quad (D.18)$$

$$V = 4/3 \pi a^2 b \quad (D.19)$$

$$V_s = 4/3 \pi a^3 = 4/3 \pi b^3 \quad (D.20)$$

Now $a > b$ but $a/b = 1 + \Delta$ where Δ is less than 1. This is an experimental fact and of course is not generally true. Equation D.17 can be rewritten in terms of Δ

$$A = 2\pi b^2 \left[1 + 2\Delta + \Delta^2 + \frac{1 + \Delta}{\sqrt{2\Delta + \Delta^2}} \ln(\sqrt{2\Delta + \Delta^2} + 1 + \Delta) \right] \quad (D.21)$$

or

$$A = 2\pi a^2 \left[1 + \frac{1}{(1 + \Delta)\sqrt{2\Delta + \Delta^2}} \ln(\sqrt{2\Delta + \Delta^2} + 1 + \Delta) \right] \quad (D.22)$$

Now if the area of the sphere is based on a (rather than b)

$$A = \frac{A_s}{2} \left[1 + \frac{1}{(1 + \Delta)\sqrt{2\Delta + \Delta^2}} \ln(\sqrt{2\Delta + \Delta^2} + 1 + \Delta) \right] \quad (D.23)$$

For convenience, define

$$F = 1 + \frac{1}{(1 + \Delta)\sqrt{2\Delta + \Delta^2}} \ln(\sqrt{2\Delta + \Delta^2} + 1 + \Delta) \quad (D.24)$$

Referring back to equation 3.34, the starting point for the

derivation of equation 3.38,

$$\frac{dn}{dt} = -N_A \cdot \text{area} \quad (\text{D.25})$$

where D.25 now becomes

$$\frac{dn}{dt} = -N_A \left(\frac{4\pi a^2}{2} \right) \cdot F \quad (\text{D.26})$$

Before integration, a must be written in terms of the volume as before. Now, however, the volume of the ellipsoid must be used.

$$V = (4/3) \pi a^2 b \quad (\text{D.27})$$

while

$$V_s = (4/3) \pi a^3 \quad (\text{D.28})$$

but

$$b = a/1 + \Delta \quad (\text{D.29})$$

and

$$V = \frac{(4/3)\pi a^3}{1 + \Delta} = \frac{V_s}{1 + \Delta} \quad (\text{D.30})$$

Now introducing the ideal gas law one can solve for a^2 ,

$$V = \frac{4/3 \pi a^3}{1 + \Delta} = \frac{n R \Theta'}{P} \quad (\text{D.31})$$

and

$$a^2 = \left(\frac{n R \Theta'}{P} \right)^{2/3} (1 + \Delta)^{2/3} (3/4 \pi)^{2/3} \quad (\text{D.32})$$

Substitution of D.32 into D.26 gives

$$\frac{dn}{dt} = - N_A 2 \pi \left(\frac{n R \theta'}{P} \right)^{2/3} (1 + \Delta)^{2/3} \left(\frac{3}{4\pi} \right)^{2/3} \cdot F \quad (D.33)$$

If one defines $F' = (1 + \Delta)^{2/3} F$, integrating D.33 will give

$$\frac{1}{3} (n^{1/3} - n_0^{1/3}) = 2 \left(\frac{R \theta'}{P} \right)^{2/3} \left(\frac{3}{4\pi} \right)^{2/3} (T)(F') \quad (D.34)$$

only if F' is a constant. In Table III are presented the a and b values and the Δ values for Take 4 Reel 6. The take was chosen without design, and it is believed to be typical of the results obtained in the present investigation. Notice that the Δ 's range from 0.27 to 0.04. The arithmetic average is 0.12. For $\Delta = 0.27$, $F' = 2.02$ and $\Delta = 0.04$, $F' = 1.987$, a deviation of 1.7 per cent with an average value of about two. The reader will notice that the slope in equation D.34 apart from the F' factor is one-half that in equation 3.38; so that the value of two for F' cancels with the one-half and the slope remains unchanged. In Table IV are recorded the F' values for each Δ given in Table III.

Consequently the conclusion is made that the assumption of spherical geometry introduces little error into equation 3.38. Further, the $n^{1/3}$ was computed by $4/3 \pi a^2 b$ so

TABLE III
 APPARENT HORIZONTAL AND VERTICAL DIAMETERS AND
 THEIR RATIO, REEL 6 TAKE 4

Time 10^{-2} sec	AHD* 10^{-2} inch	AVD* 10^{-2} inch	$\frac{\text{AHD}}{\text{AVD}} = 1 + \Delta$	Δ
0	86	67.5	1.27	0.27
4	76	69.5	1.09	.09
7.5	76	64	1.19	.19
10	75	67	1.12	.12
15	74	64	1.16	.16
20	70.5	62	1.14	.14
25	68	60	1.14	.14
30	65	59	1.10	.10
35	62.5	55	1.14	.14
40	59	54.5	1.09	.09
45	56	52.5	1.07	.07
50	55	50	1.10	.10
55.5	51	47	1.09	.09
60	47.2	45	1.05	.05
66	45	43.5	1.04	.04
70	43.5	41.8	1.05	.05
75	41	38.5	1.06	.06
80	37.5	36	1.04	.04
85	35.5	33	1.08	.08
90	33.2	32	1.04	.04
100	29	27.5	1.05	.05
110	26.5	25.5	1.04	.04

*AHD = apparent horizontal diameter.
 AVD = apparent vertical diameter.

TABLE IV
 F' VALUES FOR REEL 6 TAKE 4

<u>Time</u> <u>1/100 sec</u>	<u>Δ</u>	<u>F'</u>
0	0.27	1.99
4	.09	1.99
7.5	.19	2.00
10	.12	2.01
15	.16	2.16
20	.14	2.02
25	.14	2.02
30	.10	2.01
35	.14	2.02
40	.09	1.99
45	.07	2.00
50	.10	2.01
55.5	.09	1.99
60	.05	2.00
66	.04	2.01
70	.05	2.00

that the results obtained from the plots are a little better than inferred from equation 3.38.

APPENDIX E

SAMPLE CALCULATIONS AND EXPERIMENTAL DATA

SAMPLE CALCULATIONS AND EXPERIMENTAL DATA

All of the original data are recorded on pages 15628-15650, 23751-23800, and 10551-10600 of Original Record of Research Notebooks located in the office of Professor H. F. Johnson, Department of Chemical Engineering, University of Tennessee.

The mass of the bubbles was determined assuming that the bubbles were oblate spheroids. An oblate spheroid is a surface generated by the rotation of an ellipse about its minor axis. In the case here the minor axis was vertical or parallel to the MEA flow. In the notebooks the following nomenclature was used:

V = volume of bubble

AHD = apparent horizontal diameter

AVD = apparent vertical diameter

THD = true horizontal diameter

TVD = true vertical diameter

ACD = apparent capillary tube diameter

TCD = true capillary tube diameter

The capillary tube appeared in the photographs, and its diameter was measured so that the magnification factor could be determined. The true diameter was taken to be the average of ten measurements, namely 0.2547 inches. Thus

$$\text{THD} = \frac{0.2547}{\text{ACD}} \times \text{AHD} \quad (\text{E.1})$$

and

$$\text{TVD} = \frac{0.2547}{\text{ACD}} \times \text{AVD} \quad (\text{E.2})$$

For an oblate spheroid

$$\begin{aligned} V &= \frac{4}{3} \pi (\text{THD}/2)^2 (\text{TVD}/2) \\ V &= \pi/6 (\text{THD})^2 (\text{TVD}) \end{aligned} \quad (\text{E.3})$$

Substitution of E.1 and E.2 gives finally

$$V = 5.006 \times 10^{-6} \frac{(\text{AHD})^2 (\text{AVD})}{(\text{ACD})^3} \text{ft}^3 \quad (\text{E.4})$$

For computation of the mass the ideal gas law was assumed so that

$$n = \frac{PV}{R\theta} \quad (\text{E.5})$$

where

n = mass of gas in bubble, pound-moles

P = pressure of gas, cm Hg

θ = absolute temperature, °R or °K

R = gas law constant

Since the manometer tap was located about $7\frac{1}{2}$ inches above the bubble the hydrostatic head caused by this column of liquid had to be taken into account. Therefore

$$P = P_A + \Delta P_M - \Delta P_C \quad (\text{E.6})$$

where

P_A = barometric pressure

ΔP_M = manometer pressure

and the factor ΔP_C comes from the above hydrostatic head and the MEA in the manometer arm connected to the absorption cell. The factor will vary somewhat for different MEA solutions because of the change in density.

Finally

$$n = \frac{9.06 \times 10^{-8} (P_A - \Delta P_M - \Delta P_C) (\text{AHD})^2 (\text{AVD})}{\theta' (\text{ACD})^3} \quad (\text{E.7})$$

if θ' is in $^{\circ}\text{R}$. Occasionally AVD was greater than AHD as the bubble's shape fluctuated. Equation E.7 was still used, however.

The procedure was to first determine ACD, AHD, and AVD from the film. These values are recorded in the notebooks mentioned in the first paragraph, but they are not included in this report. By equation E.7 the mass of the bubbles was computed and these values are recorded in Tables III, IV, V, VI, VII, VIII, and IX, where B_0 is the initial MEA concentration in moles per liter, θ is the temperature in degrees centigrade, C is the CO_2 concentration in grams per liter, T is time in seconds and n is in pound moles.

TABLE V

EXPERIMENTAL DATA
REEL 3, $B_0 = 1.49$

$T \times 10^2$ sec	$n \times 10^9$ lb-moles	$T \times 10^2$ sec	$n \times 10^9$ lb-moles	$T \times 10^2$ sec	$n \times 10^9$ lb-moles
<u>Take 3</u> $\theta = 24.5^\circ\text{C}$ $C = 1.25$ gms/l		<u>Take 5 (cont'd)</u>		<u>Take 7 (cont'd)</u>	
0	1.535	18	.573	110	.116
2	1.58	23	.418	115	.081
6	1.68	28	.4325		
13	1.45	34	.373	<u>Take 9</u> $\theta = 24.5^\circ\text{C}$ $C = 3.30$ gms/l	
16	1.405	40	.344	0	1.38
22.5	1.39	48	.294	3	1.43
28	1.12	53	.1697	6	1.345
33	0.81	58	.145	10	1.21
38	.917	66	.145	15	1.025
43	.956	71	.145	20	0.995
49	.618	78	.145	25	.891
53	.388	<u>Take 7</u> $\theta = 24.5^\circ\text{C}$ $C = .240$ gms/l		30	.864
58	.547	0	1.025	38	.737
63	.515	3	1.27	45	.728
68	.515	9	1.08	52	.602
73	.292	11.5	1.142	59	.470
78	.314	14	1.41	63	.480
83	.349	17	1.11	70	.417
88	.268	25	0.65	75	.322
93	.1925	30	.65	80	.307
98	.220	35	.59	85	.294
103	.156	40	.534	90	.261
108	.213	45	.569	95	.244
113	.142	50	.349	100	.188
118	.197	55	.349	105	.150
<u>Take 5</u> $\theta = 24.5^\circ\text{C}$ $C = 1.70$ gms/l		65	.39	110	.160
0	1.22	71	.298	115	.1508
2	1.045	77.5	.274	120	.1072
6	0.81	85	.308	125	.085
11.5	.694	90	.192	130	.1182
15	.673	95	.151	135	.050
		100	.128	138	.046
		105	.159		

TABLE V (continued)

$T \times 10^2$ sec	$n \times 10^9$ lb-moles	$T \times 10^2$ sec	$n \times 10^9$ lb-moles	$T \times 10^2$ sec	$n \times 10^9$ lb-moles
<u>Take 11</u> $\theta = 24.5^\circ\text{C}$ $C = 4.46 \text{ gms/l}$		<u>Take 15 (cont'd)</u>		<u>Take 21</u> $\theta = 24.5^\circ\text{C}$ $C = 8.85 \text{ gms/l}$	
0	1.39	68	0.3935	0	1.42
3	1.105	73	.345	5	1.035
10	0.965	78	.237	15	0.943
18	.796	83	.236	20	.982
23	.682	88	.249	25	.834
28	.660	93	.204	30	.725
33	.604	98	.193	35	.585
38	.635	103	.158	40	.543
39	.510	108	.145	45	.520
43	.510	113	.0965	50	.520
48	.445	118	.0872	55	.446
53	.400	<u>Take 17</u> $\theta = 24.5^\circ\text{C}$ $C = 6.85 \text{ gms/l}$		60	.417
58	.368	0	1.68	65	.419
63	.282	3	1.315	70	.376
68	.256	9	1.205	75	.346
73	.226	14	1.07	80	.301
78	.160	19	1.01	85	.249
83	.111	25	0.829	90	.261
<u>Take 15</u> $\theta = 24.5^\circ\text{C}$ $C = 5.73 \text{ gms/l}$		29	.761	95	.236
0	1.44	34	.626	100	.173
3	1.3	39	.670	105	.1735
8	1.22	44	.399	110	.196
13	1.13	49	.461	115	.146
18	0.954	53	.433	125	.114
23	.970	56	.298	130	.125
28	.840	59	.354	134	.097
33	.721	64	.433	140	.070
38	.748	79	.313	155	.0342
43	.735	89	.236	161	.0514
47	.582	99	.222		
51	.550	104	.1595		
55	.573	109	.215		
58	.501	119	.150		
63	.436				

TABLE VI
EXPERIMENTAL DATA
REEL 4, $B_0 = 1.95$

$T \times 10^2$ sec	$n \times 10^9$ lb-moles	$T \times 10^2$ sec	$n \times 10^9$ lb-moles	$T \times 10^2$ sec	$n \times 10^9$ lb-moles
<u>Take 2</u> $\theta = 25^\circ\text{C}$ $C = 1.07 \text{ gms/l}$		<u>Take 3 (cont'd)</u>		<u>Take 4 (cont'd)</u>	
0	1.44	9	0.890	67	.2422
0.5	1.38	13	.810	72	.248
3	1.379	18	.711	75	.202
8	1.149	24	.622	77	.201
9	1.20	28	.541	82	.156
13	1.095	33	.504	87	.124
18	1.058	38	.403	92	.0905
19	1.025	43	.369	98	.0784
23	0.799	48	.334	102	.0622
28	.791	53	.254	<u>Take 6</u> $\theta = 25^\circ\text{C}$ $C = 5.01 \text{ gms/l}$	
33	.737	58	.241	0	1.154
40	.603	63	.196	2	1.076
43	.480	68	.147	6	1.006
45	.443	73	.138	11	0.955
48	.424	77	.130	17	.856
53	.436	93	.078	22	.801
58	.319	98	.0658	27	.697
59	.326	132	.0350	32	.625
63	.326	<u>Take 4</u> $\theta = 25^\circ\text{C}$ $C = 3.66 \text{ gms/l}$		37	.508
68	.270	0	1.380	42	.496
72	.2237	2	1.269	47	.430
77	.193	7	1.027	52	.371
83	.1586	15	0.911	57	.331
88	.1206	18	.870	62	.295
93	.1128	22	.818	67	.236
98	.0830	27.5	.735	71	.218
108	.0518	32	.637	76	.194
<u>Take 3</u> $\theta = 25^\circ\text{C}$ $C = 1.92 \text{ gms/l}$		37	.581	81	.173
0	1.231	42	.517	86.5	.139
1	1.164	47	.444	92	.113
5	0.9724	52	.412	97	.100
		57	.339	107	.0673
		62	.291	117	.0548

TABLE VI (continued)

$T \times 10^2$ sec	$n \times 10^9$ lb-moles	$T \times 10^2$ sec	$n \times 10^9$ lb-moles	$T \times 10^2$ sec	$n \times 10^9$ lb-moles
<u>Take 8</u> $\theta = 25^\circ\text{C}$ $C = 7.90$ gms/l		<u>Take 11 (cont'd)</u>		<u>Take 15</u> $\theta = 26^\circ\text{C}$ $C = 12.55$ gms/l	
0	1.066	65	.257	0	1.526
4	0.818	70	.267	2	1.480
11	.724	75	.223	7	1.187
14	.662	80	.182	12	1.140
18	.631	85	.170	17	0.983
23	.543	93	.134	22	.935
28	.526	106.5	.0980	27	.815
31	.454	125	.0634	32	.819
34	.440	<u>Take 13</u> $\theta = 26^\circ\text{C}$ $C = 10.73$ gms/l		37	.691
38	.374	0	1.302	42	.582
43	.343	4	1.225	47	.574
48	.339	8	1.086	52	.479
54	.236	12	0.963	57	.442
58	.224	17	.921	67	.377
63	.188	22	.885	77	.308
68	.157	28	.734	87	.242
78	.150	32	.652	97	.202
83	.115	37	.632	107	.137
88.5	.077	42	.570	117	.0921
<u>Take 11</u> $\theta = 25^\circ\text{C}$ $C = 9.97$ gms/l		48	.489	<u>Take 17</u> $\theta = 26^\circ\text{C}$ $C = 13.96$ gms/l	
0	1.353	52	.429	0	1.226
2	1.225	58	.362	1.5	1.218
5	1.176	62	.331	5	1.126
10	0.940	67	.268	10	0.977
15	.797	72	.252	15	.979
20	.805	77	.228	20	.962
25	.667	82	.184	25	.722
30	.581	87	.156	30	.708
35	.574	92	.142	35	.618
40	.521	97	.0938	40	.563
45	.462	105	.0843	45	.532
50	.416	117	.0532	50	.427
55	.365	122	.0438	55	.423
60.5	.304			60	.389

TABLE VII
 EXPERIMENTAL DATA
 REEL 6, $B_0 = 2.97$

$T \times 10^2$ sec	$n \times 10^9$ lb-moles	$T \times 10^2$ sec	$n \times 10^9$ lb-moles	$T \times 10^2$ sec	$n \times 10^9$ lb-moles
<u>Take 2</u> $\theta = 27^\circ\text{C}$ $C = 2.18$ gms/l		<u>Take 3(1)(cont'd)</u>		<u>Take 4(cont'd)</u>	
0	1.436	61	0.0830	10	1.122
7.5	1.115	67	.0630	15	1.043
10	1.071	71	.0554	20	0.917
15	0.984	76	.0430	25	.826
20	.772	<u>Take 3(2)</u> $\theta = 27^\circ\text{C}$ $C = 2.80$ gms/l		30	.742
25	.649	0	1.264	35	.639
30	.597	5	1.028	40	.565
35	.425	10	0.952	45	.490
39	.414	15	.839	50	.450
45	.343	20	.688	55.5	.364
50	.278	25	.592	60	.299
55	.231	30	.551	66	.262
59	.206	35	.409	70	.235
65	.152	40	.374	75	.193
71	.110	45	.299	80	.151
75	.0952	50	.287	85	.124
85	.0553	55	.235	90	.105
90	.0039	60	.209	100	.0688
<u>Take 3(1)</u> $\theta = 27^\circ\text{C}$ $C = 2.80$ gms/l		66	.159	110	.0533
0	0.652	70	.135	<u>Take 5(1)</u> $\theta = 27^\circ\text{C}$ $C = 9.29$ gms/l	
8.5	.512	75	.118	0	1.358
11	.513	80	.0869	3	1.200
15	.411	85	.0712	9	0.999
23	.378	90	.0441	13	1.003
26	.320	100	.039	17	0.842
31	.263	<u>Take 4</u> $\theta = 27^\circ\text{C}$ $C = 4.38$ gms/l		23	.587
37	.222	0	1.486	27	.616
40.5	.178	4	1.195	33	.584
46	.138	7.5	1.100	38	.458
51	.110			43	.399
56.5	.0958			48	.322
				53	.294
				58	.202

TABLE VII (continued)

$T \times 10^2$ sec	$n \times 10^9$ lb-moles	$T \times 10^2$ sec	$n \times 10^9$ lb-moles	$T \times 10^2$ sec	$n \times 10^9$ lb-moles
<u>Take 14 (cont'd)</u>		<u>Take 16(1)</u>		<u>Take 16(2)</u>	
		$\theta = 27^\circ\text{C}$		$\theta = 27^\circ\text{C}$	
		$C = 28.06 \text{ gms/l}$		$C = 28.06 \text{ gms/l}$	
110	0.174	0	1.229	0	1.487
116	.148	10	.981	10	1.236
131	.100	15	.919	20	0.863
137	.0736	20	.723	24	1.004
<u>145.5</u>	<u>.0594</u>	25	.754	48	0.614
<u>Take 15</u>		33	.625	55	.484
$\theta = 27^\circ\text{C}$		40	.578	60	.517
$C = 28.06 \text{ gms/l}$		48	.486	64	.429
0	0.916	55	.394	70	.364
3	.953	60	.360	80	.260
9	.916	70	.246	90	.205
15	.780	80.5	.195	95	.184
20	.736	91	.152	100	.172
26	.598	96	.128	105	.135
32	.557	100	.117	<u>110</u>	<u>.0929</u>
39	.523	110.5	.0886		
<u>44.5</u>	<u>.417</u>	120	.0638		
54	.344	<u>130</u>	<u>.0397</u>		
59	.298				
65.5	.267				
73	.213				
79	.182				
89	.143				
94	.117				
99	.105				
105	.0884				
109	.0649				
<u>114</u>	<u>.0460</u>				

TABLE VIII
 EXPERIMENTAL DATA
 REEL 7, $B_D = 1.06$

$T \times 10^2$ sec	$n \times 10^9$ lb-moles	$T \times 10^2$ sec	$n \times 10^9$ lb-moles	$T \times 10^2$ sec	$n \times 10^9$ lb-moles
<u>Take 2</u> $\theta = 25^\circ\text{C}$ $C = 15.54$ gms/l		<u>Take 4</u> $\theta = 25^\circ\text{C}$ $C = 1.55$ gms/l		<u>Take 6 (cont'd)</u>	
0	1.775	0	1.754	36	0.866
4	1.770	7	1.062	44	.759
16.5	1.470	17	1.098	54	.617
24	1.341	27	0.887	64	.706
39	1.457	37	.640	66	.617
44	1.296	47	.566	74	.533
59	1.232	62	.466	84	.444
74	1.102			93	.370
89	1.012	<u>Take 5</u> $\theta = 25.5^\circ\text{C}$ $C = 2.05$ gms/l		104	.306
104	0.845	0	1.309	114	.239
114	.721	2	1.413	124	.191
124	.736	12.5	1.209	134	.158
134	.786	23	0.951	139	.140
145	.689	32	.726	144	.140
154	.648	42	.634	<u>Take 7</u> $\theta = 26^\circ\text{C}$ $C = 1.77$ gms/l	
164	.589	53	.454	0	1.373
174	.545	62.5	.402	11	1.112
194	.461	72	.367	22	0.845
		82	.316	31	.631
		92	.229	41	.566
		102	.224	51	.485
		127.5	.152	61	.350
				66	.331
		<u>Take 6</u> $\theta = 25.8^\circ\text{C}$ $C = 2.05$ gms/l		71	.318
		0	2.010	88.5	.230
		4	1.493	101	.152
		14	1.229	<u>Take 8(1)</u> $\theta = 26^\circ\text{C}$ $C = 2.67$ gms/l	
		19	1.161	0	1.798
		24	1.055	1.5	1.671
		29	0.952	4	1.443
				14	1.210

TABLE VIII (continued)

$T \times 10^2$ sec	$n \times 10^9$ lb-moles	$T \times 10^2$ sec	$n \times 10^9$ lb-moles	$T \times 10^2$ sec	$n \times 10^9$ lb-moles
<u>Take 8(1)(cont'd)</u>		<u>Take 9(cont'd)</u>		<u>Take 12</u> $\theta=27^\circ\text{C}$ $C=5.28$ gms/l	
24	0.839	60	0.313	0	0.886
34	.739	70	.206	10	.827
44	.695	80	.168	20	.669
54	.606			30	.640
64	.578	<u>Take 11</u> $\theta=27^\circ\text{C}$ $C=3.73$ gms/l		40	.540
74	.506			49.5	.508
84	.398	0	1.882	60	.446
101	.306	10	1.658	70	.330
104	.310	21	1.029	78	.301
114	.234	30.5	0.927	96	.236
124	.191	40	.846	110	.155
<u>Take 8(4)</u> $\theta=26^\circ\text{C}$ $C=2.67$ gms/l		50	.747	120	.131
0	2.203	60	.676	<u>Take 13(1)</u> $\theta=26.5^\circ\text{C}$ $C=5.28$ gms/l	
4.5	1.894	70	.628	0	1.571
9	1.486	80	.494	10	1.323
18.5	1.403	90.5	.416	20	1.062
39	1.095	100	.336	30	0.862
49	0.829	110	.276	40	.749
59	.679	120	.240	50	.701
69	.638	130	.175	60	.610
79	.520	140	.172	70	.565
89	.424	150	.156	<u>Take 13(2)</u> $\theta=26.5^\circ\text{C}$ $C=5.28$ gms/l	
99	.322	160	.122	0	1.582
109	.204	170	.107	9	1.441
129	.139			19	0.808
<u>Take 9</u> $\theta=26.8^\circ\text{C}$ $C=3.35$ gms/l				29	.704
0	0.967				
10	.798				
20	.654				
30	.579				
40	.445				
50	.376				

TABLE IX

EXPERIMENTAL DATA
REEL 8, $B_0 = 6.06$

$T \times 10^2$ sec	$n \times 10^9$ lb-moles	$T \times 10^2$ sec	$n \times 10^9$ lb-moles	$T \times 10^2$ sec	$n \times 10^9$ lb-moles
<u>Take 1</u> $\theta = 25^\circ\text{C}$ $C = 0.65$ gms/l		<u>Take 3</u> $\theta = 25.5^\circ\text{C}$ $C = 5.80$ gms/l		<u>Take 4(2)(cont'd)</u>	
0	1.190	0	1.413	16.5	1.092
9.5	0.868	5	1.149	27	0.851
15	.772	10.5	0.888	37	.759
25	.617	15	.888	47	.656
35	.452	19.5	.757	57	.530
45	.314	25	.590	67	.426
55	.178	30	.578	77	.311
65	.137	35	.526	87	.196
75	.0931	45	.457	97.5	.144
		55	.324	107	.102
		65	.226		
		75	.155	<u>Take 5</u> $\theta = 25^\circ\text{C}$ $C = 12.36$ gms/l	
		85	.0932	0	1.620
<u>Take 2</u> $\theta = 25^\circ\text{C}$ $C = 2.56$ gms/l		<u>Take 4(1)</u> $\theta = 24.5^\circ\text{C}$ $C = 12.36$ gms/l		6	1.336
0	1.509	0	0.989	9.5	1.114
5	1.201	16	.750	20	1.051
10	1.091	27	.739	30	0.883
15	0.978	36	.608	35	.787
20	.777	46	.471	40	.709
25	.754	56	.416	50	.583
30	.610	67	.269	60	.460
35	.566	76	.197	70	.349
40	.486	86	.131	80	.270
45	.458	96	.0977	90.5	.173
50	.364			100.5	.106
56	.304			111	.0800
60	.271				
64.5	.211			<u>Take 6</u> $\theta = 24^\circ\text{C}$ $C = 15.53$ gms/l	
70.5	.179			0	1.647
81	.104			9.5	1.076
90	.0608			20	0.940
		<u>Take 4(2)</u> $\theta = 24.5^\circ\text{C}$ $C = 12.36$ gms/l			
		0	1.625		
		7	1.194		

TABLE IX (continued)

$T \times 10^2$ sec	$n \times 10^9$ lb-moles	$T \times 10^2$ sec	$n \times 10^9$ lb-moles	$T \times 10^2$ sec	$n \times 10^9$ lb-moles
<u>Take 6(cont'd)</u>		<u>Take 8(1)(cont'd)</u>		<u>Take 9(2)</u> $\theta=25^\circ\text{C}$ $C=19.82$ gms/l	
30	0.673	50	0.497	0	1.573
40	.533	60.5	.407	5	1.330
50	.455	70	.316	15	1.108
60.5	.316	80	.253	25	0.915
70.5	.183	90	.183	35	.759
80	.155	95	.144	45	.613
90	.114	105	.112	55	.479
<u>Take 7</u> $\theta=24.5^\circ\text{C}$ $C=15.53$ gms/l		<u>Take 8(2)</u> $\theta=25^\circ\text{C}$ $C=15.52$ gms/l		65.5	.355
0	1.971	0	1.686	75	.289
5	1.527	10	1.455	85	.210
10	1.246	20	1.101	95.5	.151
20	0.977	30	1.000	105	.129
25	.845	40	0.776	<u>Take 11</u> $\theta=25^\circ\text{C}$ $C=23.03$ gms/l	
30	.790	50	.616	0	1.683
39.5	.642	60	.506	5	1.339
50	.560	70	.397	10	1.125
55	.501	80	.311	20.5	0.955
60	.416	90	.204	30	.750
70	.276	100	.165	40	.668
80	.231	110	.109	49.5	.531
90	.164	<u>Take 9(1)</u> $\theta=25^\circ\text{C}$ $C=19.82$ gms/l		60	.445
100	.108	0	1.137	70	.325
110	.0704	10	0.810	80	.216
<u>Take 8(1)</u> $\theta=25^\circ\text{C}$ $C=15.53$ gms/l		18.5	.723	90	.161
0	1.504	28.5	.610	100	.115
5	1.355	38.5	.477	<u>Take 12</u> $\theta=26^\circ\text{C}$ $C=24.62$ gms/l	
10	1.119	48.5	.391	0	1.584
16	1.027	58.5	.298	5	1.202
20	0.955	68.5	.221	10	1.167
30	.782	78.5	.149		
40.5	.636	88.5	.0885		

TABLE IX (continued)

$T \times 10^2$ sec	$n \times 10^9$ lb-moles	$T \times 10^2$ sec	$n \times 10^9$ lb-moles	$T \times 10^2$ sec	$n \times 10^9$ lb-moles
<u>Take 12 (cont'd)</u>		<u>Take 13(2)(cont'd)</u>		<u>Take 14(2)(cont'd)</u>	
20	1.014	35.5	0.868	98.5	0.129
30	0.8291	45.5	.676	109	.0822
40	.746	55	.534	<u>Take 15(1)</u>	
50	.590	65	.368	$\theta = 25.5^\circ\text{C}$	
59.8	.418	75	.239	$C = 25.85 \text{ gms/l}$	
80	.282	85	.149	0	1.637
90	.175	95	.0847	3	1.450
100	.116	<u>Take 14(1)</u>		8	1.157
110	.0700	$\theta = 26^\circ\text{C}$		13	1.010
<u>Take 13(1)</u>		$C = 25.85 \text{ gms/l}$		18	0.993
$\theta = 27^\circ\text{C}$		0	1.505	28	.679
$C = 24.62 \text{ gms/l}$		5.5	1.238	38	.590
0	1.688	11	1.036	48	.432
2	1.489	20.8	0.973	58	.334
5	1.417	31	.734	68	.242
10	1.074	41	.599	78	.153
15	1.051	51	.479	88	.116
20	0.989	61	.385	98	.0837
25	.887	71.5	.298	<u>Take 15(2)</u>	
30	.795	81	.224	$\theta = 25.5^\circ\text{C}$	
41	.741	91	.164	$C = 25.85 \text{ gms/l}$	
49	.652	100.5	.123	0	1.708
60	.555	111	.0863	6	1.508
70	.437	<u>Take 14(2)</u>		10.5	1.374
80	.331	$\theta = 26^\circ\text{C}$		15	1.237
90	.252	$C = 25.85 \text{ gms/l}$		25	1.000
100	.172	0	1.601	35	0.858
110	.124	9.5	1.154	45	.706
<u>Take 13(2)</u>		19	1.061	55	.614
$\theta = 27^\circ\text{C}$		28.5	0.801	65	.454
$C = 24.62 \text{ gms/l}$		39	.704	75	.371
0	1.612	49	.550	85	.278
5	1.495	59	.436	95	.213
11	1.191	69	.340	105	.163
15	1.147	79	.229	115	.111
25	0.904	89	.172		

TABLE IX (continued)

$T \times 10^2$ sec	$n \times 10^9$ lb-moles	$T \times 10^2$ sec	$n \times 10^9$ lb-moles	$T \times 10^2$ sec	$n \times 10^9$ lb-moles
<u>Take 16</u>		<u>Take 17(1)</u>		<u>Take 17(2)</u>	
$\theta = 24^\circ\text{C}$		$\theta = 25^\circ\text{C}$		$\theta = 25^\circ\text{C}$	
$C = 25.85$ gms/l		$C = 26.28$ gms/l		$C = 26.28$ gms/l	
0	2.150	0	1.738	0	1.646
1.5	1.868	1.5	1.605	5	1.313
6	1.655	5	1.453	10	1.097
10	1.349	10	1.216	20	0.985
15	1.157	14.5	1.083	30	.752
20	1.029	20.5	1.046	40	.655
30.5	0.862	29.5	0.781	50.5	.598
39.5	.820	40	.704	60	.502
50	.695	50.5	.598	70	.366
60	.521	60	.472	80	.290
85	.259	70	.408	90	.209
90	.224	80	.326	100	.170
109.5	.163	90	.244	110	.108
120.5	.115	99.5	.167		
		110	.116		
		120.5	.0791		

In Table X are recorded the a and b values of the equation

$$n^{1/3} = a + bT$$

for each take. The constants were determined by the least squares method which states ultimately that

$$a = \frac{\sum T^2 \sum n - \sum T \sum Tn}{N \sum T^2 - (\sum T)^2} \quad (\text{E.8})$$

$$b = \frac{N \sum Tn - \sum T \sum n}{N \sum T^2 - (\sum T)^2} \quad (\text{E.9})$$

where N = number of points.

Since the absorption rates N_A were determined from b , it is desirable to know how reliable the b values are. The variance $p(b)$ is given by

$$p(b)^2 = \frac{p(n^{1/3})^2}{\sum T^2 - (\sum T)^2/N} \quad (\text{E.10})$$

and $p(n^{1/3})$ is the variance in the $n^{1/3}$ values defined by

$$p(n^{1/3})^2 = \frac{\sum (n^{1/3} - a - bT)^2}{N - 2} \quad (\text{E.11})$$

These equations may be found in any text on statistics or texts devoted to treatment of data. See for example (28) and (46). The variance was not calculated for every b but

TABLE X

LEAST SQUARES PARAMETERS a AND b
AND THE PERCENTAGE VARIANCE IN b

<u>Reel</u>	<u>Take</u>	$a \times 10^3$ <u>lb-moles</u>	$-b \times 10^3$ <u>lb-moles/sec</u>	<u>% p(b)</u>
3	3	1.186	0.605	
	5	0.980	.693	
	7	1.069	.548	
	9	1.116	.534	
	11	1.073	.667	
	15	1.118	.573	
	17	1.073	.512	
	21	1.044	.451	
4	2	1.107	0.680	5.3
	3	1.000	.611	-
	4	1.089	.681	1.0
	6	1.041	.599	-
	8	0.970	.612	1.0
	11	1.038	.565	3.3
	13	1.077	.614	0.0
	15	1.110	.572	-
	17	1.052	.52	-
	18	0.918	.546	-
	21	.956	.544	2.2
	23	1.053	.508	-
	6	2	1.100	0.871
3(1)		0.861	.699	0.0
3(2)		1.043	.755	2.0
4		1.107	.699	0.0
5(1)		1.090	.851	1.4
5(2)		1.111	.743	-
6		1.049	.765	1.5
7		1.029	.641	-
8		1.056	.629	-
9		1.064	.648	0.0
11		1.057	.576	0.0
12(2)		1.056	.609	1.5
13		1.049	.560	-
14		1.146	.530	-
15		1.019	.581	-
16(1)		1.043	.552	-
16(2)	1.126	.590	-	

TABLE X (continued)

<u>Reel</u>	<u>Take</u>	<u>ax10³</u> <u>lb-moles</u>	<u>-bx10³</u> <u>lb-moles/sec</u>	<u>% p(b)</u>
7	2	1.190	0.218	-
	3	1.000	.365	0.0
	4	1.043	.508	-
	5	1.086	.489	0.0
	6	1.149	.459	
	7	1.075	.559	
	8(1)	1.132	.464	88
	8(4)	1.245	.576	8
	9	0.992	.554	0
	11	1.139	.418	84
	12	0.967	.378	500
	8	1	1.045	0.816
2		1.108	.788	
3		1.066	.714	
4(1)		0.911	.666	
4(2)		1.085	.596	
5		1.155	.649	
6		1.031	.699	
7		1.064	.648	
8(1)		1.122	.624	
8(2)		1.183	.644	
9(1)		0.954	.616	
9(2)		1.098	.628	
11		1.138	.658	
12		1.137	.639	
13(1)		1.167	.600	
13(2)		1.165	.685	
14(1)		1.160	.594	
14(2)		1.064	.630	
15(1)		1.043	.696	
15(2)		1.173	.607	
16	1.083	.556		
17(1)	1.087	.550		
17(2)	1.076	.557		

those that were calculated are reported in Table X. The results are given in percentage of the value b quoted. The percentage variance is denoted simply by $\% p(b)$.

VITA

The author was born in 1931 in Johnson City, Tennessee, where he attended the public schools. After a year at East Tennessee State College in Johnson City, he transferred to the University of Tennessee, Knoxville, where he obtained his B.S. and M.S. degrees in Chemical Engineering. During his graduate studies the author had an opportunity to take a somewhat abstract mathematics course in group and matrix theory under Dr. J. A. Cooley. He chanced to meet in that course hermetian matrices, abelian groups, and Miss Joyce Gillenwater, a blue-eyed blond who sat right between the author and Dr. Cooley. The following year they were married. This occasion is taken to point out that Math. 415 was one mathematics course which proved to have very practical results.

The author wishes to express his heartfelt gratitude to his wife, Joyce, for her patience, help and understanding during the preparation of this dissertation. To his parents, Mr. and Mrs. R. C. Mottern, the author will always be grateful, for no matter what hardship it incurred, they never denied his selfish wish for an education.